

**MANIPULATING RAB GTPASE ACTIVITY  
IN WHEAT TO ALTER GLUTEN QUALITY  
FOR BREADMAKING**

**ADAM MICHAEL TYLER, BSc. (Hons)**

**Thesis submitted to the University of Nottingham for the  
degree of Doctor of Philosophy**

**MAY 2012**

## I. Abstract

In the developing endosperm of bread wheat (*Triticum aestivum*), seed storage proteins are produced on the rough endoplasmic reticulum (ER) and transported to protein bodies, specialised vacuoles for the storage of protein. The important gluten proteins of wheat are transported to the protein bodies they are stored in by two distinct routes. One route consists of vesicles that bud directly off the ER, while the other involves transport through the Golgi (Arcalis *et al*, 2004). In plants, the RabD clade mediates ER to Golgi vesicle transport (Batoko *et al*, 2000).

Available sequence information for Rab GTPases in *Arabidopsis*, rice, *Brachypodium* and bread wheat was compiled and compared in phenetic trees. Partial genetic sequences were assembled using the first draft of the Chinese Spring wheat genome.

A suitable candidate gene from the *RabD* clade (*TaRabD2a*) was chosen for down-regulation by RNA interference (RNAi) and an RNAi construct was used to transform wheat plants. Using real time PCR, all four available *RabD* genes were shown to be knocked down in the developing endosperm of transgenic wheat.

The transgenic grain was found to produce flour with significantly altered processing properties when measured by farinograph and extensograph. SE-HPLC found that a smaller proportion of HMW-GS and large LMW-GS are incorporated into the glutenin macropolymer in the transgenic dough. Lower protein content but a similar protein profile on SDS-PAGE was seen in the transgenic grain.

## **II. Acknowledgements**

The glasshouse work at Rothamsted Research, including potting up and harvest of T0 plants and sowing, potting up and harvesting of T1 and T2 plants, was done by Mrs Fiona Gilzean, Mr Anthony Griffin and Mrs Melloney St Leger. The biolistic transformation work was performed by Amanda Riley at Rothamsted Research and the screening of the T0 lines was performed by Caroline Sparks. A sample of pHMW-Adh-Nos plasmid vector was provided by Huw Jones.

Agilent RNA gels were performed at Sutton Bonington by Linda Staniforth and Ruth Cornock. Doug Smith at Campden BRI performed the 2D-PAGE and SE-HPLC of T3 flour and assisted with the SDS-PAGE of T1 seeds. Milling of T3 grain was performed by Leigh Wyatt at Campden BRI. Rheology of T3 dough and Dumas protein content measurement was carried out by the Cereals and Milling Department at Campden BRI.

I would also like to thank my supervisors Grantley Lycett, Chungui Lu, Huw Jones, Johnathan Napier and Mervin Poole for their considerable help and input throughout the project.

Finally I would like to thank the BBSRC and Campden BRI for funding through the Industrial CASE Partnership Award.

### **III. List of Contents**

I. Abstract.....	ii
II. Acknowledgements .....	iii
III. List of Contents .....	iv
IV. List of Figures.....	xi
V. List of abbreviations .....	xv
1 General Introduction .....	1
1.1.1 Functions of the Rab GTPase family.....	1
1.1.2 Development of wheat and cereal seeds .....	2
1.1.3 Storage molecules of cereal and wheat seeds.....	5
1.1.4 The role of gluten proteins in baking performance.....	6
1.1.5 Transport of seed storage proteins during wheat endosperm development.....	7
1.1.6 Potential for manipulation of Rab GTPase activity in the developing endosperm of bread wheat.....	9
2 General Materials and Methods .....	10
2.1.1 Laboratory chemicals and reagents .....	10
2.1.2 Primers & DNA .....	10
2.1.3 Genomic DNA extraction from wheat leaf.....	10
2.1.4 Polymerase Chain Reaction (PCR) .....	11
2.1.5 Agarose gel.....	12
2.1.6 DNA precipitation from PCR product .....	12

2.1.7	Gel purification of DNA fragments .....	13
2.1.8	Plasmid miniprep .....	14
2.1.9	Escherichia coli glycerol stock.....	14
2.1.10	E. coli transformation and culture .....	14
2.1.11	Spectrophotometric analysis of nucleic acids .....	15
2.1.12	DNA sequencing .....	15
2.1.13	Cloning of PCR products for sequencing .....	15
2.1.14	Total RNA extraction from developing wheat endosperm.....	16
2.1.15	cDNA synthesis using random hexamer primers.....	17
2.1.16	Quantitative reverse transcriptase polymerase chain reaction (qPCR) .....	18
3	Bioinformatics of wheat Rab GTPases .....	20
3.1	Introduction .....	20
3.1.1	The protein life-cycle of Rab GTPase .....	20
3.1.2	Membrane fusion of vesicle and target compartments	24
3.1.3	Rab GTPases in the plant endomembrane system .....	25
3.1.4	The RabD/Rab1 clade of Rab GTPases .....	26
3.2	Materials and Methods .....	28
3.2.1	Sequence data and analysis .....	28
3.2.2	Gene expression profiling.....	28
3.2.3	Phenetic analysis .....	29

3.3	Results.....	30
3.3.1	Sequence collection and analysis .....	30
3.3.2	Phenetic analysis of the Rab GTPase family .....	31
3.3.3	Construction of RabD gene sequences using PCR and GSS database.....	38
3.3.4	Expression of RabD genes in developing wheat endosperm.....	42
3.4	Discussion .....	46
3.4.1	Rab gene sequences .....	46
3.4.2	Rab genes in the wheat genome .....	47
4	Cloning of vector construct, transformation and screening of transgenic wheat.....	49
4.1	Introduction .....	49
4.1.1	The RNA interference technique.....	49
4.2	Materials and Methods .....	53
4.2.1	cDNA synthesis using specific primers .....	53
4.2.2	Reverse transcriptase polymerase chain reaction (RT-PCR).....	53
4.2.3	Cloning of RNAi construct .....	53
4.2.4	Wild-type wheat growth and seed collection .....	55
4.2.5	Preparation of wheat embryos and gold particles for transformation.....	56
4.2.6	Biolistic transformation of wheat embryos.....	58

4.2.7	Regeneration of T0 transgenic wheat plants .....	59
4.2.8	PCR screening of T0 plants for transgene .....	61
4.2.9	96-well plate DNA extraction .....	62
4.2.10	96-well plate to 1.5ml tube DNA extraction .....	62
4.2.11	Transgene screening PCR to eliminate null and hemizygous T2 lines .....	63
4.3	Results .....	65
4.3.1	Single target Rab strategy .....	65
4.3.2	RabD consensus strategy .....	65
4.3.3	RNAi target region selection and PCR primer design ...	68
4.3.4	PCR to amplify RabD2a target region .....	68
4.3.5	Cloning of RNAi vector construct .....	74
4.3.6	Screening of T0 plants for transgene .....	77
4.3.7	Transgene screening PCR to eliminate null and hemizygous lines from T1 plants .....	78
5	Analysis of transgenic wheat .....	82
5.1	Introduction .....	82
5.1.1	Gluten protein structure and function - High molecular weight glutenin subunits .....	82
5.1.2	Gluten protein structure and function - Low molecular weight glutenin subunits .....	84
5.1.3	Gluten protein structure and function - Gliadins .....	86
5.1.4	Gluten protein genetics .....	87

5.1.5	Wheat processing quality .....	88
5.2	Materials and Methods .....	92
5.2.1	Sodium dodecyl sulphate polyacrylamide gel electrophoresis of T1 seeds .....	92
5.2.2	Sowing and tagging of T1 wheat, harvesting during development and harvesting when mature .....	94
5.2.3	Sodium dodecyl sulphate polyacrylamide gel electrophoresis (SDS-PAGE) of T2 seeds.....	95
5.2.4	Grain size and shape analysis.....	97
5.2.5	Milling of T2 grain .....	99
5.2.6	Determination of flour moisture content .....	100
5.2.7	Measurement of flour protein content.....	100
5.2.8	Small-scale breadmaking quality test - Reomixer.....	101
5.2.9	Sowing, transport and potting up of T2 wheat .....	103
5.2.10	Tagging and harvesting of developing T3 seeds and harvest of mature seeds .....	104
5.2.11	Milling of T3 grain .....	104
5.2.12	Size exclusion high-performance liquid chromatography (SE-HPLC).....	105
5.2.13	Statistical analysis .....	108
5.2.14	Two-dimensional polyacrylamide gel electrophoresis (2D PAGE) .....	108
5.2.15	Brabender farinograph.....	108

5.2.16	Brabender extensograph.....	110
5.3	Results.....	114
5.3.1	Protein analysis of grain from T0 plants .....	114
5.3.2	T2 grain size and shape analysis.....	114
5.3.3	T2 grain protein analysis.....	121
5.3.4	T2 dough rheology .....	125
5.3.5	Expression of RabD genes in T3 RabD knockdown line.....	127
5.3.6	T3 grain size and shape analysis.....	131
5.3.7	Yield of T3 grain harvest.....	133
5.3.8	Analysis of T3 grain protein content .....	133
5.3.9	Two-dimensional gel analysis of T3 lines.....	135
5.3.10	Analysis of glutenin macropolymer composition in T3 dough.....	135
5.3.11	T3 dough rheology .....	143
5.4	Discussion .....	145
5.4.1	Protein content of transgenic wheat .....	145
5.4.2	Gluten bonding strength .....	146
5.4.3	Potential post-translation modification differences in storage proteins of transgenic wheat.....	147
6	General Discussion.....	150
6.1.1	Expression of RabD genes in developing wheat endosperm of wild type and transgenic Cadenza wheat .....	150

6.1.2	Effect of RNAi on Rab gene expression .....	152
6.1.3	Trafficking of gluten proteins .....	154
6.1.4	Gluten quality in transgenic wheat .....	155
6.1.5	Future prospects.....	157
7	References.....	161
8	Appendix .....	179
8.1	Alignment of wheat RabD nucleotide sequences .....	179
8.2	SDS-PAGE gels .....	184

## IV. List of Figures

Fig. 1.1 – Cellularisation during early endosperm development in cereals (adapted from Olsen, 2004).....	4
Fig. 3.1 - Model of the Rab GTPase cycle (adapted from Ebine & Ueda, 2009) .....	21
Fig. 3.2 - General mechanism of vesicle tethering and fusion (adapted from Ebine & Ueda, 2009).....	23
Fig. 3.3 - Phenogram comparing available wheat Rab protein sequences. ....	32
Fig. 3.4 - Phenogram with Rab D protein sequences of wheat, <i>Brachypodium</i> , rice, <i>Arabidopsis</i> and tobacco.....	33
Fig. 3.5 - Phenogram containing wheat and <i>Arabidopsis</i> Rab coding sequences. ....	35
Fig. 3.6 - Phenogram containing rice and wheat Rab protein sequences. ....	36
Fig. 3.7 – Circular phenogram containing 175 Rab protein sequences from <i>Arabidopsis</i> , rice, <i>Brachypodium</i> and wheat.....	37
Fig. 3.8 – Examples of Bioanalyser results from RNA of acceptable quality extracted from developing endosperm of Cadenza wheat. .	43
Fig. 3.9 - Expression of <i>RabD</i> genes in the developing endosperm of Cadenza wheat. ....	44
Fig. 4.1 - Plant silencing pathways induced by an RNAi vector (adapted from Hirai & Kodama, 2008).....	50
Fig. 4.2 - Vector map of pHMW-Adh-Nos (Nemeth <i>et al</i> , 2010).....	54
Fig. 4.3 – Results of <i>RabD</i> CDS alignments to find $\geq 21$ nt matches. ....	66

Fig. 4.4 – The Ta.54382 (wheat <i>RabD2a</i> ) coding sequence showing selected target region. ....	69
Fig. 4.5 - Primers designed to anneal to the target sequence in PCR. ....	70
Fig. 4.6 - Gradient PCR results. ....	72
Fig. 4.7 - Gradient RT-PCR results. ....	73
Fig. 4.8 – Vector cloning strategy. ....	75
Fig. 4.9 - Placement and orientation of vector primers used in cloning colony screening. ....	76
Fig. 4.10 - Example of results of the first round colony screening PCR. ....	79
Fig. 4.11 - Results of the second round colony screening PCR. ....	80
Fig. 5.1 - Primary structure of glutenin subunits and gliadins (adapted from Delcour <i>et al</i> , 2012; Shewry & Tatham, 1997; D'Ovidio & Masci, 2004; Qi <i>et al</i> , 2006).....	83
Fig. 5.2 - Features of a farinogram .....	89
Fig. 5.3 – DigiEye apparatus .....	98
Fig. 5.4 – Reomixer apparatus .....	102
Fig. 5.5 – Subunit distribution for SE-HPLC .....	107
Fig. 5.6 – Extensograph apparatus .....	111
Fig. 5.7 – Plan area of grain from T2 lines. ....	115
Fig. 5.8 – Perimeter of grain from T2 lines.....	116
Fig. 5.9 – Length of grain from T2 lines.....	117
Fig. 5.10 – Width of grain from T2 lines. ....	118
Fig. 5.11 – Circularity of grain from T2 lines. ....	119
Fig. 5.12 – Mean size and shape values of grain from T2 lines.....	120

Fig. 5.13 – SDS-PAGE of mature T2 seeds.....	122
Fig. 5.14 – Examples of densitometry analysis of T2 SDS-PAGE. .	123
Fig. 5.15 – Protein content of flour from 20 shortlisted T2 lines as a percentage of dry weight.....	124
Fig. 5.16 – Six examples of torque traces during mixing of dough made with flour from T2 lines. ....	126
Fig. 5.17 – Quality map of T2 flour reomixer data.....	128
Fig. 5.18 - Expression of <i>RabD</i> genes at 14 and 21 days post anthesis in the developing endosperm of T3 wheat. ....	130
Fig. 5.19 – Mean size and shape values of grain from T3 lines.....	132
Fig. 5.20 – Protein and starch content of flour from knockdown and control T3 lines as a percentage of dry weight.....	134
Fig. 5.21 – Aligned and overlaid images of 2D gels from T3 flour.	136
Fig. 5.22 – SE-HPLC traces of protein from T3 flour samples. ....	137
Fig. 5.23 – Farinograph traces of dough made with flour from T3 lines. ....	139
Fig. 5.24 – Results from farinograph mixing of T3 dough.....	140
Fig. 5.25 – Extensograph traces of dough made with flour from T3 lines. ....	141
Fig. 5.26 – Measurement of T3 dough processing properties by extensograph.....	142
Fig. 8.1 – SDS-PAGE of mature T1 seeds.....	184
Fig. 8.2 – SDS-PAGE of mature T2 seeds.....	185
Fig. 8.3 – SDS-PAGE of mature T2 seeds.....	186
Fig. 8.4 – SDS-PAGE of mature T2 seeds.....	187
Fig. 8.5 – SDS-PAGE of mature T2 seeds.....	188

Fig. 8.6 – SDS-PAGE of mature T2 seeds.....189

## V. List of abbreviations

2D PAGE	Two dimensional polyacrylamide gel electrophoresis
BLAST	basic local alignment search tool
cDNA	complementary deoxyribonucleic acid
CDS	coding sequence
DNA	deoxyribonucleic acid
dNTPs	deoxyribonucleotide
dsRNA	double stranded ribonucleic acid
ER	endoplasmic reticulum
ESR	embryo surrounding region
GAP	GTPase-activating protein
GDF	GDI displacement factor
GDI	GDP dissociation inhibitor
GDP	guanosine diphosphate
GEF	guanine exchange factor
GGTT	geranylgeranyl pyrophosphate
GMP	glutenin macropolymer
GTP	guanosine triphosphate
HMW-GS	high molecular weight glutenin subunit
LWM-GS	low molecular weight glutenin subunit
miRNA	micro ribonucleic acid
mRNA	messenger ribonucleic acid
RabGGTase	Rab geranylgeranyl transferase
REP	Rab escort protein
RER	rough endoplasmic reticulum

RISC	RNA-induced silencing complex
RNA	ribonucleic acid
RNAi	ribonucleic acid interference
RT-PCR	reverse transcription polymerase chain reaction
PCR	polymerase chain reaction
qPCR	quantitative real-time polymerase chain reaction
SDS-PAGE	sodium dodecyl sulphate polyacrylamide gel electrophoresis
SE-HPLC	size exclusion high performance liquid chromatography
siRNA	small interfering ribonucleic acid
SNARE	soluble NSF attachment protein receptor
TGN	trans-Golgi network
YFP	yellow fluorescent protein

# 1 General Introduction

## 1.1.1 Functions of the Rab GTPase family

In the Ras superfamily of small GTPases, plants contain Rab, Rho, Arf, and Ran GTPases but not the Ras subfamily present in mammals (Vernoud *et al*, 2003). The plant Rab GTPases are best characterised in *Arabidopsis thaliana* with 56 members, each of which is considered to be involved in a particular trafficking step. Rab GTPases are molecular switches that regulate the transport of vesicles between membranous compartments of the exocytic and endocytic pathways of eukaryotes. As well as vesicle budding, tethering and docking, Rab proteins are also involved in the regulation of vesicle and compartment motility through recruitment of motor proteins to the membrane (Stenmark, 2009; Zerial & McBride, 2001).

There are 8 clades of Rab GTPase in plants, designated A-H. They are generally related to mammalian Rab classes 11, 2, 18, 1, 8, 5, 7 and 6 respectively (Pereira-Leal & Seabra, 2001). There are exceptions however, including Rab F1 in plants, which has no homologue in mammalian or yeast systems (Woollard & Moore, 2008). Plant Rab GTPases are well conserved within clades and are usually more similar to homologues in other (even distant) species than closely related Rabs within the same species (Rojas *et al*, 2012). This suggests that Rab GTPase functions are highly conserved between species, though not necessarily separate from each other. A study looking at the effects of knocking out *RabD* genes individually in *Arabidopsis* have shown a lack of phenotype

indicating functional redundancy or overlapping roles (Pinheiro *et al*, 2009).

Early plant secretory traffic involves GTPases of the Rab B and Rab D clades (Rutherford & Moore, 2002) which have been shown to target proteins to the Golgi (Batoko *et al*, 2000; Cheung *et al*, 2002; Zheng *et al*, 2005). A member of the large Rab A subclass has been implicated in trafficking to the cell wall in tomato (Lu *et al*, 2001; Rehman *et al*, 2008). Vesicle transport to the vacuole has been shown to be mediated by Rabs from the F clade and the G3 subclade (Lee *et al*, 2004; Mazel *et al*, 2004; Ueda *et al*, 2004). Studies demonstrate the Rab A, Rab E and Rab F subclasses to be involved in post-Golgi secretory traffic and endocytic cycling (Woollard & Moore, 2008). However, there is little information relating to the function of Rab GTPases from the Rab C and Rab H clades, as well as several of those in the Rab G and Rab A classes.

### *1.1.2 Development of wheat and cereal seeds*

During seed development, protein and starch are laid down in the endosperm as a store for future utilisation at germination. In grasses, the endosperm has 3 major stages of development - early development, differentiation and maturation (Sabelli & Larkins, 2009).

Early development involves creation of the primary endosperm nucleus by fusion of a sperm nucleus and two polar nuclei. In wheat and many other grasses this happens at the same time as syngamy (the fusion of the egg cell nucleus with a sperm

nucleus) (Bennett *et al*, 1975). The triploid (in diploid cereals, nonaploid in bread wheat) endosperm nucleus then rapidly duplicates several times without cytokinesis or cell wall production, to form the syncytium (Olsen, 2004). The number of nuclei reached inside the coenocytic endosperm can exceed 2000 in some species of *Triticum* (Bennett *et al*, 1975). With the nuclei located around the outside of the syncytium, their division is then followed by cytokinesis. This cellularisation proceeds towards the centre of the syncytium until the central cavity is completely filled with endosperm cells (Fig. 1.1).

The differentiation of cereal endosperm results in 4 main types of cell - transfer, aleurone, embryo surrounding region (ESR) and starchy endosperm. The function of transfer cells is to act as a gateway for nutrients between the maternal cells of the seed and the starchy endosperm. In wheat, rice and maize the aleurone layer is one cell thick and covers the starchy endosperm, except where transfer cells are in contact with the starchy endosperm (Sabelli & Larkins, 2009). Functions of the aleurone include assisting in starchy endosperm growth (Lid *et al*, 2004; Olsen, 2004) and releasing enzymes to break down the mature starchy endosperm during germination upon gibberellic acid signal from the embryo (Sabelli & Larkins, 2009). The ESR cells cover the early embryo after the cellularisation phase before reducing in number during development, occupying only a small area at the base of the endosperm. Potential roles of the ESR include the supply of sugars to the embryo (Bate *et al*, 2004; Cossegal *et al*, 2007), defence against pathogens

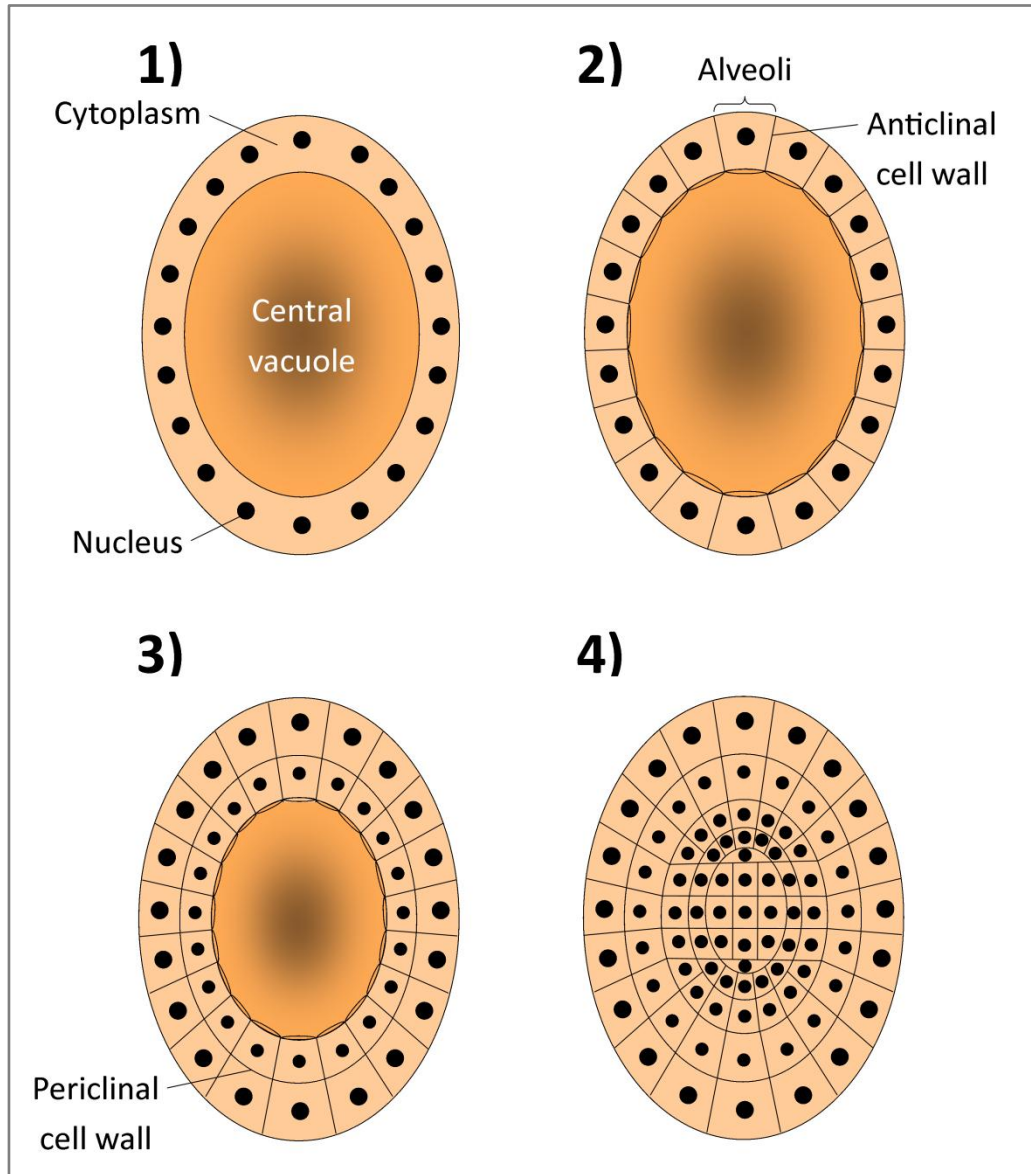


**Fig. 1.1 – Cellularisation during early endosperm development in cereals (adapted from Olsen, 2004)**

1) Endosperm syncytium formation is complete. Evenly spaced nuclei are contained in the cytoplasm surrounding the central vacuole; 2) Open ended tubes (alveoli) are formed by anticlinal cell walls. Each alveolus contains one nucleus and the open end faces the central vacuole; 3) Alveolar nuclei divide before periclinal cell wall formation separates the outer layer of cells from the inner layer of alveoli; 4) The alveoli continue to divide inwards, leaving further layers of cells behind until the central vacuole disappears and cellularisation is complete.

(Balandin *et al*, 2005) and signalling between the embryo and endosperm (Bonello *et al*, 2002; Cock & McCormick, 2001).

### *1.1.3 Storage molecules of cereal and wheat seeds*

The starchy endosperm of cereal seeds accumulates important energy and protein stores during seed development. Approximately 70% of the dry weight of cereal seed is starch while the protein content varies depending on species and variety. Storage protein generally accounts for 10-15% of the dry mass of wheat seeds. In wheat and other Triticeae starch granules form as two types: simple - one large granule per amyloplast; and compound - small polyhedral 'multigranules' within an amyloplast (Shapter *et al*, 2008). Cereal storage proteins include the major types - globulins and prolamins - plus a number of additional minor proteins (Shewry & Halford, 2002). Together, the prolamins make up 50-60% of the total endosperm protein of wheat (Sabelli & Larkins, 2009). Prolamins are rich in proline and glutamine due to the high frequency of Pro and Gln repeats in their amino acid sequences. They are notably lacking in the essential amino acids lysine and tryptophan.

The important gluten proteins of wheat are members of the prolamin superfamily (Kreis *et al*, 1985). They are divided into the monomeric gliadins, which only contain intra-chain disulphide bonds, and polymeric glutenins. Glutenin proteins form inter-chain disulphide bonds which enable a complex polymer structure. Glutenin subunits are divided into high molecular weight (HMW-GS)

and low molecular weight (LMW-GS) subunits. Gliadins are sub-classified as  $\alpha$ -,  $\beta$ -,  $\gamma$ - and  $\omega$ -, depending on fractionation by acidic PAGE (Woychik *et al*, 1961). Gluten proteins are synthesised by membrane-bound polyribosomes on the RER before moving into the ER lumen. Within the ER processing occurs including folding, disulphide bond formation (including inter-chain bonds in glutenins) and hydrogen bonding. The latter can cause the gluten protein to precipitate, forming hydrated protein particles (Tosi *et al*, 2009).

#### *1.1.4 The role of gluten proteins in baking performance*

The prolamins of wheat - gliadins and glutenins - are the major components of the gluten protein fraction, which gives wheat its unique bread making and general baking qualities. Gluten proteins are insoluble in water or aqueous salt solutions, which allows gluten to be easily isolated by gently washing dough to remove the starch and other soluble material. The physical properties of gluten are commonly described as a viscoelastic, i.e. a combination of elasticity and extensibility. The elasticity (ability to return to original shape after deformation) of the dough is responsible for trapping the CO<sub>2</sub> released by yeast during baking, causing the dough to rise, and is therefore a critical property of a good bread wheat. A 'weak' (less elastic) bread flour will let CO<sub>2</sub> escape, while an excessively strong flour confers so much elasticity that expansion is reduced. Both lead to bread failing to rise properly and therefore produce poor quality bread.

The different classes of gluten proteins have their own effects

on the dough - the elasticity can generally be attributed to the polymeric glutenins and the extensibility to the monomeric gliadins (Shewry *et al*, 1995). Wheat of good bread making quality is classically characterised by its high protein content, but also by the types of proteins present.

#### *1.1.5 Transport of seed storage proteins during wheat endosperm development*

Rubin *et al* (1992) proposed that two different types of protein body appear to accumulate in developing wheat endosperm. The first contains relatively dense protein and seems to bud off directly from protein aggregates in the ER that, it is suggested, are too large and insoluble to enter the Golgi apparatus. HMW glutenin subunits are found almost exclusively in these protein bodies throughout development. The second type is less dense and accounts for proteins trafficked via the Golgi. However, these results were contradicted in fluorescence and electron microscopy studies by Loussert *et al* (2008) using specific antibodies for each of  $\alpha$ -,  $\beta$ -,  $\gamma$ - and  $\omega$ - gliadins, HMW and LMW glutenin subunits. The authors could not bring to light any differences in the distribution of the different gluten proteins during endosperm development. Protein sorting into different protein bodies was however shown by Tosi *et al* (2009) using one antibody specific to a LMW glutenin subunit and another, less specific antibody that recognised other gluten proteins. The study also showed that gluten trafficking via the Golgi is favoured during early seed development but later on, during the

intense grain filling phase, protein aggregation in the RER was much increased, which suggests greater frequency of ER-derived protein bodies. This is in agreement with other studies (Levanony *et al*, 1992; Loussert *et al*, 2008) which indicate that prolamins are only processed by the Golgi between 7-16 days post anthesis (dpa). It has also been observed that Golgi stacked cisternae structures are no longer visible in the starchy endosperm after 12dpa (Loussert *et al*, 2008; Tosi *et al*, 2009).

Throughout much of seed development starch and protein are being produced, transported and stored. Small (1-2 $\mu$ m) protein bodies containing prolamins begin to appear around 7 dpa. From about 15dpa the protein bodies begin to increase in size and then visibly merge and/or aggregate. By 21dpa the effect is widespread in the cell and from 33dpa protein is present as a matrix between starch granules and organelles, no longer contained within distinct protein bodies (Loussert *et al*, 2008).

As well as prolamins, wheat seeds also contain 7S globulins located mostly in the embryo but also present in small quantities in the endosperm (Burgess & Shewry, 1986). Triticins are legumin-related globulins present in the starchy endosperm of wheat and comprise about 5% of the total seed protein (Singh *et al*, 1988). Wheat globulins are synthesised in the same way as prolamins and they are trafficked via the Golgi but, unlike the prolamins, are not thought to form protein bodies directly from the ER (Kermode & Bewley, 1999).

### *1.1.6 Potential for manipulation of Rab GTPase activity in the developing endosperm of bread wheat*

Previous efforts to alter the quality of breadmaking wheat using biotechnology have been focused on the gluten proteins themselves, particularly the HMW glutenin subunits. However, the transport of these important wheat proteins has not been well studied and until now no attempts have been made to manipulate trafficking in order to affect breadmaking quality.

In a study on the tetraploid durum wheat by Di Luccia *et al* (2005) a dominant-negative Rab1B from tobacco (Rab D2) was thought to influence the transport of gluten proteins within the secretory system of the developing endosperm by down-regulating the trafficking step from the ER to the Golgi. The result was an increase in insoluble glutenin and an alteration in functional properties of the grain compared to the wild type Rab1 control, indicating improved gluten quality.

If the expression of a *RabD2* gene was reduced in the developing endosperm of hexaploid wheat leading to a restriction of ER to Golgi trafficking, an increase in gluten quality may be induced, improving breadmaking potential.

The objectives of this study include gathering, producing and analysing sequence and expression data on the Rab family of GTPases in *Triticum aestivum*, generating transformed wheat plants in which cell trafficking is altered in the developing endosperm and analysing the transgenic grain to assess the effects of the transgene on gluten quality.

## **2 General Materials and Methods**

### *2.1.1 Laboratory chemicals and reagents*

Chemicals and reagents were supplied by Fisher Scientific (Fisher Scientific UK Ltd, Bishop Meadow Road, Loughborough, LE11 5RG) or Sigma-Aldrich (Sigma-Aldrich Corporation, 3050 Spruce Street, St. Louis, MO, United States) unless otherwise stated.

### *2.1.2 Primers & DNA*

Primers were obtained from Eurofins MWG Operon (Anzingerstr. 7a, 85560 Ebersberg, Germany). The dNTPs used in PCR were obtained from Promega (Promega UK Ltd, Delta House, Southampton Science Park, Southampton, Hampshire, SO16 7NS). Primers and dNTPs were diluted as in the manufacturer's instructions and stored at -20°C. Stock concentration for primers was 100pmol ml<sup>-1</sup> and for dNTPs was 2.5mM per dNTP (or 10mM total). dNTPs were used directly from the stock solution, whilst primers were further diluted to 10pmol ml<sup>-1</sup> before use.

### *2.1.3 Genomic DNA extraction from wheat leaf*

Wheat genomic DNA was extracted from leaf tissue using the following protocol. Leaf tissue was placed in a 1.5ml microcentrifuge tube along with 400µl DNA buffer (200mM Tris-HCl (pH8), 25mM EDTA, 250mM NaCl, 0.5% SDS) and macerated with a centrifuge tube pestle. Following maceration, 135µl of 5M potassium acetate was added, the tube vortexed and incubated on ice for 10 minutes.

The tube was spun in a microcentrifuge at 16,200g (13,000 rpm) for 15 minutes before transferring the supernatant into fresh tube. This was followed by the addition of 0.8 volumes -20°C isopropanol and the tube was mixed gently before incubating at -20°C for 30 minutes. The tube was centrifuged at 16,200g (13,000 rpm) for 15 minutes then the supernatant was discarded and pellet washed with 600µl of chilled 70% ethanol. The tube was then centrifuged at 16,200g (13,000 rpm) for 5 minutes then the supernatant was discarded and pellet washed with 300µl of chilled 100% ethanol. The tube was again centrifuged at 16,200g (13,000 rpm) for 5 minutes before discarding the supernatant and vacuum drying the pellet, which was dissolved in H<sub>2</sub>O.

#### *2.1.4 Polymerase Chain Reaction (PCR)*

Originally described by Saiki *et al* (1988), PCRs were performed using an Eppendorf Mastercycler PCR machine. Each reaction tube contained a total reaction mixture of 20µl composed of 12.8µl H<sub>2</sub>O, 2µl 10x PCR buffer, 0.6µl 50mM MgCl<sub>2</sub>, 1.6µl 2.5mM dNTPs, 0.4µl forwards primer, 0.4µl reverse primer, 2µl DNA template, 0.2µl *Taq* polymerase. PCR buffer and MgCl<sub>2</sub> solutions were supplied by Bioline (Bioline Reagents Ltd., Unit 16 The Edge Business Centre, Humber Road, London, NW2 6EW). Unless otherwise stated, the DNA template used in PCR was from a sample of wheat DNA extracted from leaf tissue of Cadenza variety wheat. The general PCR programme used was 94°C for 5 minutes, followed by a denaturing, annealing, amplification cycle (repeated 35 times)

of 94°C, 60°C (for non-gradient PCR), 72°C. Once complete, this repeated cycle was followed by 72°C for 10 minutes prior to removal of tubes from machine and storage at 4°C. Gradient PCRs used a temperature gradient during the annealing step.

### *2.1.5 Agarose gel*

Electrophoresis gels were 2% molecular biology grade agarose (Bio-Rad Laboratories Inc., 2000 Alfred Noble Drive, Hercules, CA 94547, USA), made up with 0.5x TBE buffer (5x TBE buffer: 53g Tris base, 27.5g boric acid, 10mM EDTA, made up to 1 litre with H<sub>2</sub>O). 0.01% v/v 10mg/ml ethidium bromide was mixed into the buffer once the agarose had been dissolved by heating in a microwave oven and the liquid had begun to cool. Gels were left to solidify in a microgel former with appropriate combs before being placed in a microgel bath and submerged in 0.5x TBE buffer. Next 2µl of loading buffer (10ml loading buffer: 25mg xylene cyanol, 25mg bromophenol blue, 3ml glycerol, made up to 10ml with H<sub>2</sub>O) was added to 10µl of PCR product in each of the experiment wells (mixed before loading) and 5µl of DNA ladder was added to each marker well. Once PCR products and marker had been loaded, gels were run at 10V/cm then photographed under ultraviolet light.

### *2.1.6 DNA precipitation from PCR product*

DNA was precipitated directly from PCR products by ethanol precipitation as follows. One tenth volume of 3M sodium acetate was added to the PCR product in a 1.5ml or 2ml centrifuge tube,

followed by 3 volumes of ethanol at -20°C. The tube was incubated at -20°C for 30 minutes then spun in a microcentrifuge at 16,200g (13,000rpm) for 10 minutes. The supernatant was discarded and the pellet washed with 1ml 70% ethanol before spinning the tube again at 16,200g (13,000rpm) for 2 minutes. The supernatant was discarded and the pellet was vacuum dried before resuspending the pellet in water and storage at 4°C.

### *2.1.7 Gel purification of DNA fragments*

DNA was purified from agarose gel using the following protocol. A 0.5ml centrifuge tube was labelled and a hole made in the top and bottom using a small gauge needle. A small piece of wet filter paper was placed in the bottom of the tube. A frozen gel slice containing a DNA band was then thawed and placed in the tube, which was then frozen in liquid nitrogen. This tube was placed in a 1.5ml centrifuge tube which was spun in a microcentrifuge at 10,000rpm for 3 minutes. The 0.5ml tube was transferred to a new 1.5ml tube, which was spun at 16,200g (13,000 rpm) for 2 minutes. The contents of the two 1.5ml tubes were combined and 0.05 volumes dextran ( $10\text{mg ml}^{-1}$ ) was added followed by 3 volumes ethanol. The tube was incubated at -20°C for 1 hour then spun in a microcentrifuge at 16,200g (13,000 rpm) for 10 minutes. The supernatant was discarded and the pellet washed with 1ml 70% ethanol. The tube was spun at 16,200g (13,000 rpm) for 2 minutes before discarding the supernatant and vacuum drying the pellet, which was resuspended in water.

### 2.1.8 Plasmid miniprep

Plasmid was recovered from transformed *E. coli* culture using a Fermentas GeneJET™ plasmid miniprep kit (Fermentas GmbH, Opelstrasse 9, 68789 St. Leon-Rot, Germany) following the manufacturer's instructions.

### 2.1.9 *Escherichia coli* glycerol stock

Transformed *E. coli* were stored in the form of a glycerol stock. 1.5ml culture was added to 0.5ml of 60% glycerol in a cryotube, vortexed, then frozen in liquid N<sub>2</sub> and stored at -70°C.

### 2.1.10 *E. coli* transformation and culture

Method adapted from Sambrook *et al* (1989). A sample of pHMW-Adh-Nos vector was obtained from Dr Huw Jones (Rothamsted Research, Harpenden, Hertfordshire, AL5 2JQ). Competent DH5- $\alpha$  *E. coli* cells were transformed using a sample of vector, after which 100 $\mu$ l competent cells were added to 5-10 ng of plasmid DNA and an empty control tube. The tubes were mixed gently then placed on ice for 30 minutes. Tubes were placed in a 37°C water bath for 2 minutes then 900 $\mu$ l LB medium was added to each tube, and the tubes were kept at 37°C for a further 30 minutes. After this time, 100 $\mu$ l and 10 $\mu$ l were transferred from the transformed tube onto separate LB+ampicillin plates (LB+ampicillin plates: 100ml LB agar microwaved until liquid. Once sufficiently cooled, 100 $\mu$ l 100mgml<sup>-1</sup> ampicillin was added and mixed, and 25ml was poured into each of 3 sterile Petri dishes and left to cool) and

100µl of the control tube was transferred onto the third plate. After 5 minutes the plates were inverted and incubated at 37°C for 16 hours.

Transformed, ampicillin-selected colonies were then visible, of which 2 were used to inoculate LB+ampicillin medium (LB+ampicillin medium: 10ml sterile LB medium mixed with 10µl 100mg ml<sup>-1</sup> ampicillin) in separate flasks which were incubated at 37°C in a shaking incubator. Plasmid was recovered from the culture using a plasmid miniprep kit (Fermentas). A sample of the remaining culture was used to make a glycerol stock, from which further *E. coli* cultures could be made when more plasmid was required.

#### *2.1.11 Spectrophotometric analysis of nucleic acids*

A NanoDrop 1000 machine (NanoDrop products, 3411 Silverside Rd, Bancroft Building, Wilmington, DE 19810, USA) was used to quantify DNA and RNA samples using manufacturer's instructions.

#### *2.1.12 DNA sequencing*

DNA samples were sequenced by Eurofins MWG Operon. DNA samples were prepared for sequencing by following the instructions provided.

#### *2.1.13 Cloning of PCR products for sequencing*

A Fermentas CloneJET kit was used to clone DNA extractions from gel excisions or PCR products into a sequencing vector using

the “sticky-end” cloning protocol included with the kit.

Transformation and culture of DH5- $\alpha$  *E. coli* was carried out as in “*E. coli* transformation and culture”. Two different colonies were cultured from each plate that contained two or more colonies. Plasmid was recovered from each culture using a plasmid miniprep kit and sequenced.

#### *2.1.14 Total RNA extraction from developing wheat endosperm*

Total RNA was extracted from wheat endosperm tissue using a modified version of the method used by Chang *et al* (1993). First, 300 $\mu$ l  $\beta$ -mercaptoethanol was added to 15ml extraction buffer (extraction buffer: 2% CTAB, 2% PVP, 100mM Tris-HCl (pH 8), 25mM EDTA, 2M NaCl. The buffer autoclaved then 0.5g l<sup>-1</sup> spermidine was added) in a 50ml centrifuge tube and warmed to 65°C in a water bath. Ground endosperm from 2-3 caryopses (0.2g) was added and mixed completely by inverting the tube, followed by incubation at 65°C for 1 minute. An equal volume of chloroform:IAA was added and carefully mixed by inversion before phases were separated at 10,000rpm (12,857g) for 10 minutes at room temperature. The upper layer was transferred to a new 50ml tube using a 10ml disposable pipette before centrifuging with an equal volume of chloroform:IAA a second time and the upper layer was extracted again. One quarter volume 10M of LiCl was added to the tube containing the upper layer extract and mixed. The tube was incubated on ice overnight to precipitate the RNA.

The 50ml tube was centrifuged at 10,000rpm (12,857g) for 20 minutes at 2°C and the supernatant was decanted off. A heating block was used to warm 500µl SSTE (SSTE: 1.0M NaCl, 0.5% SDS, 10mM Tris-HCl (pH 8.0), 1mM EDTA) to 37°C in a 2ml microcentrifuge tube. The SSTE was used to dissolve the pellet in the 50ml tube before being transferred back to 2 ml tube. An equal volume of chloroform:IAA was added to the 2ml tube and phases were separated at 10,000rpm (10,621g) for 10 minutes at 2°C. The upper layer was then transferred to a new 2ml tube using a pipette, to which 2 volumes of -20°C chilled 100% ethanol were added. The tube was incubated at -70°C for 30 minutes and centrifuged at 14,000rpm (20,817g) for 20 minutes at 2°C to pellet RNA. The supernatant was decanted off and the pellet was washed with 500µl of chilled 70% ethanol then centrifuged at 10,000rpm (10,621g) for 5 minutes at 2°C. The pellet was vacuum-dried and resuspended in DEPC-treated H<sub>2</sub>O before being left to dissolve at room temperature for 5 minutes. The RNA was then mixed by pipette before samples were taken for analysis by Nanodrop™ 1000 spectrophotometer and Agilent™ 2100 bioanalyser (Agilent Technologies Inc., Life Sciences and Chemical Analysis Group, 5301 Stevens Creek Boulevard, Santa Clara, CA 95051-7201, USA), and RNA was stored at -70°C.

#### *2.1.15 cDNA synthesis using random hexamer primers*

Method was adapted from that described by Parr *et al* (1992). A 10µl dilution of total RNA was made to 100ngµl<sup>-1</sup> in a 0.2ml PCR tube on ice, using DEPC-treated water. Random hexamer primers

(2µl) were added along with 18µl of DEPC-treated water. The tube was incubated at 70°C for 5 minutes then placed on ice.

A 10µl volume of M-MLV RT 5x buffer was added to a 0.5ml centrifuge tube followed by 2.5µl dNTPs, 1µl RNasin, 2µl M-MLV reverse transcriptase and 4.5µl DEPC-treated water. This reaction mixture was transferred to the RNA/primer mix on ice. The PCR tube was then incubated at room temperature for 10 minutes then 42°C for 1 hour before adding 150µl DEPC-treated water and storage at -20°C.

Random hexamer primers, RT enzyme, buffer, RNasin RNase inhibitor and dNTPs were supplied by Promega.

#### *2.1.16 Quantitative reverse transcriptase polymerase chain reaction (qPCR)*

Real time quantitative PCR first described by Heid *et al* (1996). For each well of a 384-well PCR plate that was to be used, a 10µl PCR mix was added. This mix was made up of 1.6µl of water, 7.5µl SYBR Green I Master Mix, 0.45µl forwards primer and 0.45µl reverse primer. A 5µl volume of cDNA (synthesised using random hexamer primers) was added to each well of PCR mix on the plate. Two technical replicates and three biological replicates were used for each combination of primer pair and seed developmental stage.

For each primer pair, a "no template" control and a "no RT" control were included, each with two technical replicates. For the "no template" control, water was added to the qPCR plate instead of the cDNA template. For the "no RT" control, water was added

instead of the M-MLV reverse transcriptase during cDNA synthesis and the RNA template was made up of an equal mixture of all RNA samples used in the cDNA synthesis.

This cDNA mix was also used to set up a calibration curve for each primer pair as follows: 5 reactions, each with 2 technical replicates, were made up using the cDNA mix at concentrations of  $10^0$ ,  $10^{-1}$ ,  $10^{-2}$ ,  $10^{-3}$  and  $10^{-4}$  as DNA template.

The 384-well PCR plate was then loaded onto a Roche LightCycler 480 and the following program was run: 95°C for 5 minutes; 45 cycles of 95°C for 10 seconds, 60°C for 15 seconds, 72°C for 15 seconds; 95°C for 5 seconds, 65°C for 1 minute, slow ramp to 97°C, 40°C for 10 seconds.

The LightCycler 480 software (Roche) was used to calculate a calibration curve for each primer pair from which RNA concentrations were automatically determined.

## **3 Bioinformatics of wheat Rab GTPases**

### **3.1 Introduction**

#### *3.1.1 The protein life-cycle of Rab GTPase*

Rab GTPases are 'molecular switches' that cycle between an active GTP-bound, membrane-associated state and an inactive GDP-bound, cytosolic state (Fig. 3.1). Active membrane-bound Rab GTPases are involved in the recruitment of tethering and fusion factors, at which point docking and fusion of a trafficking vesicle with its acceptor membrane may occur (Gurkan *et al*, 2005; Pfeffer & Aivazian, 2004).

Shortly after being newly synthesised, Rab proteins are prenylated (hydrophobic molecules added to a protein) in their GDP-bound form, which makes them insoluble. This process is carried out by a complex of Rab escort protein (REP), Rab geranylgeranyl transferase (RabGGTase) and geranylgeranyl pyrophosphate (GGTP). RabGGTase performs the actual prenylation but cannot bind to the Rab without REP, while GGTP increases the affinity of the RabGGTase towards the Rab-REP complex (Woollard & Moore, 2008).

Rab proteins are activated when bound GDP is exchanged for GTP by a guanine exchange factor (GEF) specific to each Rab. In active form Rab GTPases recruit effector proteins to the vesicle membrane, which can mediate one of a range of functions. These can include coats to initiate vesicle budding; motility along the microtubule and/or actin cytoskeleton via kinesin or dynein/dynactin

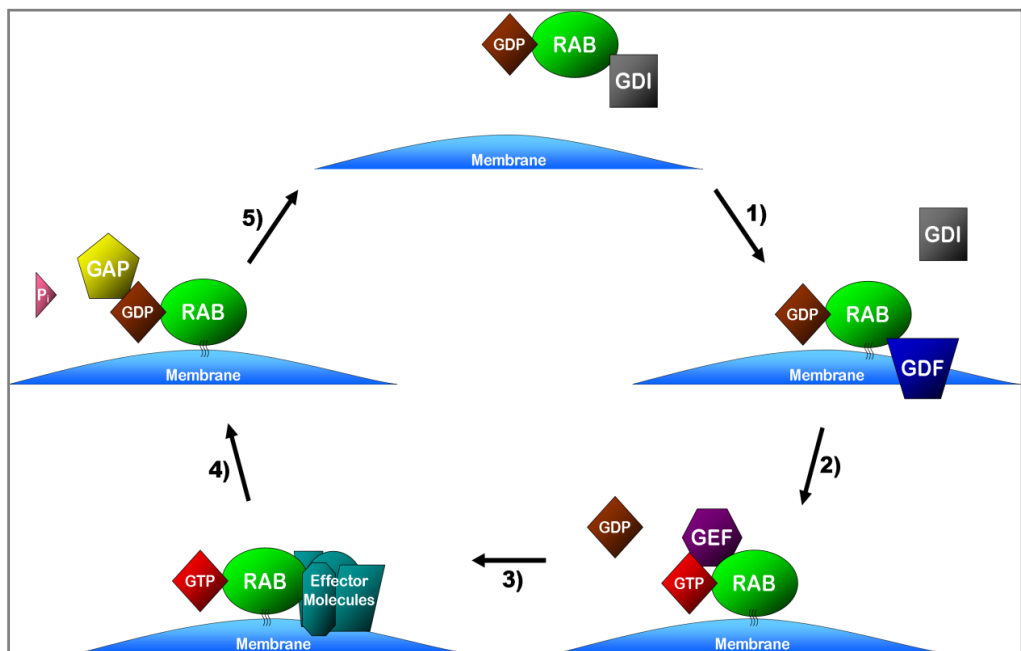


**Fig. 3.1 - Model of the Rab GTPase cycle (adapted from Ebine & Ueda, 2009)**

1) Dissociation of Rab from Rab GDP Dissociation Inhibitor (Rab GDI) is mediated by a GDI displacement factor (GDF), which then keeps Rab attached to the membrane; 2) Activation of Rab occurs with the exchange of bound GDP for GTP, which is catalyzed by a specific Guanine nucleotide Exchange Factor (GEF) ; 3) Effector molecules are recruited to the membrane by the activated Rab, initiating a range of downstream functions, including vesicle tethering and vesicle movement; 4) GTPase Activating Protein (GAP) catalyses the hydrolysis of GTP on Rab, converting Rab to the GDP-bound inactive form; 5) The inactivated GDP-bound Rab is detached from the membrane by Rab GDI and remains in the cytosol until the next round of the Rab GTPase cycle.

motors; tethers for docking to the target membrane; and SNAREs for fusion of the vesicle membrane with that of the target compartment (Horgan & McCaffrey, 2011). In mammals and yeast it has been shown that due to the wide variety of Rab effectors it is likely that each Rab utilises a particular set of effectors (Grosshans *et al*, 2006). In addition, most of the tethering complexes (which tether vesicles to their target membranes) have been demonstrated to be effectors of a single Rab GTPase (Cai *et al*, 2007). This suggests that transport vesicle tethering to a target compartment membrane appears to be a conserved function within Rab protein family, yet individual Rab GTPases each have their own specific role in plants (Ebine & Ueda, 2009).

Following vesicle fusion with the acceptor membrane, the GTP bound to the Rab protein is hydrolysed to GDP in the presence of GTPase activating protein (GAP). The hydrolysis causes a binding target for Rab GDP dissociation inhibitor (GDI) to be generated on the GDP-bound, inactive Rab, which results in removal of the Rab from the target membrane by GDI. The GDI-bound inactive Rab resides in the cytosol until the GDI is separated from the Rab by GDI displacement factor (GDF), at which point the Rab is bound to the donor membrane (DiracSvejstrup *et al*, 1997). The Rab is then receptive to activation by GEF and the GDI binding target is rendered inactive.

Rab GDIs in plants are functionally conserved with broad substrate specificity (Ueda *et al*, 1996; Ueda *et al*, 1998; Zarsky *et al*, 1997). This distinguishes them from GEFs and GAPs, each of

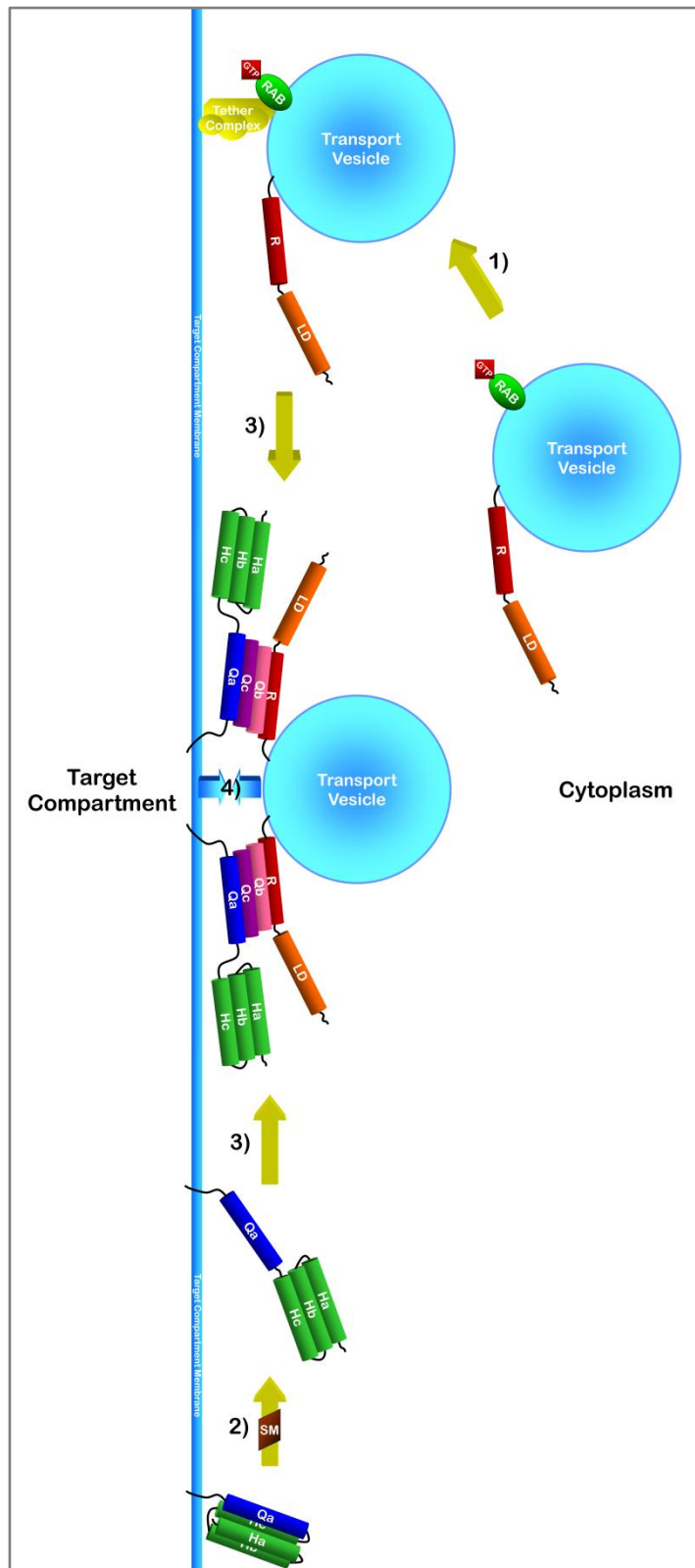


**Fig. 3.2 - General mechanism of vesicle tethering and fusion (adapted from Ebine & Ueda, 2009)**

1) Transport vesicles are attached to the target membranes by some Rab effectors, which are called "tethers"; 2) The conformation of the Qa-SNARE is converted from the "closed" conformation to the "open" conformation. A conserved protein family, Sec1/Munc18 (SM) proteins, is believed to be responsible for the refolding of the Qa-SNARE ; 3) Assembly into the SNARE complex; 4) Fusion of the vesicle membrane with that of the target compartment and delivery of vesicle contents; The SNARE complex comprises one each of Qa-, Qb-, Qc- and R-SNAREs. H: autoinhibitory domain of Qa-SNARE comprising three helices (Ha, Hb, Hc). LD: longin domain

which interacts only with a certain Rab protein. Like GDIs, GDF proteins also have broad substrate specificities. The Rab GDF function has been found in Yip3 in yeast (Sivars *et al*, 2003) and PRA1 (Prenylated Rab Acceptor 1) in animals and plants (Bahk *et al*, 2009; Rho *et al*, 2009). Interestingly, SidM/DrrA in bacteria (*Legionella pneumophila*) performs dual Rab effector functions as both a Rab GEF and GDF (Suh *et al*, 2010).

### *3.1.2 Membrane fusion of vesicle and target compartments*

Once the Rab GTPase has tethered the vesicle to the target membrane, SNARE proteins mediate the fusion process (Fig. 3.2). The SNARE protein family is characterised by a common heptad-repeat motif and is conserved throughout all eukaryotes. Depending on the amino acid at the '0-layer' position in the SNARE motif, they are classified into R- (arginine at 0-layer) or Q- (glutamine at 0-layer) SNAREs. Based on sequence similarity Q-SNAREs are further classified into Qa-, Qb- and Qc-SNAREs (Antonin *et al*, 2002; Fasshauer *et al*, 1998). SNAP-25-like proteins contain motifs from both Qb- and Qc-SNAREs within the same sequence.

The SNARE complex is made up of either the 4 different SNAREs or of 3 SNAREs in complexes containing SNAP-like proteins, with the SNAREs anchored onto the vesicle or target compartment membrane by a transmembrane domain or fatty acylation. The SNARE complex may only form once the conformation of the Qa-SNARE is altered from its closed, inactive form to the open, receptive conformation. The putative catalyst for the reaction is the

Sec1/Munc18 (SM) protein family (Burgoyne & Morgan, 2007; Toonen & Verhage, 2007). The formation of the SNARE complex causes the membranes of the vesicle and target compartment to pull together closely enough to fuse (Hong, 2005; Wickner & Schekman, 2008). The combination of a specific Rab GTPase, tethering complex and the particular SNARE proteins involved in the SNARE complex is what is thought determine membrane fusion specificity (Ebine & Ueda, 2009).

### *3.1.3 Rab GTPases in the plant endomembrane system*

In plants the RabA clade is a large and diverse group consisting of 26 members in 6 subclades in *Arabidopsis* (Pereira-Leal & Seabra, 2001). On the other hand, the RabA6 subclass is not found in monocots, whilst yeasts and animals generally only have 1 to 3 members in the entire clade (Woollard & Moore, 2008). RabA2 and A3 were shown to transport YFP to a brefeldin-A sensitive compartment that partially overlaps with the TGN, and which was consequently named the Rab-A2/A3 compartment (Chow *et al*, 2008). This compartment is thought to be on the Golgi to plasma membrane route in the secretory pathway (Woollard & Moore, 2008). Proteins of the RabA1 subclade have been implicated in secretory trafficking in plants, usually from the TGN to the plasma membrane (de Graaf *et al*, 2005; Heo *et al*, 2005; Rehman *et al*, 2008). A member of the RabA4 subclade, RabA4b, was found to localise to a vesicular-tubular *trans*-Golgi compartment that accumulates near the tips of growing root hairs in *Arabidopsis*

(Preuss *et al*, 2006).

The RabE subclade has 5 members in *Arabidopsis* and is related to Rab8 in mammals (Pereira-Leal & Seabra, 2001). YFP-tagged RabE1d was found to localise to the Golgi stacks in tobacco and is thought to act downstream of RabD GTPases in the Golgi to plasma membrane biosynthetic secretory pathway (Zheng *et al*, 2005).

Certain cellular processes are also thought to be regulated by Rabs, for instance it has been shown that RabA2, A3 and F2 are involved in cytokinesis in *Arabidopsis* (Baluska *et al*, 2006; Dhonukshe *et al*, 2006).

#### *3.1.4 The RabD/Rab1 clade of Rab GTPases*

The RabD clade in plants is equivalent to Rab1 in animals and Ypt1 in yeasts, and is split into 2 subclades - RabD1 and RabD2 (Rutherford & Moore, 2002). In yeast, Ypt1p affects docking of ER-derived vesicles and also regulates Uso1p-dependent tethering of donor vesicles to the target membrane (Cao *et al*, 1998) suggesting the mediation of Ypt1p in tethering of ER-derived vesicles before membrane fusion occurs. Several studies have demonstrated a similar role for the mammalian Rab1. It was shown to mediate the docking of ER-derived vesicles with the *cis*-Golgi compartment by recruitment of cytosolic tethering factors (Allan *et al*, 2000) and displayed interaction with Golgi membrane proteins (Moyer *et al*, 2001). In another study Rab1-specific antibodies blocked ER to the Golgi and also intra-Golgi trafficking (Plutner *et al*, 1991).

The role in traffic from the ER to the Golgi of a member of the RabD clade, Rab D2a, was demonstrated by the over-expression of a dominant-negative form of RabD2a (N121I) which resulted in accumulation of secreted and Golgi markers in an ER-like reticulate compartment in *Arabidopsis* (Batoko *et al*, 2000). However, inhibition by the dominant-negative in several other plant species did not affect trafficking to the protein storage vacuole in leaf protoplasts (Park *et al*, 2004), which would indicate independent secretory traffic pathways. The trafficking of peroxisomal membrane proteins AtPEX2 and AtPEX10, suggested to be transported to the peroxisome via the ER, was shown insensitive to the dominant-negative RabD2a as well as a drug causing the ER and Golgi to fuse (brefeldin A) (Sparkes *et al*, 2005).

In order to study the Rab family in wheat, sequence information for wheat Rab proteins and genes was collected and compared against that from other plant species (*Arabidopsis*, rice and *Brachypodium*). Expression of wheat *RabD* genes in developing endosperm was also investigated.

## **3.2 Materials and Methods**

### *3.2.1 Sequence data and analysis*

*Arabidopsis thaliana* Rab GTPase proteins and their associated genes and coding sequences (CDS) were found mainly by string searches of the NCBI Protein database. After the *Arabidopsis* Rabs database had been produced, subsequent sequence searches were mostly by BLAST (Basic Local Alignment Search Tool) using sequences already gathered. Full wheat Rab proteins and genes were sought using online bioinformatic search engines such as NCBI BLAST, followed by searching for wheat ESTs showing similarity to the *Arabidopsis RAB* genes. Each EST in the search results belonged to a particular unigene, the name of which was noted before the sequences of all the ESTs belonging to each unigene were aligned using Geneious (Drummond *et al*, 2010) to produce consensus sequences, which were then analysed to find CDS with Rab-like features.

### *3.2.2 Gene expression profiling*

The Array Express and NASC Arrays websites were searched and relevant experimental data downloaded (<http://www.ebi.ac.uk/microarray-as/ae/>, <http://affymetrix.arabidopsis.info/narrays/experimentbrowse.pl>). *Rab* gene expression during seed development in wheat and *Arabidopsis* was studied using microarray data analysis software (GeneSpring GX, Agilent Technologies).

### 3.2.3 Phenetic analysis

Phenetic analyses were carried out using Rab CDS data that had been obtained by BLAST or string searches of the NCBI Nucleotide and EST databases, as well as Rab protein sequences that had been obtained by following links from corresponding entries in the NCBI Nucleotide database or by translating from a CDS that had been assembled from ESTs. The plant species included were *Arabidopsis thaliana*, *Oryza sativa*, *Brachypodium distachyon*, *Triticum aestivum* and *Nicotiana tabacum*. Alignments and phenetic tree files for rectangular trees were generated using MAFFT version 6 online (Kato & Toh, 2010). Alignments and phenograms for circular trees were produced in MEGA 5 (Tamura *et al*, 2011). All trees were neighbour-joining with 1000 bootstrap replicates, shown on branches as percentage confidence values (Felsenstein, 1985; Saitou & Nei, 1987). Branches corresponding to partitions reproduced in less than 50% bootstrap replicates were collapsed. The trees were drawn to scale, with branch lengths in the same units as those of the evolutionary distances used to infer the phenetic tree. The evolutionary distances were computed using the Poisson correction method and are in the units of the number of amino acid substitutions per site.

### **3.3 Results**

#### *3.3.1 Sequence collection and analysis*

The first method of gathering information began with the production of a database of all *Arabidopsis thaliana* RAB GTPase proteins. Once this was complete the *Arabidopsis* database was used to search for wheat Rab proteins and genes using online bioinformatic search engines such as NCBI BLAST. Only three Rab proteins could be found in this way due to the lack of full wheat Rab gene and protein sequences available. The next approach was to look for wheat unigenes showing similarity to the *Arabidopsis RAB* coding sequences. All the ESTs belonging to a particular unigene were aligned using software to produce consensus sequences.

The consensus sequences produced from unigene ESTs were examined for ORFs to determine whether a region coding for a viable protein was present. Out of all the unigenes analysed, 29 contained genuine coding regions, of which three were identical to the three wheat *Rab* genes found originally.

After all available unigenes had been collected a further approach involved the use of data from microarray experiments. Those using wheat seed or endosperm tissue, including those focusing on wheat seed development, were of particular interest. *Rab* gene expression was compared to other genes, specifically storage proteins to investigate their relative expression in developing endosperm.

Rice and *Brachypodium distachyon* *Rab* coding sequence (CDS) and protein sequences were collected for comparison with

those of *Arabidopsis* and with the selection of wheat *Rab* unigenes that had been gathered, as well as with the tobacco *Rab* that has been shown to give a knockdown phenotype in durum wheat (Di Luccia *et al*, 2005). These were subjected to phenetic analysis in order to investigate the relationships between *Rabs* of different plant species and find a potential target gene for knockdown in wheat.

### 3.3.2 Phenetic analysis of the *Rab* GTPase family

Phenetic analyses were carried out using *Rab* protein and nucleotide sequence data from *Arabidopsis thaliana*, *Brachypodium distachyon*, rice, wheat and tobacco. Selected sequences were aligned together and phenetic trees were generated from those alignments in order to discern relationships between individuals and groups of *Rab* sequences.

*Rab* protein sequences from wheat were used to produce the phenogram shown in Fig. 3.3. The *Rab* D proteins show high similarity to each other, as well as greater sequence conservation within the *Rab* D2 subgroup. These results indicate similar functions, which corresponds with studies into the secretory system interactions of *Rab* Ds in *Arabidopsis* (Pinheiro *et al*, 2009).

The phenogram shown in Fig. 3.4 shows the available *Rab* D amino acid sequences from *Arabidopsis*, *Brachypodium*, rice, wheat and the tobacco *Rab* targeted in an earlier study by Di Luccia *et al* (2005). While *Rab* D2a and to a certain extent *Rab* D1 sequences appear to be conserved within their own subgroups, the *Arabidopsis* *RAB* D2b (AT5G47200) and *RAB* D2c (AT4G17530) appear to be

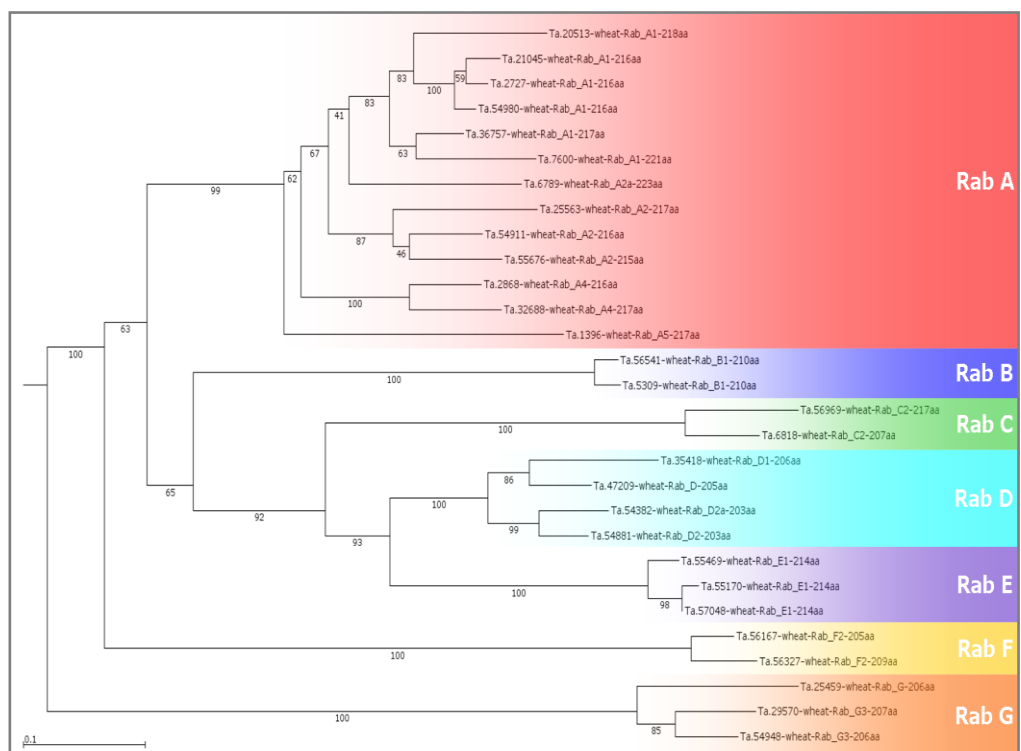


**Fig. 3.3 - Phenogram comparing available wheat Rab protein sequences.** Rab clades are labelled on the right. Alignment and phenetic tree file was generated using MAFFT version 6 online (Kato & Toh, 2010). Tree is neighbour-joining with 1000 bootstrap replicates, shown on branches as percentage confidence values.

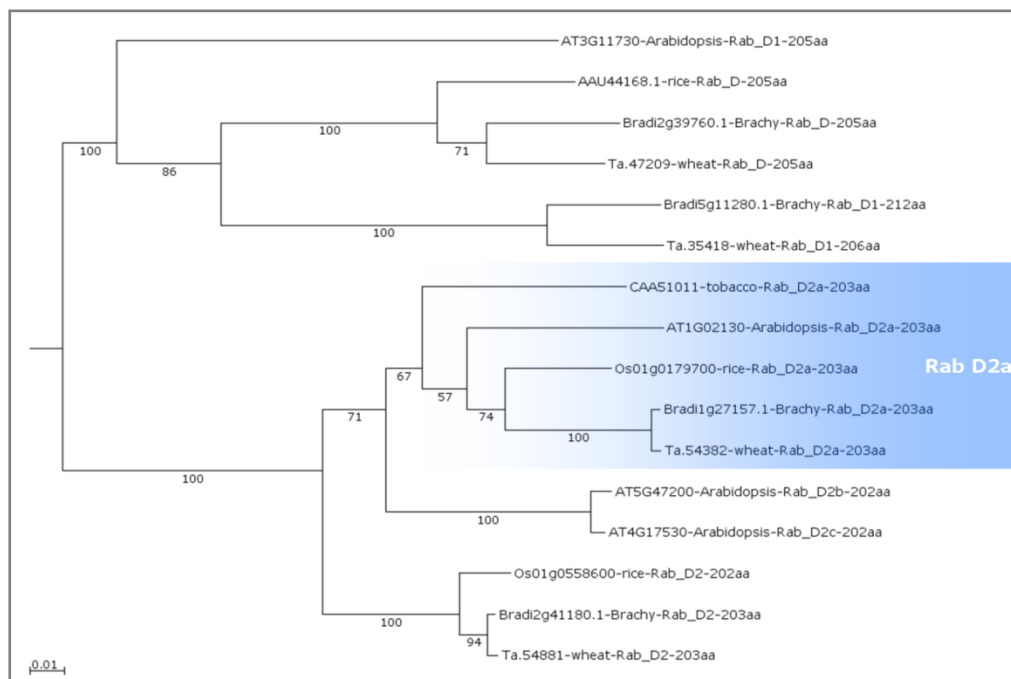


**Fig. 3.4 - Phenogram with Rab D protein sequences of wheat, *Brachypodium*, rice, *Arabidopsis* and tobacco.**  
 Rab D2a homologs are highlighted in blue. Alignment and phenetic tree file was generated using MAFFT version 6 online (Kato & Toh, 2010). Tree is neighbour-joining with 1000 bootstrap replicates, shown on branches as percentage confidence values.

more similar to each other than any Rab D2 sequences of other species. This could make it difficult to classify Rab D2 sequences that don't appear homologous to Rab D2a. The tobacco Rab D2a protein included in this phenogram was used to co-suppress the native homologue in durum wheat (*Triticum durum*) and was shown to influence protein trafficking between the ER and the Golgi.

*Rab* coding sequences from wheat and *Arabidopsis* were phenetically compared (Fig. 3.5). While each clade tends to group together in the tree, subgroups within them often show more similarity between sequences of their own species rather than the equivalent sequence(s) belonging to the other organism. The *RabD* clade is a case in point - there appears to be a reasonable level of similarity between *RabD2a* sequences from both species, however the wheat *RabD1* sequences are fairly dissimilar to the *Arabidopsis RabD1* in relation to the rest of the clade. The wheat *RabD2* (Ta.54881) also shows relatively little similarity to the other *RabD2* members. The explanation for this could be the evolutionary distance between *A. thaliana* and *T. aestivum*, or possibly the effects of hexaploidy (e.g. silencing, pseudogenes, redundancy) in wheat compared to the diploid genome of *Arabidopsis*.

To study the relationships between the Rab GTPase family of proteins in rice and wheat, a phenogram was generated that contained amino acid sequences from both organisms (Fig. 3.6). The rice Rab subfamily that shares homology with Rab 21 in mammals (Tanaka *et al*, 2008) is not found in *Arabidopsis*, which is the reason it was not given a plant-specific alphabetic designation when the

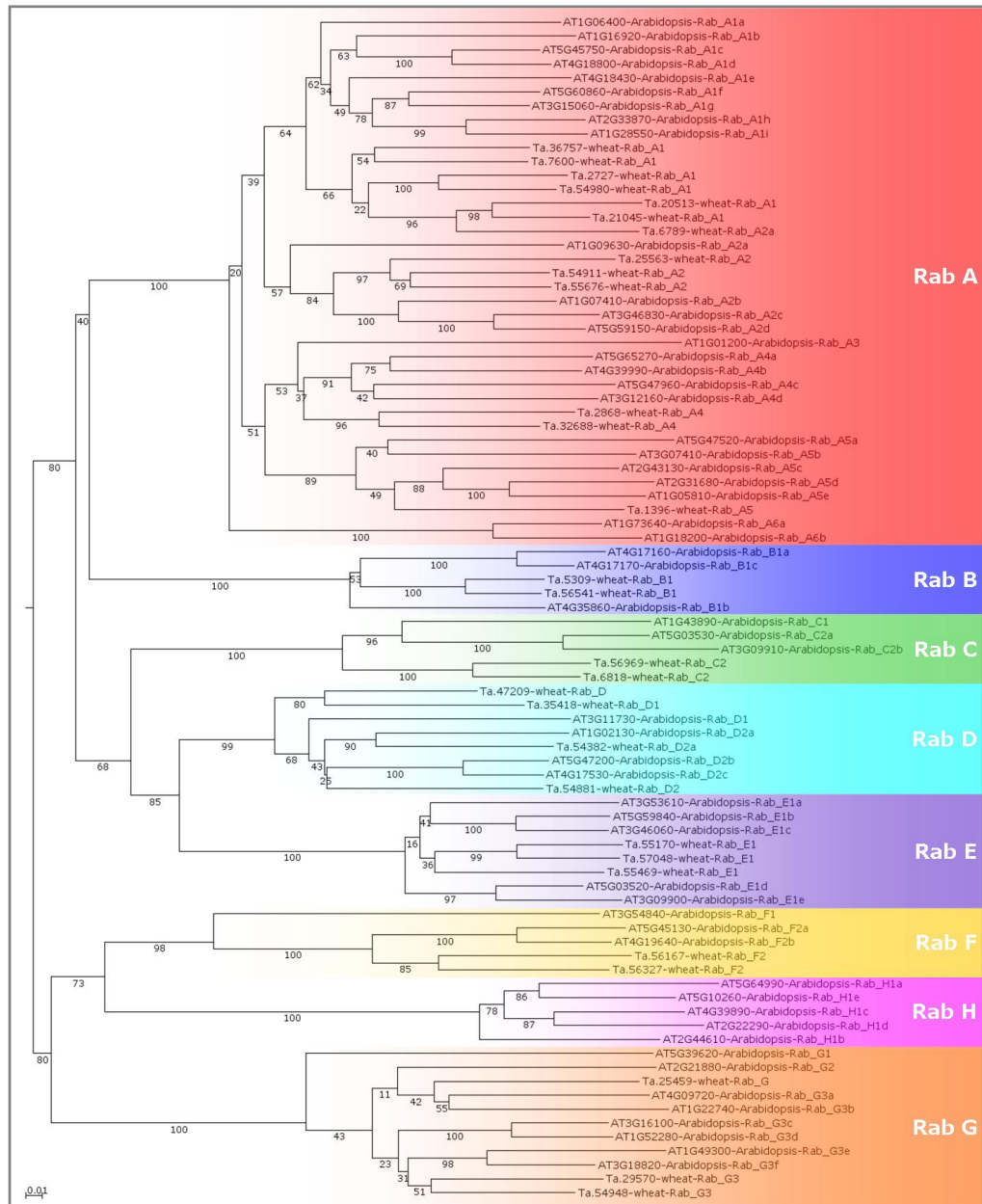


**Fig. 3.5 - Phenogram containing wheat and *Arabidopsis* Rab coding sequences.** Rab clades are indicated on the right. Alignment and phenetic tree file was generated using MAFFT version 6 online (Kato & Toh, 2010). Tree is neighbour-joining with 1000 bootstrap replicates, shown on branches as percentage confidence values.

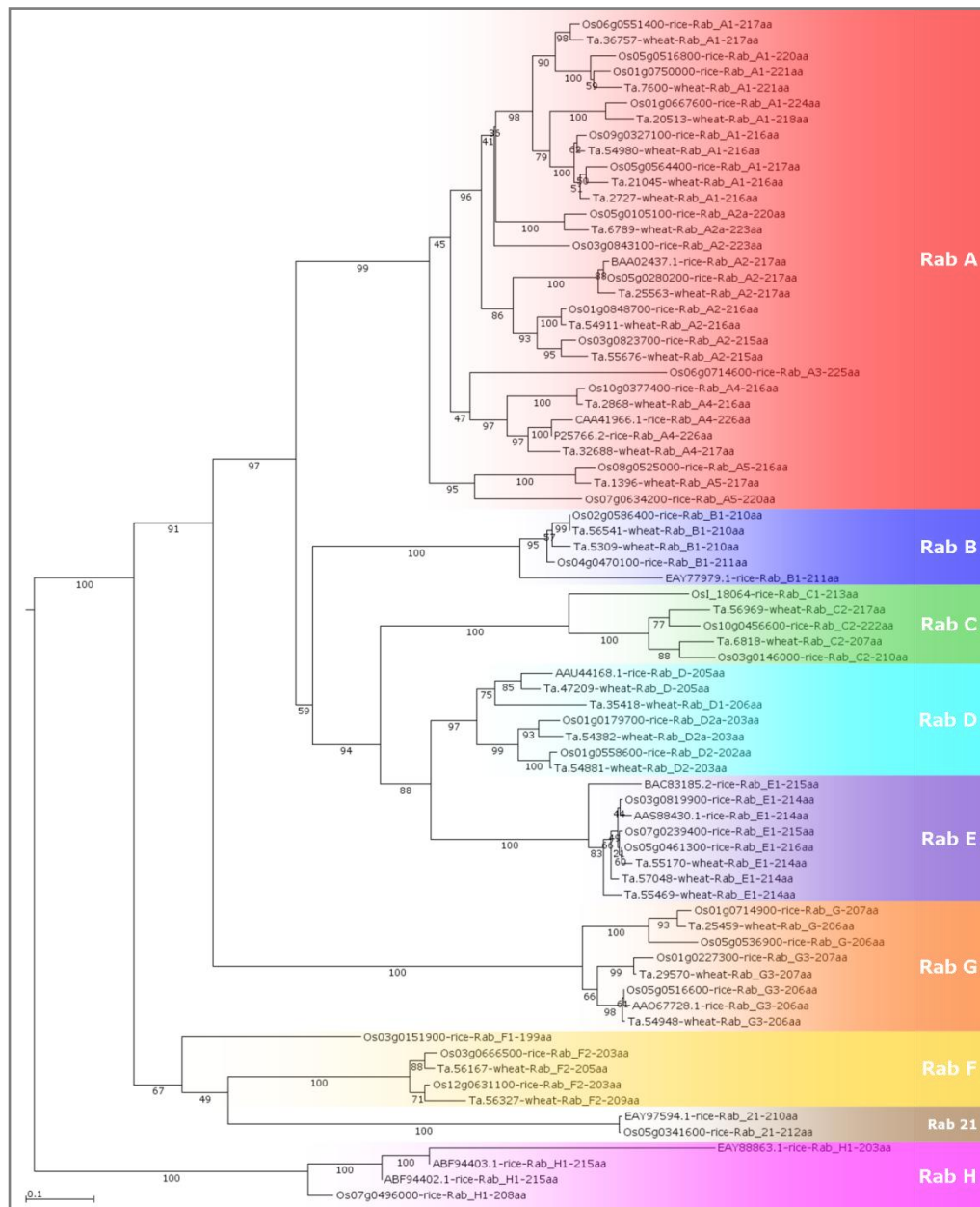


**Fig. 3.6 - Phenogram containing rice and wheat Rab protein sequences.**

Rab clades indicated on the right. Alignment and phenetic tree file was generated using MAFFT version 6 online (Kato & Toh, 2010). Tree is neighbour-joining with 1000 bootstrap replicates, shown on branches as percentage confidence values.

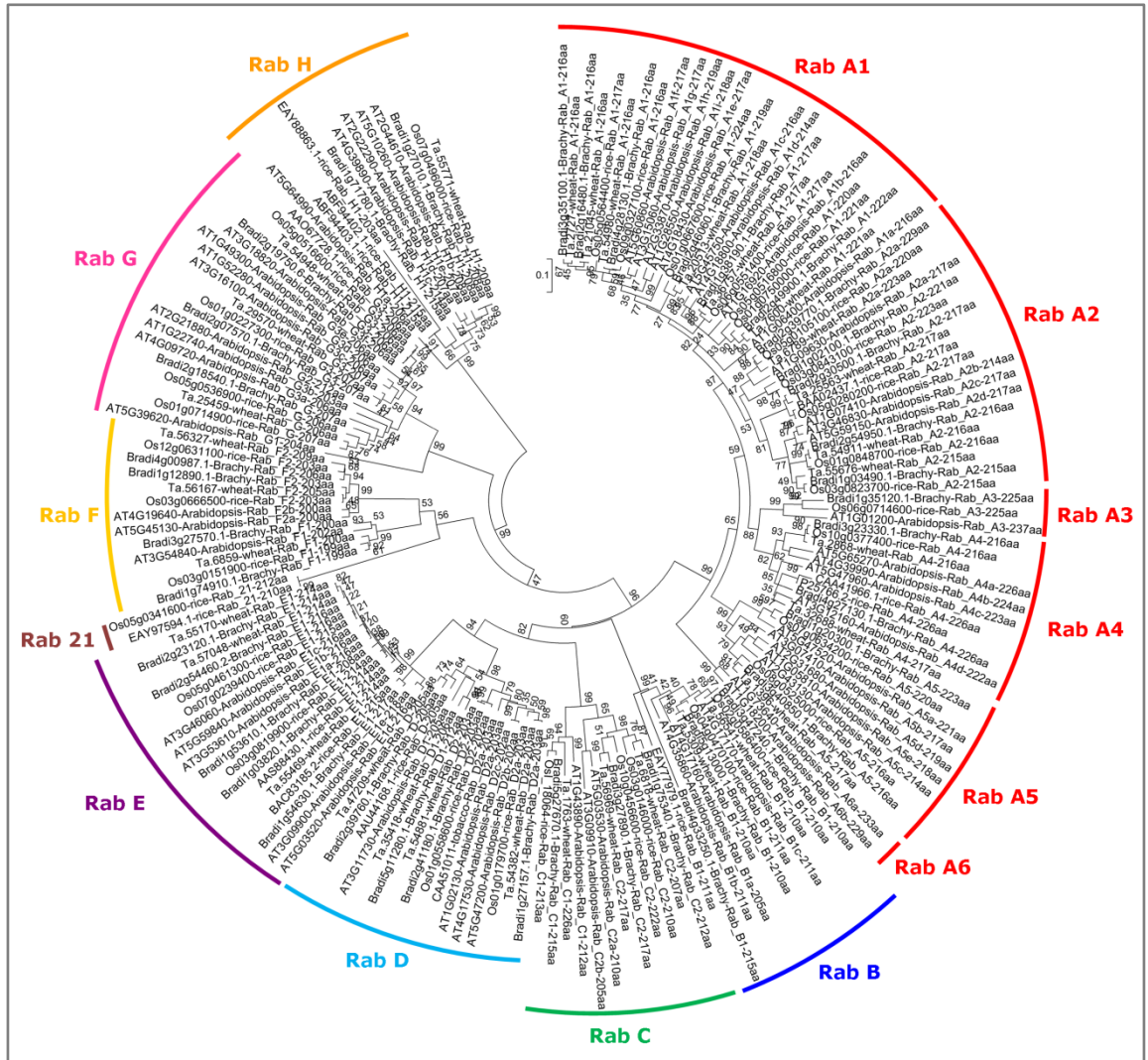


**Fig. 3.7 – Circular phenogram containing 175 Rab protein sequences from *Arabidopsis*, rice, *Brachypodium* and wheat.** Rab clades indicated on the outside. Tree is neighbour-joining with 1000 bootstrap replicates, shown on branches as percentage confidence values. Branches corresponding to partitions reproduced in less than 50% bootstrap replicates are collapsed.

system was put forward by Pereira-Leal and Seabra (2001). In addition, the Rab 21 clade that appears in rice is not present in *Brachypodium* or the selection of available wheat Rabs. The Rab protein family is conserved within clades rather than within species, demonstrating their equivalent function in the two different plants as well as the species' evolutionary proximity.

A phenogram comparing all Rab proteins compiled in the study was produced (Fig. 3.7) and proved helpful in the more specific identification of Rabs in *Brachypodium* and wheat.

### *3.3.3 Construction of RabD gene sequences using PCR and GSS database*

PCR primers were designed to amplify a 443bp region of the unigene coding sequence of wheat *Rab* Ta.54382, putatively identified as *RabD2a* (D2a-basic-F: 5'-TGC CGA TGA CTC GTA CCT GGA GA-3'; D2a-basic-R: 5'-GGC TCG CCA TCC TGT CCT TGA TT-3'). PCR was performed using wild-type Cadenza wheat DNA as DNA template and the PCR product was sequenced (see 4.3.4 PCR to amplify *RabD2a* target region). A 1379bp region of the gene was assembled from the sequencing data. This sequence was used to BLAST search a database of genome survey sequences (GSS) of Chinese Spring wheat (<http://www.cerealsdb.uk.net>). The resulting matches were aligned with the query sequence and Ta.54382 CDS using Geneious (Drummond *et al*, 2010) to give a 2019bp sequence, representing most of the gene (see 8.1 Alignment of wheat *RabD* nucleotide sequences).

Three different primer pairs were designed for each of the other 3 *RabD* unigenes found based on the CDS (Table 1). Six different combinations of primers were used in PCR for each gene with wild-type Cadenza wheat DNA as the DNA template. The PCR products were run on agarose gels and those with more than one band visible had the bands cut out and DNA extracted from the gel. DNA was purified directly from those PCR products that displayed only one band. The samples of DNA from PCR products and gels were cloned into a sequencing vector and used to transform *Escherichia coli* DH-5 $\alpha$ . Plasmid was extracted from the *E. coli* and sequenced along with purified DNA from PCR products and gel excisions.

These genomic sequences were aligned with the corresponding coding sequences. The lengths of the partial gene sequences produced were 209bp for Ta.35418 (including 1 intron), 881bp for Ta.47209 (including 2 introns) and 1703bp for Ta.54881 (including 4 introns). Several sequences for Ta.54881 aligned to the same area of the coding sequence but were not 100% homologous. The assembled partial gene sequences and coding sequences of the four *RabD* genes were aligned together (8.1 Alignment of wheat *RabD* nucleotide sequences). All four genes contained 7 introns in the same locations, however each intron varied in sequence and length between the different *RabD* genes. The information gained from this sequence data aided in the choice or design of primers for quantitative real time PCR.

<b>Primer</b>	<b>Sequence</b>
Ta.54881-RT1-F	TGACCAGGAGAGCTTCAACAAC
Ta.54881-RT1-R	TGCCAGCCTCGTAAGAAACC
Ta.54881-RT2-F	GTTGACTTCAAAATCCGCACCG
Ta.54881-RT2-R	TCGCTCTTGTCAGCAGTATC
Ta.54881-RT3-F	AAGTCTTGCCCTGCTGCTGAG
Ta.54881-RT3-R	GCAGCTTTATCGTCTTCCCATC
Ta.47209-RT1-F	TCGATGGCAAGTCGGTGAAG
Ta.47209-RT1-R	CGATAATGATTCCATGCGCTCC
Ta.47209-RT2-F	CCAGTGACAGTGTGTGCAAG
Ta.47209-RT2-R	CCCAACGATTCTGCAAAGCC
Ta.47209-RT3-F	GAAGCCATCAATGTGGAGACAG
Ta.47209-RT3-R	CATGTGAACATGGACCGTCG
Ta.35418-RT1-F	TCCGTTTCTCCGACGATTTCG
Ta.35418-RT1-R	TCCTGCTGTGTCCCAAATCTG
Ta.35418-RT2-F	AGATTTGGGACACAGCAGGAC
Ta.35418-RT2-R	AGACAATGATGATCCCGTGAGC
Ta.35418-RT3-F	GCGGTTCAGAACCATCACAAAG
Ta.35418-RT3-R	TCGATCTCGCTCAGCCATTG

**Table 1 – Primers used to investigate gene sequence of wheat *RabD* genes.**  
Sequences are 5' to 3'.

<b>Unigene</b>	<b>Primer F name</b>	<b>Primer F sequence</b>	<b>Primer R name</b>	<b>Primer R sequence</b>
Ta.35418	Ta.35418-RT1-F	TCC GTT TCT CCG ACG ATT CG	Ta.35418-RT1-R	TCC TGC TGT GTC CCA AAT CTG
Ta.47209	Ta.47209-RT4-F	AGG TCG TCG ATA CAG AGG AG	Ta.47209-RT4-R	GGC TCG CCA TCT TGT TCT TG
Ta.54832	Ta.54832-RT3-F	ATC GGA GAC TCA GGT GTT GG	Ta.54832-RT3-R	GTT CTG AAG CGT TCT TGC CC
Ta.54881	Ta.54881-RT3-F	AAG TCT TGC CTG CTG CTG AG	Ta.54881-RT2-R	TCG CTC TTG TCC AGC AGT ATC
Ta.2291	Ta.2291-P1-F	GCT CTC CAA CAA CAT TGC CAA C	Ta.2291-P1-R	GCT TCT GCC TGT CAC ATA CGC
Ta.2776	Ta.2776-P1-F	CGA TTC AGA GCA GCG TAT TGT TG	Ta.2776-P1-R	AGT TGG TCG GGT CTC TTC TAA ATG
Ta.54227	Ta.54227-P1-F	CAA ATA CGC CAT CAG GGA GAA CAT C	Ta.54227-P1-R	CGC TGC CGA AAC CAC GAG AC

<b>Unigene</b>	<b>Putative <i>Rab</i> name</b>	<b>cDNA product / bp</b>	<b>gDNA product / bp</b>
Ta.35418	<i>RabD1a</i>	122	>122
Ta.47209	<i>RabD1b</i>	141	547/866
Ta.54832	<i>RabD2a</i>	176	1176
Ta.54881	<i>RabD2b</i>	147	1517

**Table 2 – *RabD* primers used in real-time PCR.**  
Sequences are 5' to 3'.

### *3.3.4 Expression of RabD genes in developing wheat endosperm*

In order to determine the native expression of *RabD* genes in the developing endosperm of wild type Cadenza wheat a quantitative real-time PCR was performed (Fig. 3.9). Wheat seeds were harvested at 4, 7, 10, 14, 17, 21, 28 and 35 days post anthesis (dpa) and several samples of total RNA were extracted from each developmental point. The RNA was analysed by spectrophotometry and RNA gel bioanalysis (Fig. 3.8) to determine yield and quality for use in real time PCR.

Primers were designed to amplify a small (~150bp) region of the mRNA coding sequences of four wheat *RabDs* and also produce no PCR product from genomic DNA due to either the primer sequence crossing an intron boundary or a large potential PCR product including introns (Table 1). Three other genes were included in the qPCR as potential normalising genes – an ADP ribosylation factor (Ta.2291), an RNase inhibitor-like gene (Ta.2776) and a gene involved in cell division control (Ta.54227). cDNA was reverse transcribed from total RNA extracted from Cadenza wheat endosperm at 7, 10, 14, 21 and 28 days post anthesis (dpa) with 3 biological replicates (extractions from seeds harvested from separate plants) per time point. Each of the 15 cDNA samples was used as DNA template for each of the seven primer pairs with 2 technical replicates. A calibration curve was also set up for each primer pair using an equal mixture of all cDNA as the undiluted sample, with four 10-fold dilutions. Ta.2776 and Ta.54881 were

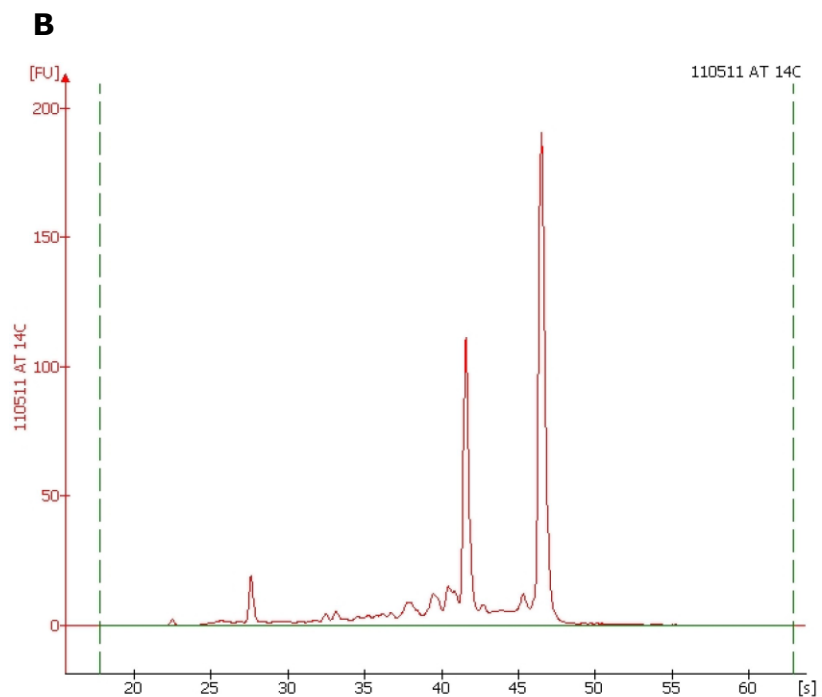
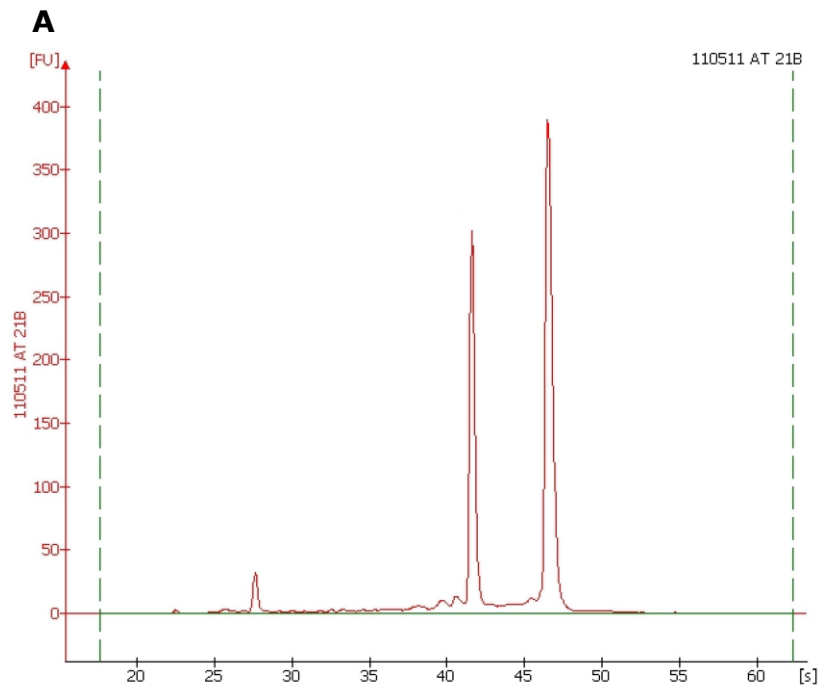


**Fig. 3.8 – Examples of Bioanalyser results from RNA of acceptable quality extracted from developing endosperm of Cadenza wheat.**

A: 21dpa – RNA area: 1005.3; RNA concentration:  $1451\text{ng}\mu\text{l}^{-1}$ ; rRNA ratio (28s:18s): 1.6. B: 14dpa – RNA area: 575.8; RNA concentration:  $831\text{ng}\mu\text{l}^{-1}$ ; rRNA ratio (28s:18s): 2.0.

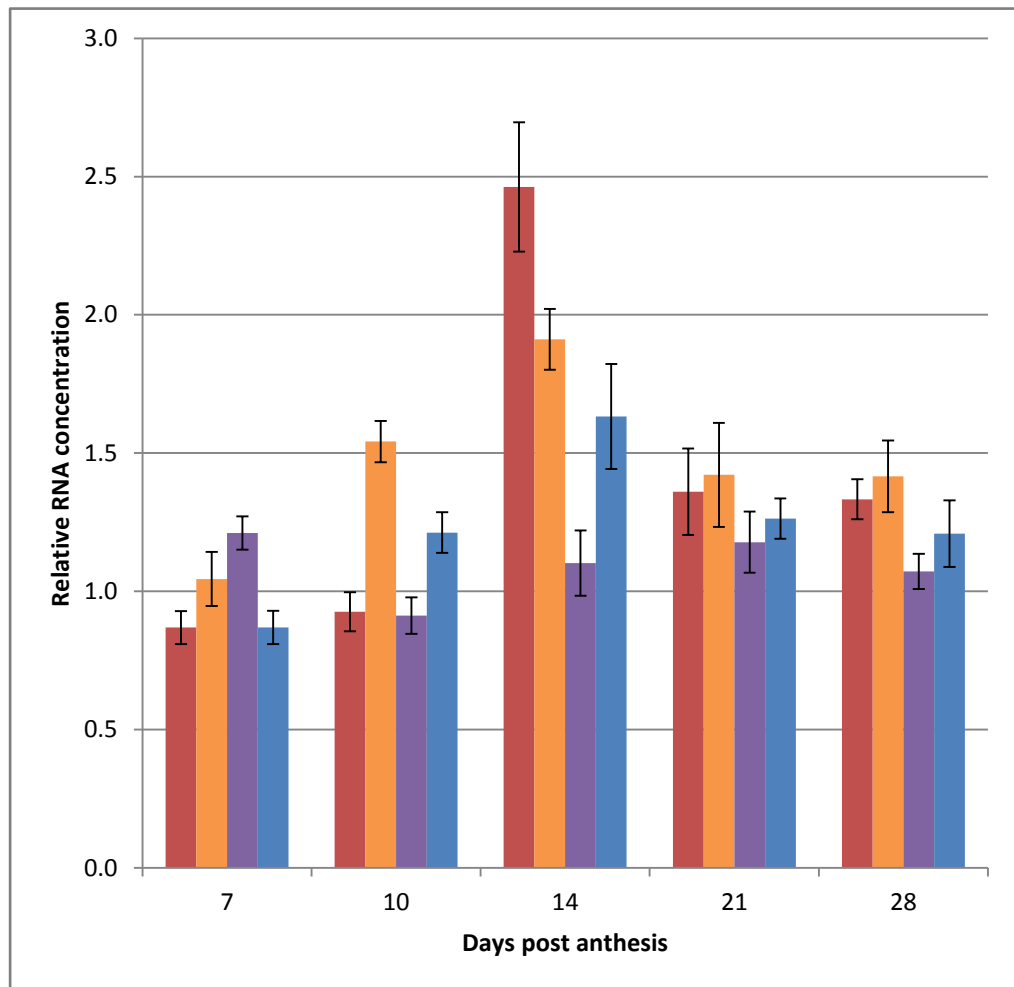


**Fig. 3.9 - Expression of *RabD* genes in the developing endosperm of Cadenza wheat.**

Red bars: Ta.35418 (*RabD1*); Orange bars: Ta.47209 (*RabD1*); Purple bars: Ta.54382 (*RabD2a*); Blue bars: Ta.54881 (*RabD2b*). Expression normalised with Ta.2776 (RNase L inhibitor-like) and Ta.54227 (cell division control) genes. Error bars indicate standard error.

chosen to normalise the RNA concentration data of *RabD* genes together using the average concentration ratios of each sample.

Ta.35418 (*RabD1*), Ta.47209 (*RabD1*) and Ta.54881 (*RabD2*) peaked in expression at 14dpa while *RabD2a* Ta.54382 maintained comparatively stable expression (Fig. 3.9). RNA concentrations at 21 and 28dpa appear similar for each *RabD* gene. This may signify that expression levels have stabilised by 21dpa or possibly that the recycling of mRNA in the endosperm has significantly slowed by 21dpa.

### **3.4 Discussion**

#### **3.4.1 Rab gene sequences**

Wheat has lacked any concerted sequencing projects until recently (Allen *et al*, 2011) meaning little sequence data is available in full, annotated form. When the gene sequences of the four available *RabD* genes were briefly studied, they appeared to each contain 7 introns in the same locations (8.1 Alignment of wheat *RabD* nucleotide sequences). While the coding sequences were highly conserved, the intron sequences varied in both length and sequence, presumably due to lack of selection pressure.

As wheat is hexaploid it might be expected to contain roughly three times the number of *Rab* genes compared to the diploid species it was compared to in phenetic analyses. However, while it was only possible to confidently identify some *Rab* sequences to the subclade level, in BLAST searches and phenetic analyses it appeared that there was never more than one wheat unigene matched with the same homologue in *Arabidopsis*, *Brachypodium* and rice when they were compared together. In fact each wheat Rab protein always had at least one *Brachypodium* or rice homologue that was unique to that wheat protein. Conversely, *Arabidopsis* sequences commonly tended to group together in twos or threes, though this was probably due to its genetic distance from the other species studied. The Rab GTPase profiles in dicots such as *Arabidopsis* have diverged from those of monocots, which include rice, *Brachypodium* and wheat, to allow for differences in development, physiology and cellular functions (Zhang *et al*, 2007).

Of flowering plants that have been sequenced, the Rab21 clade is found only in rice. Some moss and algae species also have *Rab21* genes as well as members from the Rab subfamilies 23, 24 and 28 (Diekmann *et al*, 2011). No *Rab21* unigenes were found in wheat, and the fact that *Rab21* genes are not present in *Brachypodium* suggests that wheat is also unlikely to contain genes from the *Rab21* clade.

### 3.4.2 Rab genes in the wheat genome

The relatively small number yet wide diversity of wheat Rab proteins could be due to the fact that the wheat sequences gathered are in the form of unigenes, which are made up of ESTs. Any ESTs exhibiting high homology are generally grouped into the same unigene, which means it may not be possible to distinguish between different proteins with very similar sequences using only unigene sequence data. Alternatively, homeologous *Rab* genes on different genomes of wheat may be silenced, which would also explain the lack of EST data. It may also be possible that the Rab family of wheat has significantly diversified, though based on the close homology of the amino acid sequences found with those in *Brachypodium* and rice, this appears unlikely.

An interesting clue as to the presence of homeologous *Rab* genes on the three genomes of hexaploid wheat was uncovered when PCR products amplified using Ta.54881 (*RabD2b*) primers with genomic wheat DNA were cloned into a sequencing vector and sequenced (8.1 Alignment of wheat *RabD* nucleotide sequences).

The three sequences that emerged were different, with one matching the CDS of the unigene identically, another very similar but containing a single nucleotide polymorphism (SNP) and the third containing 16 SNPs compared to the unigene CDS. However, when BLAST searched, all three nucleotide sequences were identified as *RabD2b*. This evidence suggests that homeologues of the same *Rab* gene may well be present on the three genomes of wheat, though whether they are expressed or not is unknown. Additionally, if they are expressed they may be largely functionally redundant, though it is possible that some clades may have diversified to perform a different set of roles as has happened in other plant species (Saito & Ueda, 2009; Zhang *et al*, 2007).

The number of total wheat *Rab* unigenes collected was 32, while the total number of *Brachypodium Rab* genes is 40 and in rice is 46. The 32 Rabs found in wheat might represent the total number expressed, though it is likely that this number only represents a portion of the total number of actual genes. This suggestion is based on the fact that wheat is hexaploid, alongside the sequencing results of three PCR products from wheat DNA that were highly conserved but non-identical, all of which represented the same *Rab* homologue (*RabD2b*).

The future output of wheat genome sequencing projects (Allen *et al*, 2011) will permit more thorough investigation of the *Rab* GTPases in wheat and answer questions regarding the number and locations of *Rab* genes in the hexaploid genome.

## **4 Cloning of vector construct, transformation and screening of transgenic wheat**

### **4.1 Introduction**

#### *4.1.1 The RNA interference technique*

RNA interference (RNAi) (Fire *et al*, 1998) can ectopically decrease the expression of a target gene and has been effectively utilised in strategies to demonstrate gene function (Hirai & Kodama, 2008). RNAi reduces target gene expression by a sequence-specific process and is a conserved mechanism throughout a wide variety of eukaryotes (Grewal & Moazed, 2003; Kato *et al*, 2005).

RNAi is effectively induced by double stranded RNA (dsRNA) which may be presented to the cell by different methods. Direct introduction of dsRNA into mammalian, nematode and *Drosophila* cells is sufficient to trigger RNAi, although the effect is not permanently heritable (Svoboda, 2004). Plant cells are transformed with a plasmid vector that generates hairpin RNA molecules in order to produce a heritable RNAi effect. RNAi is regularly used in plants, one example involved the introduction of an RNAi construct into *Arabidopsis* caused silencing of a homeobox gene equivalent to that of the corresponding null mutant (Chuang & Meyerowitz, 2000).

The plant RNAi construct is controlled by a strong promoter and comprises an inverted repeat of the target sequence, which is divided by a spacer fragment. Following transcription of the vector, the inverted repeat sequences anneal to form a dsRNA section (the stem) while the spacer fragment forms the loop of the hairpin RNA

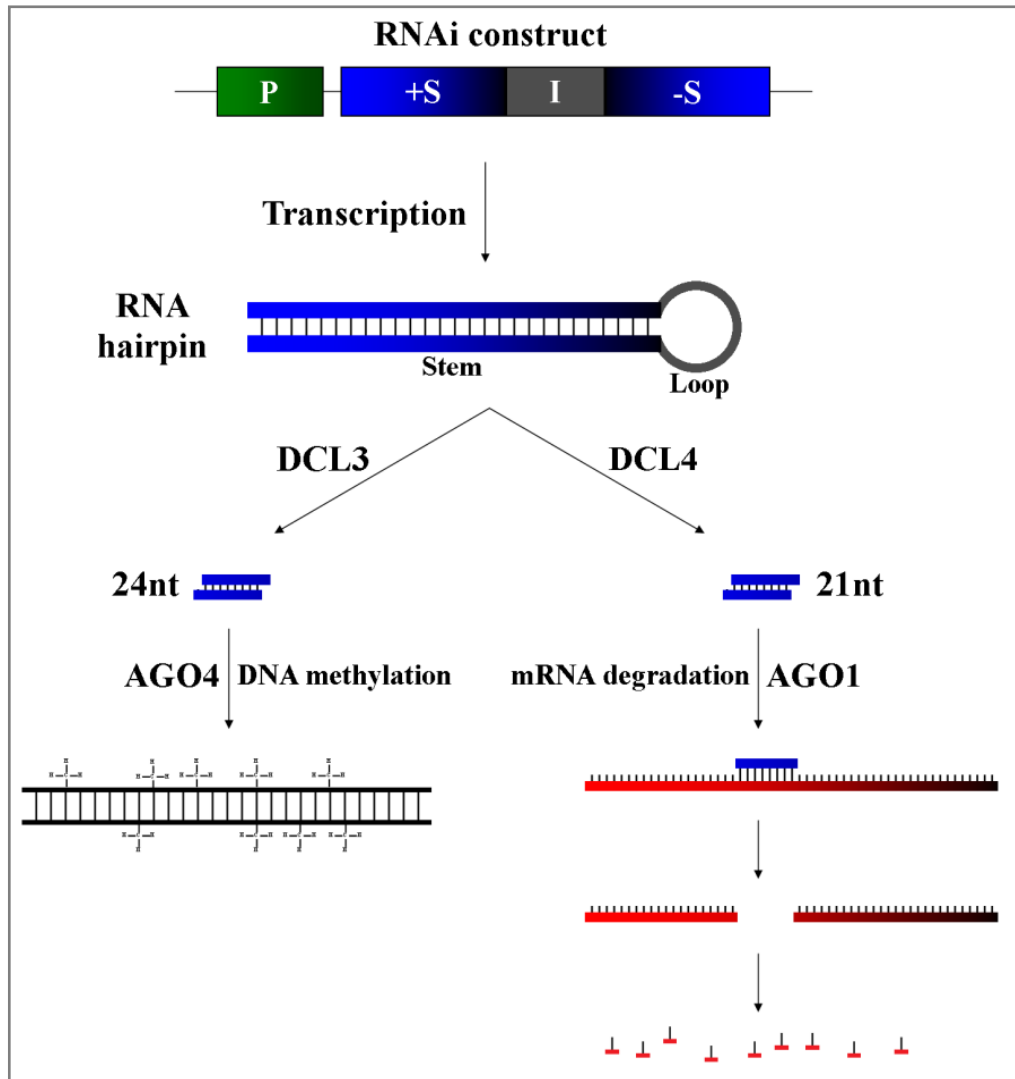


**Fig. 4.1 - Plant silencing pathways induced by an RNAi vector (adapted from Hirai & Kodama, 2008)**

An RNAi construct produces long dsRNAs after transcription. Two distinct DCL (Dicer-like) enzymes process this dsRNA. DCL3 processes dsRNAs into 24-nt long siRNAs (small interfering RNAs) which are incorporated into an AGO4 RISC. DCL4 probably produces 21-nt long siRNAs which combine with an AGO1 RISC. The siRNA incorporated into AGO1 guides the endonucleolytic cleavage of homologous RNA, and siRNAs in AGO4 guide the methylation of cytosine in the complementary genomic sequences. P, promoter; +S, sense-oriented target sequence; -S, antisense oriented target sequence.

structure (Fig. 4.1).

In *Arabidopsis*, one of the four members of the RNase III-like Dicer gene family, often paired with a dsRNA binding protein (dsRBP), recognises dsRNA and generates 21-24 nucleotide long mature micro RNA (miRNA) or small interfering RNA (siRNA) from it. The type of small RNA (sRNA) produced depends on the particular Dicer-dsRBP combination and the dsRNA source (Baulcombe, 2004; Bouche *et al*, 2006; Brodersen & Voinnet, 2006; Curtin *et al*, 2008). Fully matched dsRNA from repetitive DNA sequences, transposons, viruses, endogenous antisense gene pairs or transgene-encoded hairpins generates siRNA when processed by Dicer (Pontier *et al*, 2005; Schwarz *et al*, 2003). Alternatively, Dicer will produce miRNA upon interaction with partially complementary endogenous non-coding mRNA which forms an incomplete hairpin (Nakano *et al*, 2006). Once processed, a mature miRNA or siRNA is incorporated into the RNA-induced silencing complex (RISC) to guide sequence-specific gene silencing (Brodersen & Voinnet, 2006).

RISC is made up of a number of proteins and is thought to be located in the P-body (an RNA degradation centre in the cytoplasm) (Parker & Sheth, 2007). Along with Dicer, other proteins found in RISC include members of the dsRNA binding (dsRBP) and Argonaute (AGO) gene families. The enzyme in RISC that cleaves targeted mRNA is known as a slicer, Argonaute 1 (AGO1) being the principal slicer involved in RNAi in plants (Baumberger & Baulcombe, 2005).

RNAi exploits similar cellular mechanisms to post-transcriptional gene silencing using sense and antisense RNA (Ecker

and Davis, 1986; Hamilton *et al*, 1990; Smith *et al*, 1988; Van Der Krol *et al*, 1988). The difference being that the positive- and/or negative- sense RNA produced in the transgenic plant is copied by RNA-dependant RNA polymerase (RDR) to form dsRNA before being processed into siRNA (Baulcombe, 2005), whereas with RNAi the hairpin RNA molecule produced does not require RDR and may be processed into siRNA directly.

A wheat *Rab* gene was chosen as a target for knockdown by RNAi based largely on evidence of its function from the literature. A target region of the CDS containing a match with the most closely related *Rab* gene was amplified and ligated with an RNAi vector, which was used to transform wheat. PCR was used to screen successfully transformed T0 plants and determine zygosity of T1 plants.

## **4.2 Materials and Methods**

### *4.2.1 cDNA synthesis using specific primers*

The method was adapted from Parr *et al* (1992). Total wheat RNA from 14dpa endosperm (10µl) was added to 4µl of each of the forwards and reverse primers for the RNAi target (a 270bp section of Ta.54382 CDS) and 12µl of DEPC-treated water in a 0.2ml PCR tube. Half the mixture (15µl) was transferred to a second 0.2ml tube and both tubes were incubated at 70°C for 5 minutes before being placed on ice.

A 10µl volume of M-MLV RT buffer x5 was added to a 0.5ml centrifuge tube followed by 3µl dNTPs, 1µl RNasin, 2µl M-MLV reverse transcriptase and 4µl DEPC-treated water (reagents from Promega). Half of this reaction mixture (10µl) was transferred to each of the two RNA/primer mixes on ice. The two PCR tubes were then incubated at 42°C for 1 hour before adding 75µl of DEPC-treated water to each.

RT enzyme, buffer, RNasin RNase inhibitor and dNTPs were supplied by Promega.

### *4.2.2 Reverse transcriptase polymerase chain reaction (RT-PCR)*

RT-PCR was carried out as standard PCR method but the DNA template used was cDNA synthesised using specific primers.

### *4.2.3 Cloning of RNAi construct*

Bovine serum albumin, calf intestinal alkaline phosphatase,

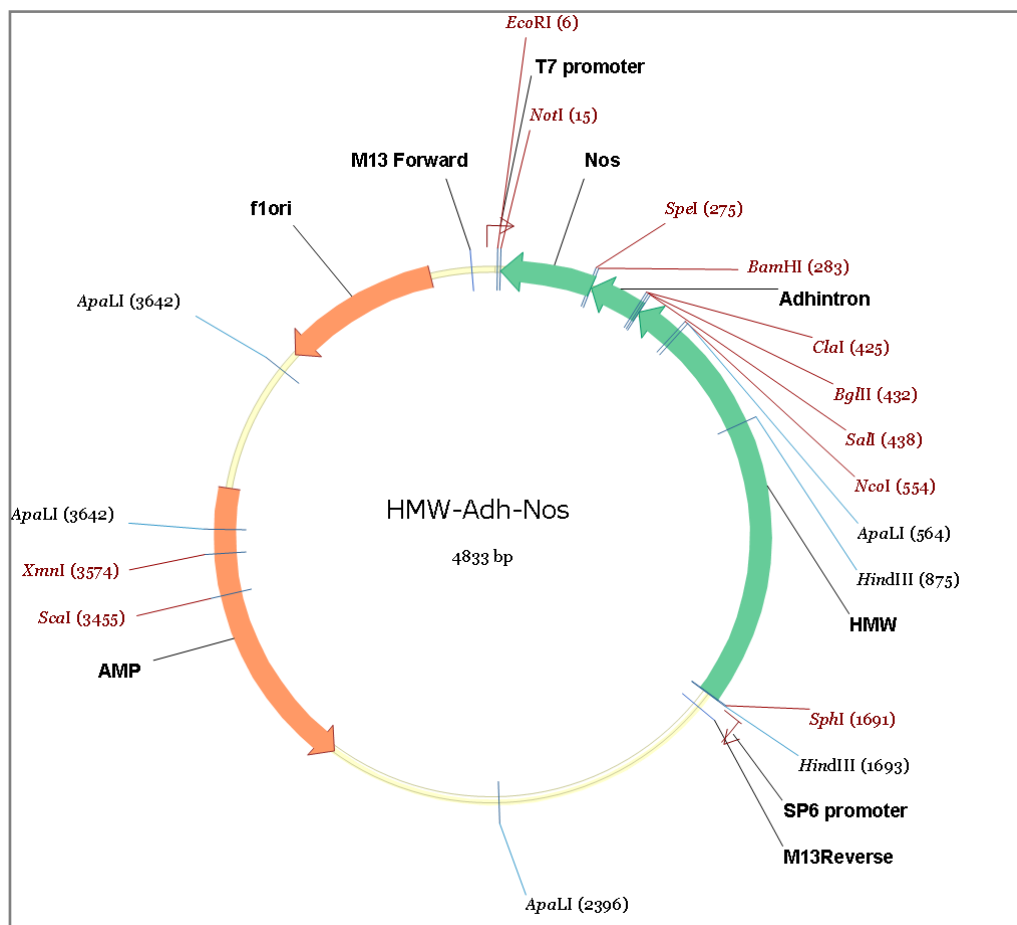


Fig. 4.2 - Vector map of pHMW-Adh-Nos (Nemeth *et al*, 2010).

T4 DNA ligase enzyme and *Bam*HI and *Bgl*II restriction enzymes were acquired from Promega. Vector (pHMW-Adh-Nos) was obtained from Huw Jones at Rothamsted Research (Fig. 4.2). Digestion and ligation of insert and vector were performed using the supplier's instructions. Negative controls used were: no enzyme digest (for both insert and vector digests), no enzyme ligation, no vector ligation, no insert ligation. Competent DH5- $\alpha$  *E. coli* cells were used for transformation. *E. coli* cells were grown in LB+ampicillin medium (Per plate: 10ml sterile LB medium mixed with 10 $\mu$ l 100mgml<sup>-1</sup> ampicillin).

#### 4.2.4 Wild-type wheat growth and seed collection

Wild-type wheat plants (*var.* Cadenza) were sown in 12-well plastic trays (tray: 225x173mm, 70mm deep. 4x3 wells per tray) in John Innes No.3 compost and potted up into 5 litre pots using the same compost. They were grown in glasshouses (glasshouse conditions: venting at 22°C, day heating at 20°C, night heating at 18°C, 16 hour day length, supplemental lighting outside of British Summer Time) at Sutton Bonington campus of University of Nottingham. The date when each ear reached anthesis was noted using the decimal code devised by Zadoks *et al* (1974). Ears were recorded as anthesed when they passed 61 on the decimal code. Seeds were harvested at 4, 7, 10, 14, 17, 21, 28 and 35 days post anthesis (dpa) and frozen in liquid nitrogen before being stored at -70°C. Seeds were dissected to obtain the endosperm after harvesting and before freezing.

#### *4.2.5 Preparation of wheat embryos and gold particles for transformation*

The following method was carried out at Rothamsted Research using materials and method as described by Jones & Sparks (2009). Wheat (Cadenza var.) spikes were collected from growth-room-grown plants approximately 10–12 weeks after sowing and caryopses were removed from the panicles. The caryopses were sterilised by rinsing in 70% (v/v) aqueous ethanol for 5 minutes then soaking in 10% (v/v) Domestos bleach (Unilever UK, Domestos, Freepost ADM1000, London, SW1A 2XX) for 15–20 minutes with occasional shaking. Caryopses were rinsed thoroughly with three changes of sterile water. The sterilized caryopses were kept in moist conditions but not immersed in water.

The embryos were isolated microscopically in a sterile environment and the embryo axis was removed to prevent precocious germination. A number of scutella (25–30) were placed within a central target area of a 9-cm Petri dish containing induction medium, orientating them with the cut embryo surface in contact with the medium. The plates were sealed with Nescofilm (Fisher Scientific) and the prepared donor material was pre-cultured in the dark at 22°C for 1–2 days prior to bombardment.

A 20mg sample of 0.6µm sub-micron gold particles (Bio-Rad) was placed in a 1.5ml microcentrifuge tube along with 1ml 100% ethanol and sonicated for 2 minutes. The tube was pulse-spun in a microfuge for 3s and the supernatant was removed. This ethanol wash was repeated twice more. 1ml of sterile H<sub>2</sub>O was added and

sonicated for 2 minutes before the tube was pulse-spun in a microfuge for 3s and the supernatant removed. This H<sub>2</sub>O wash was repeated. A 1ml volume of sterile H<sub>2</sub>O was added and the gold particles were resuspended fully by vortexing. From this suspension, 50µl was aliquotted into sterile 1.5ml tubes, vortexing between taking each aliquot to ensure an equal distribution of particles. The aliquots were stored at –20°C.

The following procedure was carried out on ice, in a sterile environment. A 50µl aliquot of prepared gold was allowed to thaw at room temperature, and then sonicated for 1–2 minutes and vortexed briefly. A 5µl sample of DNA (1 mg/ml in TE) was added, including the RNAi vector construct and a separate plasmid vector incorporating a selectable marker (bar). The tube was then vortexed briefly to ensure good contact of DNA with the particles. A gold-only control was also prepared with H<sub>2</sub>O instead of DNA. Into the lid of the tube were added 2.5M CaCl<sub>2</sub> (50µl) and 0.1M spermidine (20µl), mixed together, then briefly vortexed into the gold/DNA solution. The tube was then centrifuged in a microfuge at top speed for 3–5s pulse to pellet the DNA-coated particles. The supernatant was discarded and 150µl of 100% ethanol was added to wash the particles, resuspending them as fully as possible. The tube was then centrifuged in a microfuge at top speed for 3–5s pulse to pellet the particles and the supernatant discarded. The pellet was fully resuspended in 85µl 100% ethanol and maintained on ice.

#### *4.2.6 Biolistic transformation of wheat embryos*

The following method was carried out at Rothamsted Research using materials and method as described by Jones & Sparks (2009). DNA-coated gold particles were delivered using the PDS-1000/He particle gun (Bio-Rad) according to the manufacturer's instructions. The following settings were maintained as standard for this procedure: gap 2.5cm (distance between rupture disc and macrocarrier), stopping plate aperture 0.8cm (distance between macrocarrier and stopping screen), target distance 5.5cm (distance between stopping screen and target plate), vacuum 91.4–94.8kPa, vacuum flow rate 5.0, vent flow rate 4.5 (8).

The gun's chamber and component parts were sterilised by spraying with 90% (v/v) ethanol, which was allowed to evaporate completely. The macrocarrier holders, macrocarriers, stopping screens and rupture discs were sterilised by dipping in 100% ethanol and allowing the alcohol to evaporate completely on a mesh rack in a flow hood. The macrocarrier holders were placed into sterile 6cm Petri dishes and one macrocarrier was introduced into each holder. The coated gold particles were briefly vortexed and a 5µl aliquot was dropped centrally onto the macrocarrier membrane. The membrane was allowed to dry naturally, not in the air flow. A rupture disc (650 or 950 psi) was loaded into the rupture disc retaining cap and screwed into place on the gas acceleration tube, tightening firmly using the mini torque wrench. A stopping screen was placed into the fixed nest. The macrocarrier holder containing macrocarrier + gold particles/DNA was inverted and placed over the

stopping screen in the nest and its position maintained using the retaining ring. The fixed nest assembly was mounted onto the second shelf from the top to give a gap of 2.5 cm. A sample was placed on the target stage on a shelf to give the desired distance - the fourth shelf from the top gives a target distance of 5.5cm.

After a vacuum of 91.4–94.8kPa was drawn the gun was fired. After firing, the vacuum was released, the sample was removed and the component parts were disassembled, discarding the ruptured disc and macrocarrier. The macrocarrier holder and stopping screen were placed in 100% ethanol to re-sterilise if they were to be reused in further shots. Otherwise they were placed in 1:10 dilution Savlon (Novartis Consumer Health, West Sussex, UK) to soak. The parts were sonicated for 10 minutes prior to reuse.

#### *4.2.7 Regeneration of T0 transgenic wheat plants*

The following method was carried out at Rothamsted Research using materials and method as described by Jones & Sparks (2009). Following bombardment, the scutella were spread evenly across the medium, dividing each replicate between two or three plates of induction medium (MS 9% 0.5DAg) i.e. approximately 10 scutella per plate. The plates were sealed with Nescofilm and incubated at 22°C in the dark for induction of embryogenic callus.

After 3–5 weeks on induction medium any calli bearing somatic embryos were transferred to regeneration medium (RZDCu) in 9cm Petri dishes and incubated at 22°C in the light for 3–4

weeks. After 3–4 weeks on regeneration medium, calli were transferred to RZ + selection in 9cm Petri dishes with high lids (the selection medium was determined by the selectable marker gene in the transforming plasmid: RZPPT4 for bar or RZG50 for nptII). The plates were sealed with Nescofilm and incubated at 22°C in the light. After a further 3–4 weeks, surviving calli were transferred to regeneration medium + selection but without hormones (RPPT4 or RG50) in 9cm Petri dishes with high lids. The plates were sealed with Nescofilm and incubated at 22°C in the light. Once regenerating shoots were clearly defined and could be separated easily from the callus, they were transferred to regeneration medium + selection but without hormones (RPPT4 or RG50) in GA-7 Magenta vessels, placing no more than 4–6 plantlets per Magenta, then incubated at 22°C in the light.

Plantlets were transferred to soil once a reasonable root system has been established and leaves were approximately 10–15cm. Plantlets were carefully removed from the agar-gel-solidified medium (rinsing the roots with water if necessary to remove excess agar-gel) then potted into 8cm square plastic pots (Nursery Trades, (Lea Valley) Ltd.) using “Rothamsted prescription mix” compost (Petersfield Products, Leicestershire, UK). Plantlets were placed within a propagator to provide a high humidity for 1–2 weeks to acclimatize them from tissue culture, and grown in a GM containment glasshouse (16 hour day, 20°C day, 15°C night, automatic supplementary lighting turning on when natural daylight falls below  $300\mu\text{mol m}^{-2} \text{s}^{-1}$  and switching off when rising above

400 $\mu\text{mol m}^{-2} \text{s}^{-1}$ ). Typically it took at least 3 months from bombardment to potting into soil. Once suitably established (3–4 leaves), a leaf sample was taken from which to extract genomic DNA for analysis by PCR to establish whether the plant was transformed. Once confirmed PCR positive, the transformed plants were re-potted to 13cm diameter pots (Nursery Trades (Lea Valley) Ltd.) and grown under the same glasshouse conditions. Plants reached maturity in 3–4 months, at which point the grain was harvested from each plant separately.

#### *4.2.8 PCR screening of T0 plants for transgene*

DNA was extracted using a Promega wizard genomic DNA purification kit following the manufacturer's instructions.

Each 20 $\mu\text{l}$  PCR reaction contained 18 $\mu\text{l}$  PCR ReddyMix Master Mix (ABgene Limited (UK Head Office), Abgene House, Blenheim Road, Epsom, KT19 9AP, United Kingdom), 0.3 $\mu\text{l}$  of forward primer (20 $\mu\text{M}$ ), 0.3 $\mu\text{l}$  of reverse primer (20 $\mu\text{M}$ ), 1 $\mu\text{l}$  of DNA template and was made up to 20 $\mu\text{l}$  with sterile distilled H<sub>2</sub>O.

The PCR program for the first round of screening was as follows: 94°C for 5 minutes, 57°C for 30 seconds, 72°C for 2 minutes, 30x [94°C for 1 minute, 57°C for 30 seconds, 72°C for 2 minutes + 3 second ramp], 72°C for 10 minutes. The PCR program for the second round of screening was the same except annealing temperature was 60°C instead of 57°C.

#### *4.2.9 96-well plate DNA extraction*

A single 3mm stainless steel ball was added to each well of a 96-well collection plate containing leaf samples. A 600µl volume of DNA extraction buffer (200mM Tris-HCl (pH8), 250mM NaCl, 25mM EDTA (pH8), 0.5% SDS) was added to each well and the plate was shaken in a ball mill for 3 minutes. The plate was then spun in a plate centrifuge at 5600g for 20 minutes and 250µl liquid transferred from each well of the collection plate to the corresponding well in a storage plate to which had been added 250µl isopropanol per well. The storage plate was sealed and incubated for 3 minutes at room temperature followed by a spin of 5600g for 20 minutes in a plate centrifuge. The supernatant was then removed by aspiration and 100µl of 70% ethanol added, followed by mixing by robot for 5 minutes and another spin at 5600g for 20 minutes. The supernatant was removed by aspiration and the plate was vacuum dried. The pellets were resuspended in TE buffer at 4°C for 2 hours then stored at -20°C.

#### *4.2.10 96-well plate to 1.5ml tube DNA extraction*

A single 3mm stainless steel ball was added to each well of two 8-well strips containing leaf samples on an otherwise empty 96-well collection plate. A 600µl volume of DNA extraction buffer (200mM Tris-HCl (pH8), 250mM NaCl, 25mM EDTA (pH8), 0.5% SDS) was added to each well and the plate was shaken in a ball mill for 3 minutes. The liquid was transferred from each well of the collection plate to 1.5ml microcentrifuge tubes (1 per well). The

tubes were centrifuged at 16,200g (13,000 rpm) for 5 minutes and 500µl of the supernatant was transferred to fresh 1.5ml tubes. A 500µl volume of isopropanol was added to each tube before mixing the tubes by inversion and incubating at room temperature for 5 minutes. The tubes were then centrifuged at 16,200g (13,000 rpm) for 5 minutes before decanting off the supernatant. The pellets were washed with 1ml 70% ethanol, using a pipette tip to dislodge the pellet, vortexed and centrifuged at 16,200g (13,000 rpm) for 5 minutes. The supernatant was decanted off and the pellet was washed with 150µl 100% ethanol, vortexed then centrifuged at 16,200g (13,000 rpm) for 5 minutes. The supernatant was removed by pipette and the pellet was washed with 150µl 70% ethanol, vortexed then centrifuged at 16,200g (13,000 rpm) for 5 minutes. The supernatant was removed by pipette and the pellet was vacuum dried for 5-10 minutes before resuspending in 0.1x TE buffer at 4°C for 2 hours, then storage at -20°C.

#### *4.2.11 Transgene screening PCR to eliminate null and hemizygous T2 lines*

Seeds were sown in four 308-well trays in Levington M2 potting compost (Scotts, 14111 Scottslawn Road, Marysville, OH 43041, USA) and grown for 2 weeks in a glasshouse at Sutton Bonington (16 hour day, 22°C day, 20°C night, automatic supplementary lighting during daytime). A leaf sample was then taken from each plant and placed in ten 96-well collection plates which were stored at -20°C. Genomic DNA was extracted from all

the leaf samples using a 96-well plate DNA extraction or a 96-well plate to 1.5ml tube DNA extraction.

## **4.3 Results**

### *4.3.1 Single target Rab strategy*

With the aim of altering ER to Golgi traffic, the planned approach was to select a gene from the *Rab* family to knock down using RNAi. The minimum length of small interfering RNA (siRNA) employed in RNAi is 21 nucleotides. The target sequence must not have matches of this length or more with genes that are not being targeted for RNAi. However, as close relatives within the same clade or subclade can have similar functions, matches of this kind with those genes could be desirable. The ability of RNAi to knock down all seven members of the *OsRac* gene family simultaneously in transgenic rice was described by Miki *et al* (2005). Knockdown of multiple similar genes could ultimately produce a greater and/or more noticeable effect in the transformed organism.

As the Rab D subfamily of GTPases mediates the vesicle transport pathway of interest (ER to Golgi), coding sequences of the four available *RabD* members were aligned and compared in pairs to find regions of identity of 21nt or more (Fig. 4.3A). With a view to using a region of *RabD2a* (Ta.54382) as the target sequence, it was compared to each of the other wheat *Rab* coding sequences available. No matches of significant ( $\geq 21$ nt) length were found outside the *RabD* clade.

### *4.3.2 RabD consensus strategy*

As an alternative approach to selecting a single *Rab* gene as a target for RNAi, a consensus sequence was produced using coding

**A**

1	Ta.54382-Wheat-Rab_D2a	TGGAGAGT	TATATCAGTACTATTGGTGTGA	TTTCAAATACGTACCGTG	150
	Ta.54881-Wheat-Rab_D2b	TGGAGAGC	TATATCAGTACTATTGGTGTGA	CTTCAAATCCGCACCGTT	150
		*****	*****	*****	*****
2	Ta.54881-Wheat-Rab_D2b	AGAGCGATTTAGG	ACCATCACAAGCAGCTACTACCG	CGGTGCCCATGGCA	250
	Ta.35418-Wheat-Rab_D	GGAGCGGTCAGA	ACCATCACAAGCAGCTACTACCG	GAGGAGCTCACGGGA	250
		*****	*****	*****	*****
3	Ta.35418-Wheat-Rab_D	CTCGAGATGGATGGGAAGACCATCAAAT	TGCAGATTTGGGACACAGCAGG		197
	Ta.47209-Wheat-Rab_D	GTTGAGCTCGATGGCAAGTCGGTGAAGC	TGCAGATTTGGGACACAGCAGG		200
		* * * * *	*****		*****

**B**

<u>CGTCGGCAAGTCTGCCTCCTCCTCAGATTTGCCGATGATTCGTACCTGG</u>	50
<u>AGAGCTATATCAGTACTATTGGTGTGATTTCAAATCCGCACCGTTGAG</u>	100
<u>CAAGATGGGAAGACGATGAAGCTGCAAATTTGGGACACTGCTGGACAAGA</u>	150
<u>ACGGTTCAGAACCATCACAAGCAGCTACTACCGAGGAGCTCACGGGATCA</u>	200
<u>TTATTGTCTATGACGTGACAGACCAGGAGAGCTTCAACAATGTCAAGCAG</u>	250
<u>TGGTTGA</u>	257
Consensus match key	
<u>ATGC</u> Ta.35418	<u>ATGC</u> Ta.54382
<u>ATGC</u> Ta.47209	<u>ATGC</u> Ta.54881

**Fig. 4.3 – Results of *RabD* CDS alignments to find ≥21nt matches.**

A: Sections of alignments between wheat *RabD* coding sequences. Matches marked with \* and ≥21nt matches highlighted in yellow. B: Proposed target region of *RabD* consensus sequence showing ≥21nt matches with *RabD* CDS underlined.

sequences of the four wheat *RabD* members (Ta.35418, Ta.47209, Ta.54382 and Ta.54881,). As small interfering RNA (siRNA) is between 21 and 25 nucleotides in length, all matches of 21 nt or more with the RNAi target sequence could produce a knockdown effect on the matching gene (Xu *et al*, 2006). All wheat *Rab* coding sequences were compared to the *RabD* consensus to predict the effect on each of using RNAi with the consensus as the 'target' sequence (Fig. 4.3 B). Ta.35418 (*RabD1*) had 2 matches in the range 205-302 nt of the consensus of 50 and 24 nt length. Ta.47209 (*RabD1*) gave 2 matches of 25 and 28 nt within the range 54-310 nt of the consensus. Ta.54382 (*RabD2a*) had 3 matches of 32, 41 and 28 nt between nucleotides 109 and 539 of the consensus. Ta.54881 (*RabD2b*) had 4 matches of 29, 32, 38 and 23 nt with the consensus between 13-236 nt. Outside the *RabD* subfamily, there was a region of the consensus that gave a significant match with the *RabA* members Ta.36757, Ta.7600, Ta.54911 and Ta.55676. The match varies in length but in each case it ends at the same nucleotide (nt 66 of the consensus).

The aim is to affect vesicle trafficking only from the ER to the Golgi. Down-regulating genes that affect other pathways in the vesicle transport system could produce unwanted effects. Therefore a target sequence had to be selected from within the consensus that would have the RNAi effect on *RabD* members but not those of other clades. The nt range 54-310 of the consensus was chosen (Fig. 4.3 B) as it misses out most of the *RabA* match (only 13 nt of the match is within the selected region, which is insufficient to produce siRNA)

and includes most of the matches from the *RabD* subfamily. If this sequence was cloned into the RNAi vector as the 'target' sequence it could theoretically create an RNAi effect on at least the 4 known *RabD* genes in wheat.

#### 4.3.3 RNAi target region selection and PCR primer design

As shown in Fig. 4.4, the target region chosen within the Ta.54382 (*RabD2a*) CDS includes the 23nt match with Ta.54881 (*RabD2b*). The target region is 270 nucleotides in length from nt 55 to 324 of the Ta.54382 CDS. The RabD2a-F and RabD2a-R primers were designed to amplify this region and the RabD2a+Bam-F and RabD2a+Bgl-R primers were designed to add restriction sites onto the ends of the resulting PCR product (Fig. 4.5). The purpose of this is the ability to cut the ends of the PCR product using the restriction endonucleases *Bam*HI (site: GGATCC) and *Bg*II (site: AGATCT). Once digested, the target region may be ligated with the RNAi vector pHMW-Adh-Nos.

#### 4.3.4 PCR to amplify RabD2a target region

Primers were designed to amplify and add restriction enzyme sites onto the ends of a region of a known wheat *RabD2a* unigene (Ta.54382) and PCR experiments were performed. Fig. 4.6 shows the results of a PCR with a steep gradient of annealing temperatures using DNA extracted from wheat leaf and a pair of primers designed to amplify a 457bp region of Ta.54382 (*RabD2a*). No product was produced in lanes 4-12 but a band of approximately 1.4 kilobases is

```

ATGAATCCGGAGTATGACTATCTCTTTAAGCTTCTGCTTATCGGAGACTC 50
AGGTGTTGGCAAGTCATGCCTTCCTTAAGATTTGCCGATGACTCGTACC 100
TGGAGAGTTATATCAGTACTATTGGTGTGATTTCAAATACGTACCGTG 150
GAGCAAGATGGAAAGACTATGAAGCTGCAAATCTGGGACACTGCTGGGCA 200
AGAACGCTTCAGAACTATTACTAGCAGCTACTATCGAGGGGCTCACGGGA 250
TCATTATTGTCTATGACGTGACAGACCAGGACAGCTTCAACAATGTGAAG 300
CAGTGGTTGAACGAGATTGATCGCTATGCTAGTGAGAATGTTAACAAGCT 350
TCTTGTAGGGAACAAATCTGATCTCACTGACAAAAGAGTTGTATCATATG 400
AGACAGCGAAGGCATTTGCTGATGAGATTGGCATCCCATTCATGGAGACC 450
AGTGCAAAGAATGCCTTGAACGTTGAGCAGGCTTTCATGGCTATGTCTGC 500
TTCAATCAAGGACAGGATGGCGAGCCAGCCAGCCGAAACAGCGCTCGCC 550
CAGCCACGGTGCAGATCCGCGGGCAACCTGTGGAACAGAAGACGAGCTGC 600
TGCTCTTCT 609

```

**Fig. 4.4 – The Ta.54382 (wheat *RabD2a*) coding sequence showing selected target region.**

The 270bp target region is highlighted in yellow, with forward and reverse primer regions shown in green and cyan respectively. The 23nt match with Ta.54881 (*RabD2b*) is highlighted in dark blue.

RabD2a primer F: GTTGGCAAGTCATGCCTTC  
RabD2a primer R: GCGATCAATCTCGTTCAACC

RabD2a+Bam primer F: CTTAAGGATCCGTTGGCAAGTCATGC  
RabD2a+Bgl primer R: GGCCAAGATCTGCGATCAATCTCGTT

**Fig. 4.5 - Primers designed to anneal to the target sequence in PCR.**

The parts of the RabD2a+Bam-F and RabD2a+Bgl-R primers that match the gene (green/blue) are preceded by a restriction site (red/pink), plus extra nucleotides to ensure efficient restriction. RabD2a+Bam-F contains a *Bam*HI site and RabD2a+Bgl-R contains a *Bgl*II site.

visible in the 3 lanes with the lowest annealing temperatures (lanes 1-3). When the three visible bands were cut from the gel, purified and sequenced, it transpired that the size of the band was due to the presence of 4 introns within the target region of DNA ("Ta.54382 part gene 1 (PCR)" in 8.1 Alignment of wheat *RabD* nucleotide sequences). The likely reason the bands only appeared at lower PCR annealing temperatures was that the extension time was effectively increased to the length necessary for the longer-than-expected DNA molecule to fully polymerise due to the extra time required to change the temperature of the PCR tubes.

In order to obtain the target sequence without introns, a reverse transcription PCR (RT-PCR) was performed. Two new pairs of primers were designed (Fig. 4.5) – one to amplify a 270bp region of Ta.54382 containing a 21nt match with Ta.54881 (RabD2a-F & RabD2a-R) and another to add restriction sites (*Bam*HI and *Bgl*II) to the ends of the PCR product of the first primer pair (RabD2a+Bam-F & RabD2a+Bgl-R). RNA was extracted from developing Cadenza wheat endosperm (28dpa) and reverse transcribed to cDNA using the primer RabD2a-R. This cDNA was used as the template DNA in a gradient PCR using the RabD2a-F and RabD2a-R primers (Fig. 4.7). Bands of the expected size were obtained on agarose gel. The bands were excised from the gel and sequenced to confirm they were the expected product. To add the restriction sites onto the target region, the PCR product was used as the template in a new PCR together with the RabD2a+Bam-F and RabD2a+Bgl-R primers. The product of this PCR was then cloned into RNAi vector pHMW-Adh-Nos.

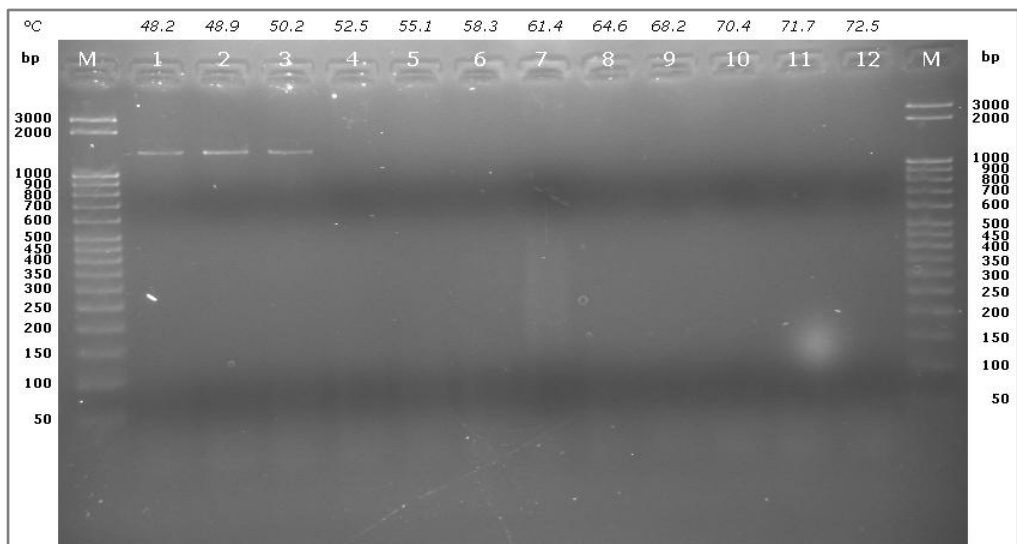


**Fig. 4.6 - Gradient PCR results.**

Annealing temperature of PCR reaction shown above each lane. Wheat DNA and original primers used.

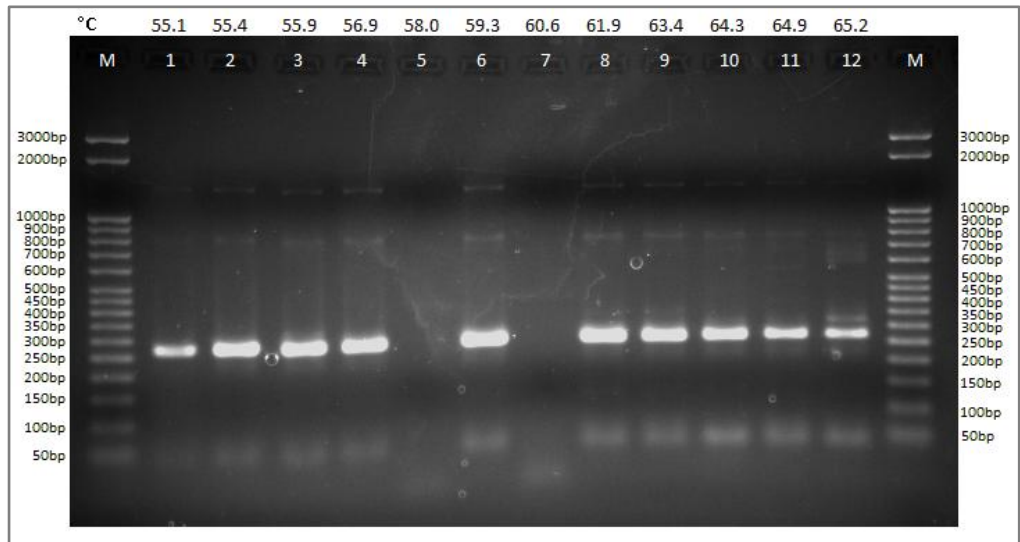


**Fig. 4.7 - Gradient RT-PCR results.**

Annealing temperature of PCR reaction is shown above each lane. Bands are between 250 and 300bp, concurrent with expected product size of 270bp.

#### 4.3.5 Cloning of RNAi vector construct

A sample of the pHMW-Adh-Nos vector to be used in the completed construct was used to transform competent *E. coli* cells. The bacteria were screened with ampicillin for colonies that had taken up the vector. Following liquid culture of individual screened colonies, vector plasmid was obtained from the *E. coli*.

The cloning strategy (Fig. 4.8) to produce the inverted repeat required was to cut the insert with both *Bam*HI and *Bgl*II enzymes to give a *Bam*HI sticky end at the 5' end and a *Bgl*II sticky end at the 3' end. Digestion of the insert (270bp region of Ta.54382) and vector (pHMW-Adh-Nos) were performed with *Bam*HI and *Bgl*II for the insert digestion, and *Bam*HI for the vector digestion. The digestion mixes were then run on agarose gel and the digested insert and linear vector were extracted. The digested insert and vector were then ligated together. The *Bgl*II sticky end of the insert was expected to ligate with a *Bam*HI sticky end on the vector as the two sites share the same overhang (GATC). This combined site should then become immune to both restriction enzymes. The ligated construct (vector + 1 insert) was used to transform competent DH5- $\alpha$  *E. coli* cells. A colony screening PCR was then performed (Fig. 4.10), in which 2 combinations of primers were used for each of 24 colonies to determine insert presence and number (1 insert = pass). Plasmid was obtained from colonies that appeared to have ligated correctly. They were then further screened using 6 different PCR primer combinations for each to confirm results and determine insert orientation (Fig. 4.11). Two colonies

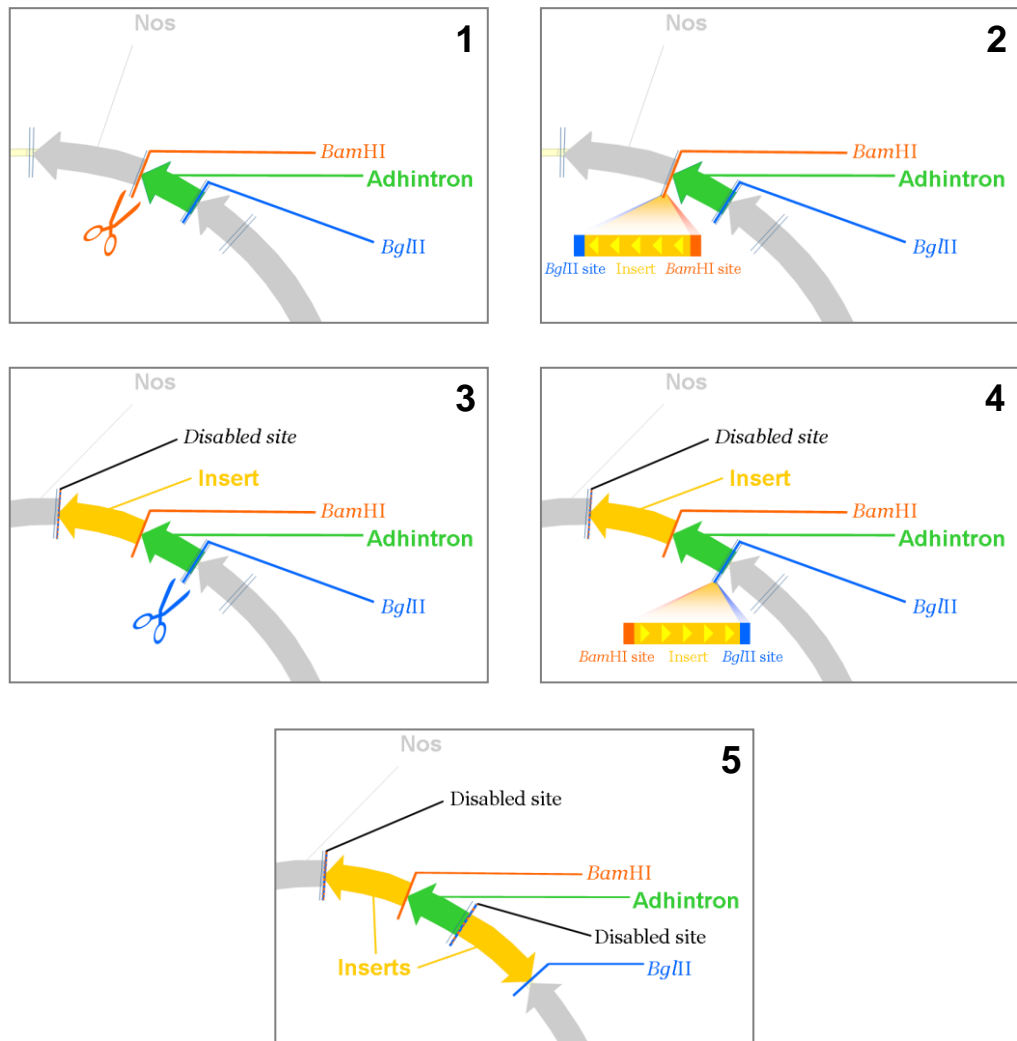


**Fig. 4.8 – Vector cloning strategy.**

1. Vector digested using *Bam*HI restriction enzyme; 2. Insert that has been digested with both *Bam*HI and *Bgl*II is ligated with the vector; 3. Vector is digested using *Bgl*II restriction enzyme; 4. Second insert is ligated with the vector; 5. Completed constructs are screened to obtain those that have successfully incorporated 2 inserts in opposite orientations.

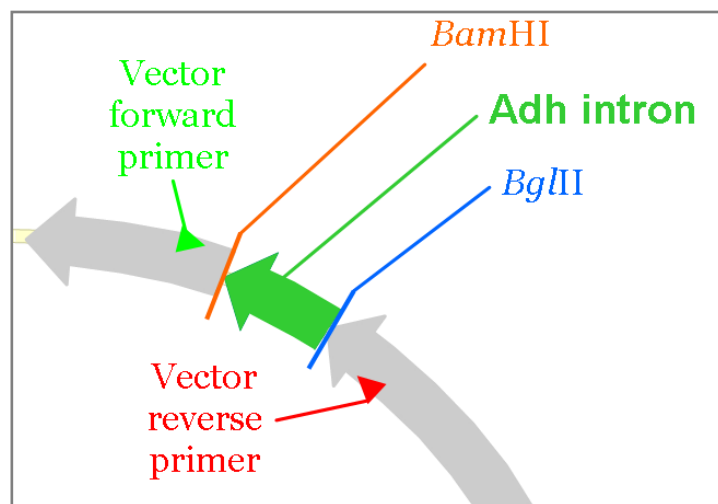


**Fig. 4.9 - Placement and orientation of vector primers used in cloning colony screening.**

(containing insert in two different orientations) were selected for the second round of cloning.

The two positive colonies selected were cultured in selective medium and the vector was obtained from each. These vectors were digested a second time using *Bgl*/II restriction enzyme and ligated with the insert. The ligated constructs were used to transform competent DH5- $\alpha$  *E. coli* cells. A colony screening PCR was performed with 2 primer combinations used for each of 24 colonies to determine insert presence and number (2 inserts = pass). Vector was obtained from colonies that ligated correctly. They were then further screened using six different PCR primer combinations for each to confirm correct insert number and determine orientation of inserts. Based on this screen one colony was selected to be sequenced to confirm PCR results before being used to transform Cadenza wheat by Amanda Riley at Rothamsted Research.

#### *4.3.6 Screening of T0 plants for transgene*

To select the T0 plants that had been successfully transformed, a PCR screen was performed by Caroline Sparks at Rothamsted Research. DNA was extracted from leaf samples taken from the T0 plants once they were suitably established (3-4 leaves). These DNA samples were used as the DNA template for a series of PCR experiments. Two sets of experiments were performed for each DNA template to be screened. The first used primers for the bar selectable marker gene that the transgene was co-transformed with (Bar 1: 5'-GTC TGC ACC ATC GTC AAC C-3'; Bar 2: 5'-GAA GTC CAG

CTG CCA GAA AC-3'). The second used primers from the RNAi vector construct (see Fig. 4.9) in two different combinations – Rab1 and Adh3'rev to amplify from the promoter through the first insert to the intron (Rab1: 5' CAC AAC ACC GAG CAC CAC AAA CT 3' Adh3'rev: 5' TGG AAA ACA CGG GAG TCT GCC 3'), and Adh5'fwd and Nos3'rev to amplify from the intron through the second insert to the terminator (Adh5'fwd: 5' GAA TCG ATC TGG GAG GCC AAG G 3'; Nos3'rev: 5' ATC GCA AGA CCG GCA ACA GG 3').

The PCR products were run on an agarose gel to determine positive or negative results. Of those T0 plants that gave positive results for both the bar selectable marker gene and the RNAi vector construct, 15 independent transformants were selected to be grown on in the next generation, along with one transformant that was positive for the bar gene but negative in both RNAi construct PCRs, as a selectable-marker-only control (henceforth known as "bar-only control").

These 16 T0 plants were grown in a glasshouse until maturation at which point they were harvested. Twelve seeds from each plant were sown and these 192 T1 plants were grown in a glasshouse and harvested at maturity. T1 seeds were also used in SDS-PAGE (see 5.3.1 Protein analysis of grain from T0 plants).

#### *4.3.7 Transgene screening PCR to eliminate null and hemizygous lines from T1 plants*

Mature T2 seeds were harvested from 192 T1 plants. Five seeds from each plant were sown and leaf samples taken from the

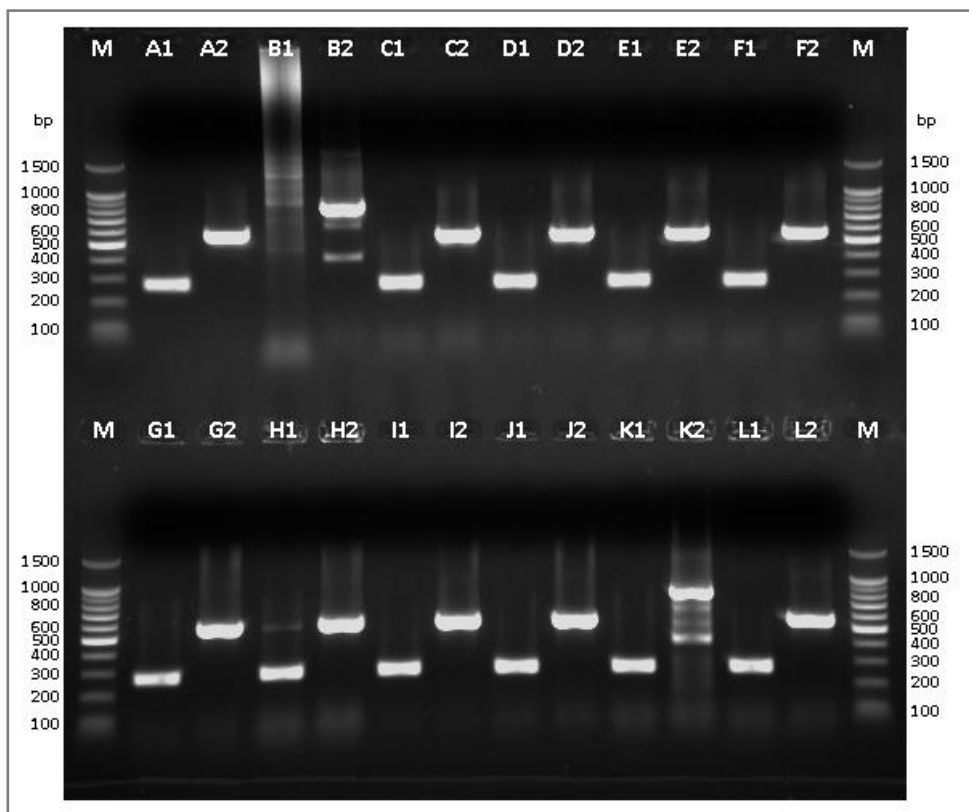


**Fig. 4.10 - Example of results of the first round colony screening PCR.**

Primers: #1 lanes = RabD2a-F and RabD2a-R (determines presence of insert); #2 lanes = Vector-F and Vector-R (primers designed to bind to the vector either side of the insert sites). A positive result is shown by a 270bp band in #1 and an 834bp band in #2 (e.g. K).

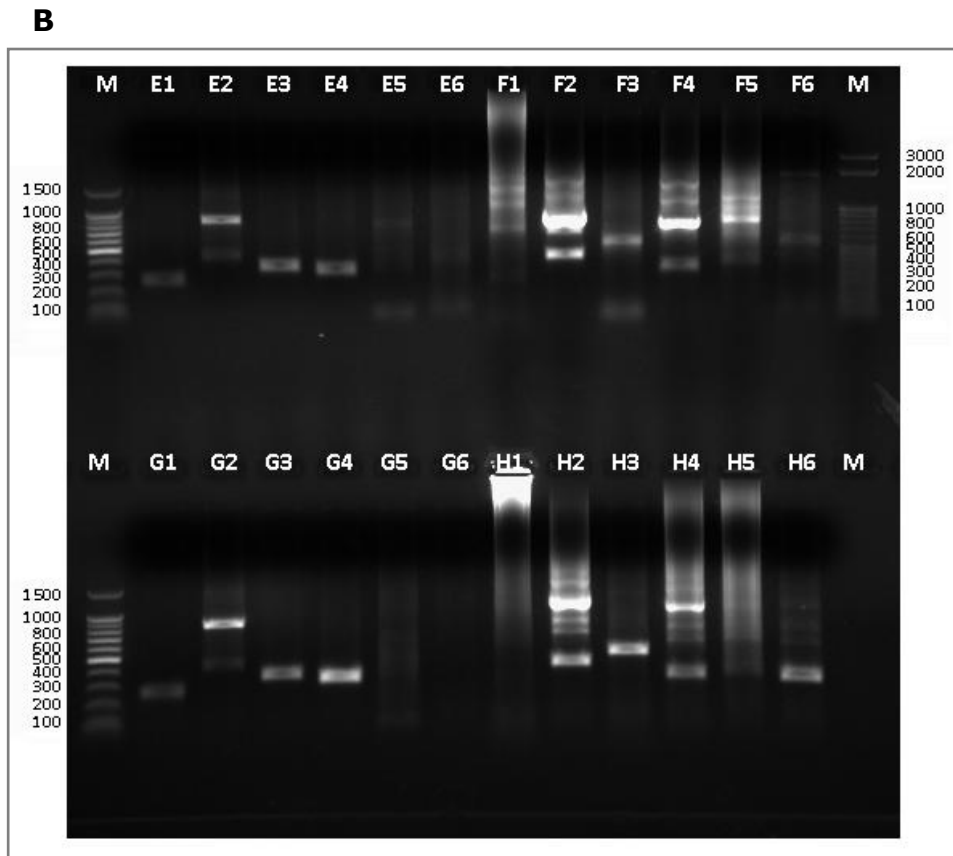
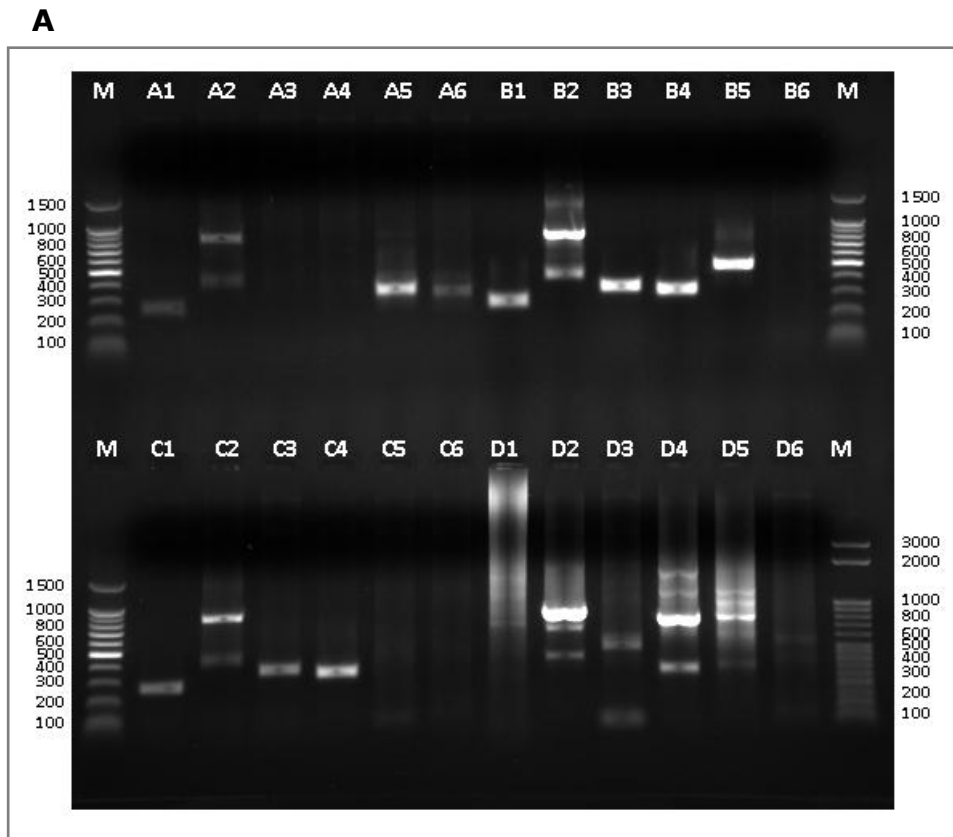


**Fig. 4.11 - Results of the second round colony screening PCR.**  
 Primers: #1 lanes = RabD2a-F and RabD2a-R (determines presence of insert); #2 lanes = Vector-F and Vector-R (primers designed to bind to the vector either side of the insert sites); #3 lanes = RabD2a-F & Vector-F; #4 lanes = RabD2a-F & Vector-R; #5 lanes = RabD2a-R & Vector-F; #6 lanes = RabD2a-R & Vector-R. A positive result is shown by a 270bp band in #1, an 834bp band in #2, then a 351bp band in #3 and 328bp band in #4 (i.e. B, C, E, G) or those two bands in #5 and #6 instead (i.e. A).

seedlings for DNA extraction. PCR was then used to determine which plants carried the transgene using 2 primer combinations – a control pair that targets a non-coding region of Ta.47209 and a transgenic pair that amplifies a part of the construct. Seedlings that showed bands of expected size in the control lane and the transgenic lane were recorded as transgene positive, while those that only showed a band in the control lane were recorded as transgene negative. Any other combinations of bands were discounted. Lines that had five positive seedlings were thought to be probably homozygous rather than hemizygous (76% likelihood based on 3:1 Mendelian ratio). Those that had both positive and negative results were identified as hemizygous and those that had only negative results were identified as null. Based on these results and the total seed weight of each line (weighed unthreshed in bags), 18 transgenic and 2 bar-only control lines were chosen to be fully threshed and winnowed, tested for breadmaking quality and sown for the next generation of transgenic plants. The transgene screening was repeated for 12 more seeds from each of these selected lines.

## **5 Analysis of transgenic wheat**

### **5.1 Introduction**

#### *5.1.1 Gluten protein structure and function - High molecular weight glutenin subunits*

Variations in the types and quantities of high molecular weight glutenin subunits (HMW-GS) are a major determinant of the elastic properties of the dough despite only making up 5-10% of total endosperm protein (Payne, 1987). They can be divided into x- and y-types based on differences in size, structure and number of cysteine amino acids (see Fig. 5.1A). Their sequences include a large central region of repeats (481 to 681bp), as well as relatively small N- and C- termini (81-104bp and 42bp respectively) that include cysteine residues involved in disulphide bonding. The resulting secondary structure is composed of small disulphide-bonding domains rich in  $\alpha$ -helices at the ends and a large central section of  $\beta$ -reverse turns where intra- and inter-chain hydrogen bonding occurs (Shewry & Tatham, 1997; Shewry *et al*, 1995). HMW-GS are thought to have a rigid rod-like tertiary structure which, along with specifically located hydrogen bonding, causes most of the elastic properties of gluten (Shewry *et al*, 1992).

Some subunits and combinations of subunits are known to have positive or negative effects on gluten strength and there have been numerous efforts to express specific subunits in wheat to alter processing quality (for recent examples see Blechl *et al*, 2007; Graybosch *et al*, 2011; Leon *et al*, 2009; Leon *et al*, 2010; Rakszegi

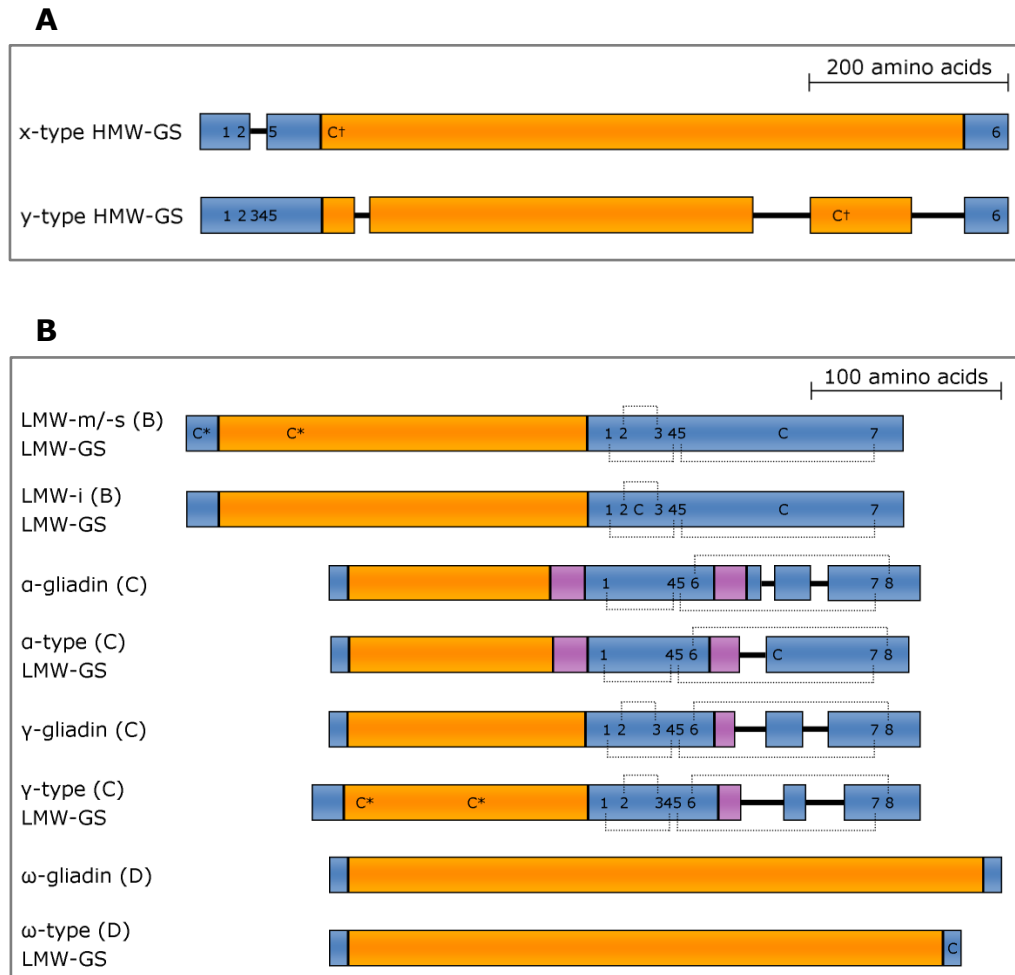


**Fig. 5.1 - Primary structure of glutenin subunits and gliadins (adapted from Delcour *et al*, 2012; Shewry & Tatham, 1997; D'Ovidio & Masci, 2004; Qi *et al*, 2006)**

A: HMW glutenin subunits - numbers indicate conserved cysteine amino acids. C<sup>+</sup> indicates a cysteine that is present in some subunits of this type but not others. Repetitive domains are coloured orange and non-repetitive domains are blue. Proteins are aligned based on their amino acid sequences.

B: LMW glutenin subunits and gliadins - numbers indicate the intra-molecular bonding cysteine residues and dotted lines indicate bonding pairs. C indicates a conserved inter-molecular bonding cysteine amino acid. Two C\* in a sequence indicates that one or other cysteine is present. Letters in brackets indicate the prolamins group (B, C or D) as determined by SDS-PAGE. Repetitive domains are coloured orange, non-repetitive domains are blue and glutamine repeats are purple. Proteins are aligned based on their amino acid sequences.

*et al*, 2008; Yue *et al*, 2008). However, expression of a subunit associated with positive effects does not always yield an improvement in processing quality. For example, a study by Popineau *et al* (2001) showed that while genetically modifying wheat to over-express strong HMW glutenin subunits did increase pure gluten strength, overall protein content of the grain was not increased and significantly deleterious effects on dough mixing performance were seen.

### *5.1.2 Gluten protein structure and function - Low molecular weight glutenin subunits*

Older studies of gluten protein focussed on HMW-GS due partly to the ease of identification by SDS-PAGE and the relatively small number of subunits. On the other hand, study of low molecular weight glutenin subunits (LMW-GS) was limited due to difficulty distinguishing them from gliadins and reducing them for electrophoresis, as well as the complexity of their coding loci and much greater number of subunits compared to HMW-GS (Masci *et al*, 1998; She *et al*, 2011). However, LMW-GS make up the majority of the glutenin fraction and the types present play a critical role in gluten quality. They have been investigated in more depth in recent years with the assistance of improved biochemical and molecular analysis techniques (She *et al*, 2011).

Typical (B-type) LMW-GS protein sequences include a short N-terminal conserved region followed by a repetitive domain containing mostly glutamine repeats, and a C-terminal region made

up of three domains (Cassidy *et al*, 1998; D'Ovidio & Masci, 2004; Ikeda *et al*, 2006) (see Fig. 5.1B). LMW-GS can be divided into two functional groups – chain extenders which can form two inter-molecular disulphide bonds, and chain terminators which only form one covalent inter-molecular bond (Kasarda, 1989). The former comprise the B-type LMW-GS known as LMW-s, LMW-m, and LMW-i, named for the first amino acid in the mature protein – serine, methionine or isoleucine. They contain eight cysteine residues, six of which are involved in *intra*-molecular bonding and two of which are available for *inter*-molecular disulphide bonding (D'Ovidio & Masci, 2004). The chain terminator group of LMW-GS is largely made up of proteins that have gliadin-like sequences and are sometimes known as aggregated gliadins. As well as having an even number of cysteine residues that bind *intra*-molecularly they, unlike gliadins, contain an extra cysteine that forms an *inter*-molecular bond, which leads to these proteins being included in the glutenin fraction (D'Ovidio & Masci, 2004).

Gluten proteins can also be classified by SDS-PAGE separation into A, B, C and D groups (Jackson *et al*, 1983; Payne & Corfield, 1979). Group A is equivalent to HMW-GS while group B is mainly composed of B-type LMW-GS (LMW-m, -s and -i). Group C comprises  $\alpha$ - and  $\gamma$ -gliadins along with  $\alpha$ - and  $\gamma$ -type LMW-GS counterparts, while  $\omega$ -gliadins and  $\omega$ -type LMW-GS make up group D (D'Ovidio & Masci, 2004).

### 5.1.3 Gluten protein structure and function - Gliadins

The proteins that make up the monomeric part of the gluten fraction are called gliadins. They are responsible for the viscosity (internal resistance to flow) and extensibility (ability to stretch without breaking) of the dough and make up approximately 40-50% of total protein in the endosperm (Qi *et al*, 2006). They were originally categorised into four groups based on their mobility in acid PAGE –  $\alpha$ -,  $\beta$ -,  $\gamma$ - and  $\omega$ -gliadins (Bushuk & Zillman, 1978; Woychik *et al*, 1961). However,  $\alpha$ - and  $\beta$ -gliadins were found to be too genetically and structurally similar to justify their separate classification, resulting in  $\beta$ -gliadins being reclassified as  $\alpha$ -gliadins (Bietz *et al*, 1977; Kasarda *et al*, 1983).

The general sequence of a gliadin begins with a short N-terminal domain of 5 to 14 amino acids, followed by a central repetitive domain containing up to 100 amino acids made up of repeat sequences of one or two motifs. These mostly include glutamine, proline, and hydrophobic amino acids (phenylalanine and tyrosine). Any cysteine residues are found in the C-terminal domain, which is a succession of glutamine repeats and unique lysine and arginine-rich sequences (Delcour *et al*, 2012; Muller & Wieser, 1997) (see Fig. 5.1B). The secondary structure of  $\alpha$ -gliadin consists of  $\alpha$ -helices in the non-repetitive regions and  $\beta$ -reverse turns in the repetitive regions, giving it a compact, globular tertiary structure (Tatham & Shewry, 1985).  $\gamma$ -gliadin has a similar secondary structure to that of  $\alpha$ -gliadin but forms an extended spiral tertiary structure (Tatham *et al*, 1990).  $\beta$ -reverse turns make up the

majority of  $\omega$ -gliadin secondary structure with few  $\alpha$ -helices or  $\beta$ -pleated sheets, suggested to produce a stiff coil tertiary structure (Shewry *et al*, 2009).

#### 5.1.4 Gluten protein genetics

HMW-GS are encoded on the long arm of chromosomes 1A, 1B and 1D by the loci Glu-A1, Glu-B1 and Glu-D1 respectively (Payne *et al*, 1980). LMW-GS are encoded by Glu-A3 (LMW-i), Glu-B3 (LMW-m and LMW-s), and Glu-D3 (LMW-m and LMW-s) on the short arm of chromosomes 1A, 1B and 1C respectively (Gupta & Shepherd, 1990; Ikeda *et al*, 2006; Jackson *et al*, 1983). Additionally, Ikeda *et al* (2006) found that some LMW-m and LMW-s proteins appeared to be encoded by the same gene and their small differences could be explained by post-translation processing at different sites. The genes that encode  $\omega$ -gliadins and most of the  $\gamma$ -gliadins are located at the Gli-1 locus on the short arm of the group 1 chromosomes, while the Gli-2 locus on the short arm of the group 6 chromosomes contains the  $\alpha$ -gliadin genes and the rest of the  $\gamma$ -gliadin genes (Bartels & Thompson, 1986; Payne, 1987; Payne *et al*, 1984; Tatham & Shewry, 1995). Gliadin genes are interspersed with gliadin-like LMW-GS genes (C- and D-type prolamins) in the Gli-1 locus (Gupta & Shepherd, 1993; Lew *et al*, 1992; Masci *et al*, 2002; Metakovsky *et al*, 1997).

Two *trans*-acting transcription factors are involved in the endosperm-specific expression of LMW-GS – ESBF-I and -II (Hammond-Kosack *et al*, 1993). They bind to the “endosperm box”

located between -326 and -160bp upstream of the transcription start point (Colot *et al*, 1987). ESBF-I occupies the E motif of the “endosperm box” promoter during early seed development, then before the stage of maximum gene expression ESBF-II also binds to endosperm box at the GLN4-like motif (Hammond-Kosack *et al*, 1993).

### *5.1.5 Wheat processing quality*

Every year, Nabim (the National Association of British and Irish Millers) produces a guide aimed at UK farmers classifying widely-grown wheat varieties into one of four groups, which relate to the potential uses of the grain (Nabim, 2011). Group 1 is composed of high quality bread wheat varieties and attracts a premium over other varieties as long as specific quality requirements are met. Group 2 contains those varieties that have potential for breadmaking but are not eligible for group 1 due to inconsistent breadmaking performance or worse performance than those in group 1. Group 3 describes soft wheat varieties for use in biscuit and cake flour, and group 4 comprises varieties that may be used for distilling or general purpose flours if they reach millers’ specific requirements or otherwise as animal feed.

There are a number of factors that are important indicators of grain quality and its suitability for different purposes. Important properties of wheat grain include specific weight in kilograms per hectolitre, 1000 grain weight in grams, protein content as a percentage, protein quality and  $\alpha$ -amylase activity (HGCA, 2012).

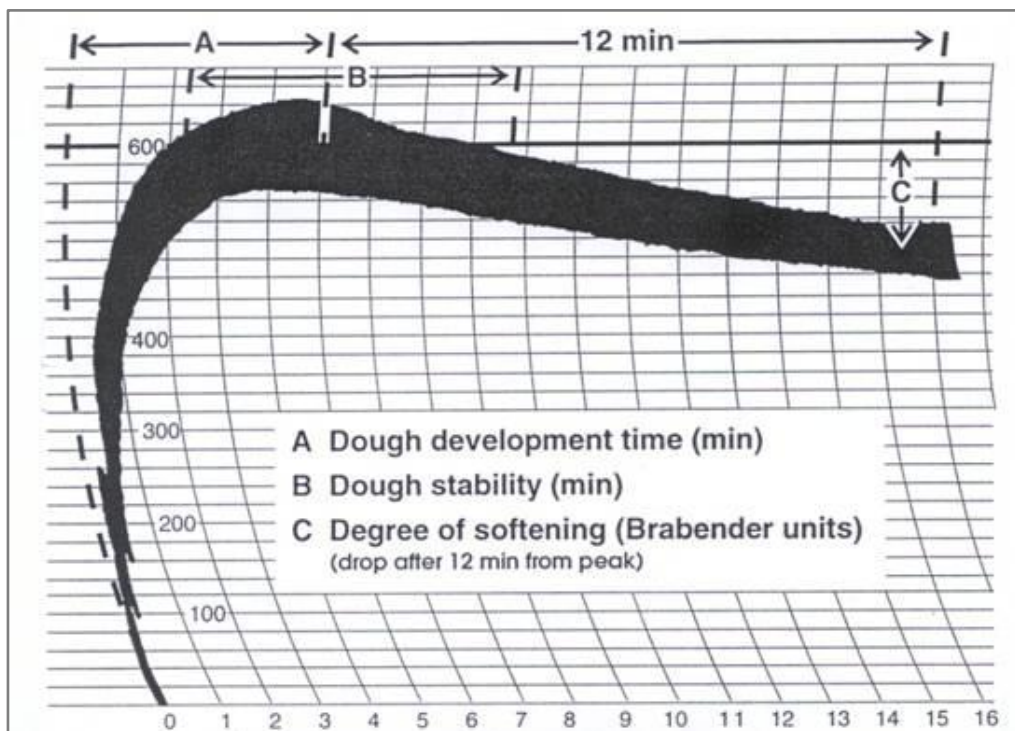


**Fig. 5.2 - Features of a farinogram**

An example of a trace produced by a farinograph, showing resistance to mixing (y-axis) over time (x-axis). Resistance is displayed in Brabender units (an arbitrary measurement) and time is measured in minutes. Dough development time (A) is the time between start of mixing and peak resistance. Dough stability (B) is the time during which the top of the trace is above the centre of the trace at peak resistance. Degree of softening (C) measures the drop in resistance (using the centre of the trace) between peak resistance and 12 minutes after peak resistance.

The falling number test was originally developed by Hagberg (1960) to assess the level of undesirable  $\alpha$ -amylase activity in flour. A higher number indicates lower activity meaning the starch is less degraded and therefore better quality. Protein content is generally higher in bread wheat varieties than biscuit varieties and can be assessed while grain is still whole or from flour samples. Protein quality of wheat grain can be measured in a number of ways. Specific requirements for the *ukp* and *uks* UK export classifications include *W* and *P/L* values as measured by the Chopin Alveograph, which relate to dough strength and extensibility (BCE, 2011).

There are a number of other rheological tests which measure similar characteristics relating to protein quality in dough, such as the Brabender™ Farinograph and Extensograph. These tests are used internationally to assess quality of dough and its suitability for various uses. The Farinograph measures and records the resistance of a dough to mixing as it is formed from flour and water, is developed and is broken down. This resistance of the dough is called consistency, the maximum of which is adjusted to a fixed value by altering the quantity of water added. This quantity, the water absorption, may be used to determine a complete mixing curve called a farinogram, the various features of which are a guide to the strength of the flour (Fig. 5.2). The dough mixed by the Farinograph is moulded on the Extensograph into a standard shape and rested under controlled conditions for a specified period. The dough is then stretched to breaking point on the Extensograph and a curve drawn recording the extensibility of the dough and its resistance to

stretching.

To investigate the effects of the transgene a variety of experiments were performed using the transformed wheat. Expression of the *RabD* genes was assessed to determine which genes had been knocked down and by how much at several stages of endosperm development. Features of the mature transgenic grain were analysed, including protein profile (ratio of different subunits), protein and starch content, grain size and shape, dough rheology and glutenin macropolymer of the dough.

## **5.2 Materials and Methods**

### *5.2.1 Sodium dodecyl sulphate polyacrylamide gel electrophoresis of T1 seeds*

Whole mature seeds were individually crushed in folded pieces of filter paper using a small hammer. A 10mg sample was then weighed out from each ground seed into separate 1.5ml microcentrifuge tubes and 500µl Laemmli loading buffer (15.3ml LLB: 13.5ml Sample solution buffer [90ml SSB: 52ml H<sub>2</sub>O, 20ml 10% SDS, 10ml Glycerol, 8ml 1M Tris-HCl (pH 6.8)], 1.5ml 1M DTT, 300µl bromophenol blue (2mg/ml). DTT and bromophenol blue solutions added immediately prior to use) was added to each of the tubes which were then vortexed. The tubes were incubated at room temperature for 2 hours, vortexing after 1 hour and at the end of the 2 hours. They were then incubated in a boiling water bath for 3 minutes on a floating holder along with a tube of protein marker (Invitrogen - Life Technologies Ltd, 3 Fountain Drive, Inchinnan Business Park, Paisley, UK, PA4 9RF) and allowed to cool before vortexing. The tubes were centrifuged at 12,000g for 5 minutes before 45µl of the supernatant was transferred to new 1.5ml tubes along with 15µl LLB.

Combs were removed from 2 pre-formed 1mmx15-well Bis-Tris 12% acrylamide gels and the wells were washed with distilled H<sub>2</sub>O. The gels were then placed into the clamping assembly of a mini dual vertical electrophoresis system (Bio-Rad Ready Gel Cell - Bio-Rad Laboratories Ltd., Bio-Rad House, Maxted Road, Hemel Hempstead, Hertfordshire, HP2 7DX). A 20x stock solution of MES

SDS running buffer (Invitrogen) was used to make up 500ml ready-for-use running buffer.

The clamping assembly including 2 gels was placed into the gel bath and running buffer was carefully poured into the upper chamber so that the level of buffer was between the lip of the inside gel cover and the top of the outside gel cover. The cooling gel pack included with the electrophoresis system was removed from storage at -20°C and placed in the lower chamber which was then filled with the remaining running buffer ensuring the level of buffer was not in danger of spilling over into the upper chamber.

Prepared wheat seed protein samples were added to the gels (10µl of each) along with the prepared protein marker, which was added to the well on the left of the protein samples. The lid was put on and the gels were run at 20V for 15 minutes then 150V until the dye front reaches the bottom of the gel (about another 60 minutes) followed by a further 45 minutes at the same voltage.

Gels were removed from their plastic covers, rinsed with distilled H<sub>2</sub>O and marked with a scalpel to aid later identification of gels. Gels were placed in a plastic tub which was filled with fixing solution (40% methanol, 7% glacial acetic acid) so that gels were covered, then left at room temperature overnight with the lid on. Colloidal Coomassie blue stain (Sigma-Aldrich) was diluted and stored as described in the manufacturer's instructions. Immediately before gels were to be stained, 25ml methanol was added to 100ml stain and mixed thoroughly. The fixing solution was poured off the gels which were rinsed with distilled water before adding of the

stain/methanol solution. The tub was placed on a rocker overnight with the lid on then the stain was poured off. A fresh tub was rinsed with distilled water and the gels were transferred to it along with 100ml destain 1 (25% methanol, 10% glacial acetic acid) which was rocked for 30 seconds. The destain 1 was then poured off and the tub and gels were rinsed with 100ml destain 2 (25% methanol) which was also decanted off before a fresh 100ml of destain 2 was added. The tub was stored at 4°C ready for imaging.

### *5.2.2 Sowing and tagging of T1 wheat, harvesting during development and harvesting when mature*

Twelve seeds from each of sixteen selected T1 lines were sown four plants per pot (three pots per line) in 21cm diameter plastic pots (Nursery Trades (Lea Valley) Ltd., Hertfordshire, UK) using "Rothamsted prescription mix" compost and grown in a glasshouse at Rothamsted Research (16 hour day, 20°C day, 15°C night, automatic supplementary lighting turning on when natural daylight falls below  $300\mu\text{mol m}^{-2} \text{s}^{-1}$  and switching off when rising above  $400\mu\text{mol m}^{-2} \text{s}^{-1}$ ).

The date when each ear reached anthesis was noted using the decimal code devised by Zadoks *et al* (1974). Ears were recorded as anthesed when they passed 61 on the scale. Some ears were removed and the developing T2 grain was harvested at 7, 14 and 21 days post anthesis (dpa). The seeds were frozen in liquid nitrogen in 1.5ml microcentrifuge tubes before being transported to Sutton Bonington in dry ice and stored at -70°C. The remaining wheat ears

were allowed to mature before harvesting. The unthreshed mature T2 seeds were placed in separate labelled paper bags for each individual plant (192 bags total) and transported to Sutton Bonington.

### *5.2.3 Sodium dodecyl sulphate polyacrylamide gel electrophoresis (SDS-PAGE) of T2 seeds*

Three mature seeds from each line to be tested were placed in separate folded pieces of paper and crushed using a pestle. One line per gel was a control line. A 10mg sample from each crushed seed was weighed out into a 1.5ml microcentrifuge tube.

A 500µl volume of Laemmli loading buffer (15.3ml LLB: 13.5ml sample solution buffer [90ml SSB: 52ml H<sub>2</sub>O, 20ml 10% SDS, 10ml glycerol, 8ml 1M Tris-HCl (pH 6.8)], 1.5ml 1M DTT, 300µl bromophenol blue (2mg/ml). DTT and bromophenol blue solutions added immediately prior to use) was added to each tube and the tubes were vortexed. The tubes were incubated at room temperature for 2 hours, vortexing after 1 hour and at the end of the 2 hours. A heating block was set to 95°C and once it had reached temperature the tubes were incubated at 95°C for 3 minutes. The tubes were left to cool before vortexing and centrifugation at 12,000g for 5 minutes. 7.5µl of the supernatant was transferred to a new 1.5ml tube along with 2.5µl LLB and 1.1µl Reducing Agent (Invitrogen).

Two pre-formed 15-well Bis-Tris 10% acrylamide gels (Invitrogen) were placed into the clamping assembly of a mini dual

vertical electrophoresis system (Sigma-Aldrich). One litre of MOPS SDS running buffer (Invitrogen) was diluted ready for use from the 20x stock solution. Of this solution, 200ml was set aside for the upper chamber, to which 500µl antioxidant (Invitrogen) was added.

The clamping assembly including 2 gels was placed into the gel bath and the 200ml running buffer for the upper chamber was carefully poured into the upper chamber so that the level of buffer was between the lip of the inside gel cover and the top of the outside gel cover. The cooling gel pack included with the electrophoresis system was removed from storage at -20°C and placed in the lower chamber which was then filled with the remaining running buffer ensuring the level of buffer was not in danger of spilling over into the upper chamber.

Prepared wheat seed protein samples were added to the gels (10µl of each) along with the prepared protein marker (Fermentas), which was added to the well on the left of the protein samples. The lid was put on and the gels were run at 20V for 15 minutes then 150V for 90 minutes.

Gels were removed from their plastic covers, rinsed with distilled H<sub>2</sub>O and marked with a scalpel to aid later identification of gels. Gels were placed in a plastic tub which was filled with fixing solution (40% methanol, 7% glacial acetic acid) so that gels were covered, then placed on a rocker for 1 hour with the lid on. Colloidal Coomassie blue stain (Sigma-Aldrich) was diluted and stored as described in the manufacturer's instructions. Immediately before gels were to be stained, 25ml methanol was added to 100ml stain

and mixed thoroughly. The fixing solution was poured off the gels which were rinsed with distilled water before adding of the stain/methanol solution. The tub was placed on a rocker for 1 hour with the lid on before the stain was poured off and gels and tub was rinsed with distilled water. Destain 1 (25% methanol, 10% glacial acetic acid) was added to the tub which was rocked for 30 seconds to remove stain from the tub. The destain 1 was then poured off and the tub and gels were rinsed with destain 2 (25% methanol) then distilled water. The tub was filled with distilled water and left on a rocker for 1 hour then the water was poured off and fresh distilled water was added. The tub was stored at 4°C ready for imaging. Phoretix 1D software by Totallab was used for densitometry analysis at Campden BRI.

#### *5.2.4 Grain size and shape analysis*

Mature wheat grains were analysed for grain size and shape using a DigiEye apparatus (VeriVide Limited, Quartz Close, Warrens Business Park, Warrens Park Way, Enderby, Leicester, LE19 4SG, United Kingdom). Grains were placed onto the platform, making sure no grains were touching each other or the side, along with a colour calibration chart (Fig. 5.3). A photograph was then taken using the DigiEye software. Several photos were taken of grain from each line using a different set of grains in each photo. The pictures were analysed using ImageJ software measuring plan area, perimeter, roundness, maximum calliper and minimum calliper of each grain image.



**Fig. 5.3 – DigiEye apparatus**

Samples were placed into the drawer along with a calibration palette and the drawer was closed before a colour- and brightness-calibrated photograph of the sample was taken and displayed on the screen. These photographs were later analysed to determine size and shape measurements.

### *5.2.5 Milling of T2 grain*

Mature T2 grain was milled using a Quadrumat milling machine (Brabender GmbH & Co. KG, Kulturstrasse 51-55, 47055 Duisburg, Germany) at Campden BRI. Before milling, wheat grain was conditioned to 16% moisture. Each sample of wheat grain was weighed into a labelled container and 1ml of water was added per 100g grain. The container was sealed and shaken vigorously for 1 minute then left to stand for 10 minutes. The mill was thoroughly cleaned with a brush and vacuum cleaner then turned on and left to run empty for 5 minutes to warm up. The grain sample was poured into the feed hopper and slowly fed into the mill. Any blockages were cleared with a brush. Once the sample had all been fed into the mill it was turned off and any material stuck on the lower roll was brushed into the lower mill. The mill was then restarted and run for 30 seconds, after which the bran from the receiving drawer was placed back into the feed hopper. The mill was run and the lower roll brushed as before, then bran placed into the feed hopper again and the process repeated once more. After this third run the inside of the mill was carefully brushed down from top to bottom until empty.

The flour was removed from the receiving drawer and sieved using a 200 $\mu$ m-aperture mesh on a rotary-shaker for 15 minutes. The flour that passed through the sieve was placed into in a labelled sealable clear plastic bag and the flour still in the sieve was discarded.

### *5.2.6 Determination of flour moisture content*

The following method was carried out at Campden BRI. A ventilated electric fan-assisted drying oven was set to 131°C and allowed to reach temperature. 60mm diameter metal dishes of 20mm height with close fitting lids were desiccated at room temperature then weighed. With an accuracy of  $\pm 0.001\text{g}$ , 1g of flour was weighed out into a pre-weighed metal dish and covered with the corresponding lid. The combined weight of the dish with lid and flour was recorded.

The oven fan was switched off and allowed to stop before opening the oven door. The dishes were uncovered and placed in the oven along with their lids, then the oven door was closed and the fan switched on. Once a temperature of 130°C was reached the flour was left to dry for 90 minutes. When drying was complete the fan was switched off and allowed to stop before the oven door was opened and lids were replaced onto their corresponding metal dish. The covered dishes were then placed in a desiccator and allowed to cool to room temperature.

The cooled dishes and contents were weighed with an accuracy of  $\pm 0.001\text{g}$ . The percentage moisture content was then calculated to the nearest 0.1% using the following formula:  $(M_0 - M_1) * 100 / M_0$  where  $M_0$  = initial weight of sample in grams and  $M_1$  = weight of sample after oven drying in grams.

### *5.2.7 Measurement of flour protein content*

Protein content was determined by Dumas combustion in an

oxygen rich environment at high temperatures. Protein is calculated using a factor of 5.7 to from total nitrogen determination. Combustion was carried out in a Leco FP528 at Campden BRI.

#### *5.2.8 Small-scale breadmaking quality test - Reomixer*

Dough rheology of flour made from T2 seeds was measured using a Reomixer machine (Reologen i Lund, Sweden). The Reomixer torque was calibrated to 2,200 g cm at an output of 10V. The analysis control parameters were set as follows: Strip width: 1.0; Max width norm: 0.70; Mov avg length: 40; Std max mix torq: 10; Plot time scale: 10; No. of title char's: 12; Time in 1 sec: 30; Time 2 dividend: 2; Time 4 dividend: 2; Mix pen width: 3; Line pen width: 1. The download parameters were set as follows: Mixing sampl freq: 200; Mixing n samples: 200; Reseved: 1. The mixing speed parameter was set to the equivalent of 93 (+/-2) rpm, checked before use. The following options were selected: Auto-save data, Large zero reading, Grid. The mixing time was set to 10 minutes. Before testing, a scrap dough was mixed followed by a control dough, the output values of which were checked to ensure they were within previously established tolerances.

The recipe for each dough was as follows: 10g flour, 4.2g 5% NaCl solution, (W-4)g distilled water. W = water absorbance percentage value / 10. The 10g flour was weighed into a reomixer mixing bowl, covered with film and placed in a water bath at 30°C, along with a glass beaker of distilled water and one of 5% NaCl solution, for 5 minutes. A three pronged well was made in the flour

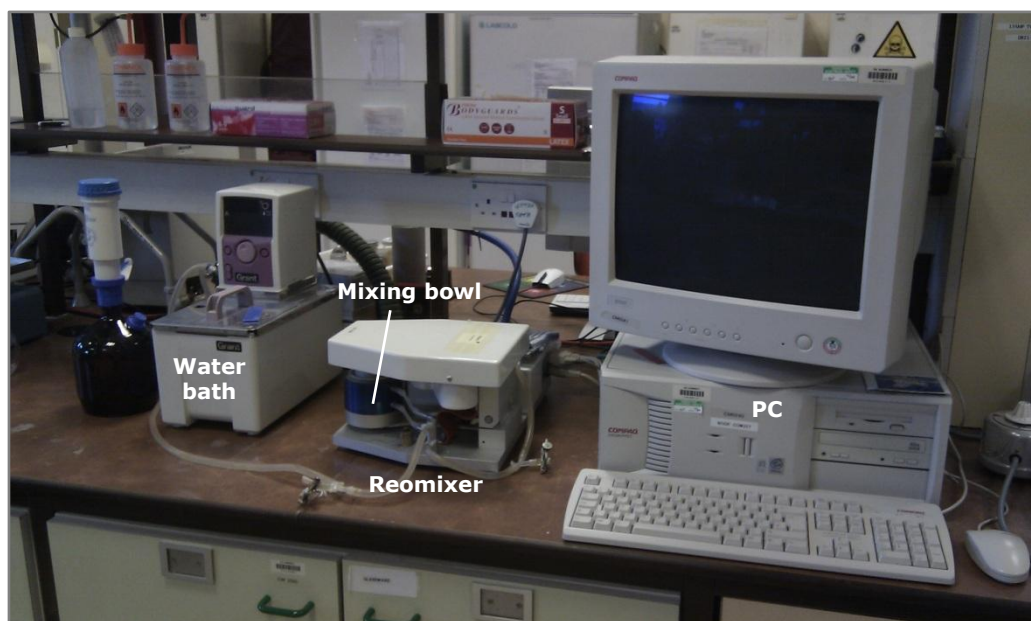


**Fig. 5.4 – Reomixer apparatus**

Flour and water samples were placed into the mixing bowl, which was kept at a constant 30°C by water circulating from a water bath. The PC was used to start the mixing and to record the resistance to mixing over a period of 10 minutes.

(between the spokes) that would contain the liquid about to be added. 4.2g 5% NaCl solution was then weighed out into the well followed by the calculated amount of distilled water. The mixing bowl was then placed into the reomixer and the mixer head was lowered into it (Fig. 5.4). The mixer was immediately started and a freezer block at -20°C was placed above the mixer head to prevent excessive heating of the dough. After the 10 minute mix was complete, the mixing bowl was removed, the dough was discarded and the bowl and mixing head were cleaned. The graph produced was saved and the smoothed trace data were exported to a text file to be later imported into spreadsheet software for further analysis.

#### *5.2.9 Sowing, transport and potting up of T2 wheat*

From each of twenty selected T2 lines (including 2 bar-only control lines) 100 seeds were sent to Rothamsted Research. Each line was sown across 2½ 40-well trays (wells: 40x40mm, 50mm deep. 5x8 wells per tray) using "Rothamsted prescription mix" compost and kept in a glasshouse at Rothamsted Research (16 hour day, 20°C day, 15°C night, automatic supplementary lighting turning on when natural daylight falls below 300µmol m<sup>-2</sup> s<sup>-1</sup> and switching off when rising above 400µmol m<sup>-2</sup> s<sup>-1</sup>). After four weeks, the seedlings of three selected transgenic lines and the two control lines were kept while the other 15 lines were discarded. One control line and two transgenic lines were transported to Sutton Bonington, potted up five plants per pot in 5 litre plastic pots using Levington C2 compost and grown in a glasshouse (16 hour day, heating to

16°C day, 15°C night, venting at 20°C, constant supplementary lighting 6am to 10pm). The other control line and transgenic line were potted up five plants per pot in 21cm diameter plastic pots at Rothamsted Research using "Rothamsted prescription mix" compost and grown in a glasshouse there (conditions as previous Rothamsted glasshouse).

#### *5.2.10 Tagging and harvesting of developing T3 seeds and harvest of mature seeds*

The date when each ear of the T2 plants at Rothamsted Research and Sutton Bonington reached anthesis was noted using the decimal code devised by Zadoks *et al* (1974). Ears were recorded as anthesed when they passed 61 on the scale. Some ears were removed and the developing T2 seeds were harvested from them at 14 and 21 days post anthesis (dpa). The seeds were frozen in liquid nitrogen in 15ml centrifuge tubes and those at Sutton Bonington were then stored at -70°C, while those at Rothamsted Research were transported to Sutton Bonington on dry ice then stored at -70°C. The remaining wheat ears were allowed to mature before they were harvested.

#### *5.2.11 Milling of T3 grain*

Milling was carried out by conditioning grain to for 14-16hrs to 16.0% from at least 1% lower grain moisture content, and milling using relevant protocols on a laboratory scale Buhler MLU 202 mill and Russell-Finex 14550 redresser at Campden BRI.

### 5.2.12 Size exclusion high-performance liquid chromatography (SE-HPLC)

SE-HPLC was carried out on flour samples using the Profilblé method developed jointly by ARVALIS - Institut du végétal (France) and l'Institut National de la Recherche Agronomique (INRA) (Morel *et al*, 2000). Flour (160mg) was dispersed in 20mL of 1% SDS in 0.1M phosphate buffer, pH 6.9. Samples in 50mL tubes were then placed on a rotary mixer in an incubator at 60°C (to inactivate major proteases) for 80 minutes to allow the soluble gluten proteins to be extracted from the flour. The SDS soluble protein extract was obtained after centrifuging the sample for 10 minutes at 5000rpm, after which an aliquot was taken from the supernatant and placed in a HPLC vial. Alternatively, the suspension was subjected to mild sonication (30 seconds at a power output level of 5 Watts RMS) treatment using a probe sonicator (Microson XL2000, Microsonix, CT, USA) to solubilise the polymeric protein fraction (sonication breaks down some intermolecular bonds and thus increases the solubility of protein in a sample). The sample was then centrifuged for 10 minutes at 5000rpm, after which an aliquot was taken from the supernatant and placed in a HPLC vial.

All SE-HPLC analysis was performed using a Jasco (Essex, UK) system comprising a LG-980-02 ternary gradient unit, a PU-980 pump, a DG-1580-53 three line degasser, an AS-950 autosampler and a UV-975 UV/VIS detector. The analytical column used was a TSKgel G 4000SW (7.5mm (ID) x 7.5cm (L), cat no. 05790, Tosoh Bioscience, Japan) and this was operated in conjunction with a

TSKgel SW guard column (7.5mm (ID) x 7.5cm (L), cat no. 05371, Tosoh Bioscience). Samples (20 $\mu$ L) were eluted using 0.1% SDS in 0.1M phosphate buffer with a flow rate of 0.7mL/min and detection at 214nm. Each chromatogram took 25 minutes to collect. Chromatograms were integrated using a combination of automatic and manual (using a fixed set of 'rules' developed by ARVALIS) methods depending on the shape of the peak associated with each of the fractions. The response for each sample for a given extraction series was normalised using the results for the control flour for that series. The control flour (supplied by ARVALIS) was a common wheat flour having a chromatographic profile typical of a flour of good baking quality. All values were quoted as a percentage of the total response of the column, i.e. as a percentage of total protein.

The overall performance of the columns on the day of analysis was determined by comparing the results for a protein standard (cytochrome C) with control values determined when the column was first used. Each combination of guard and analytical columns was characterised on first use by running the following five protein standards; cytochrome C (also used for subsequent column assessment), carbonic anhydrase, bovine serum albumin, yeast alcohol dehydrogenase and bovine thyroglobulin. The retention times for each standard are used to create a calibration curve against log molecular weight. Protein types corresponding to each peak were judged using a Profilblé legend (Fig. 5.5).

## Profilblé© SE-HPLC trace of wheat proteins

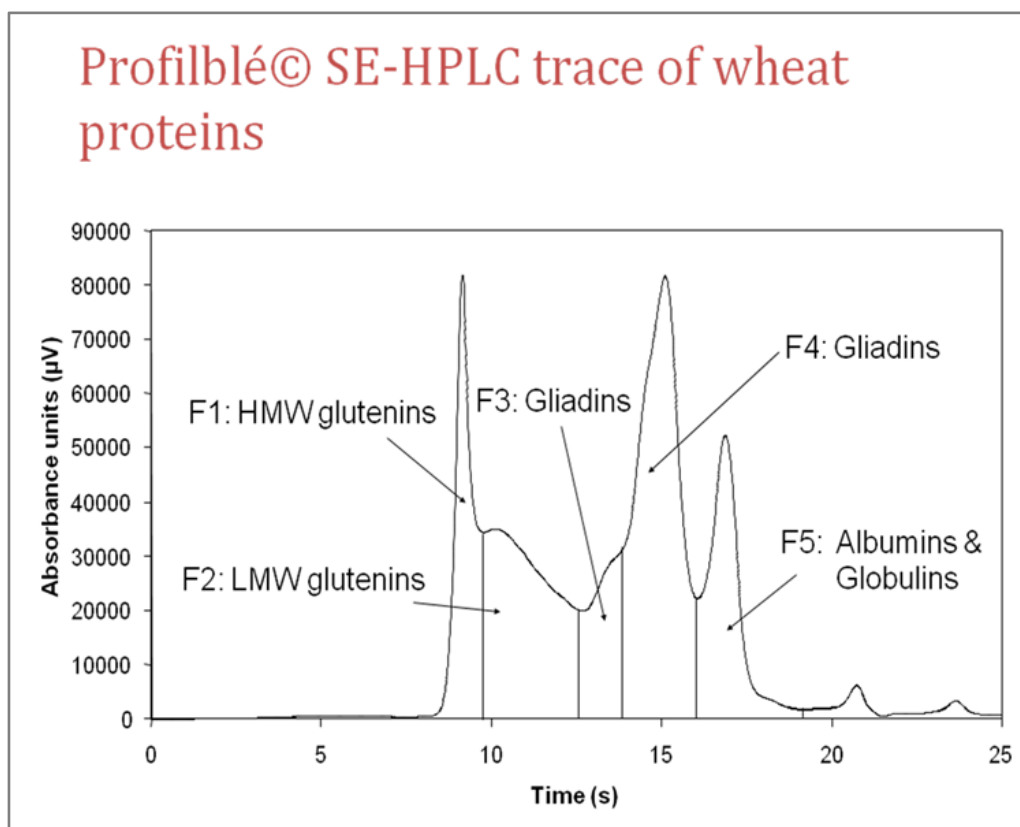


**Fig. 5.5 – Subunit distribution for SE-HPLC**

An example SE-HPLC trace of wheat seed storage proteins identifying the protein subunits present in each region of the trace.

### *5.2.13 Statistical analysis*

All statistical analyses were performed using GenStat 14<sup>th</sup> Edition (VSN International Ltd). T-tests were used to compare two distinct groups of samples and analysis of variance tests with Tukey multiple comparisons were used to compare more than two groups of samples.

### *5.2.14 Two-dimensional polyacrylamide gel electrophoresis (2D PAGE)*

Ground grain material was extracted for 1 hour in 2% NP-40, 9M urea, 1% DTT, 0.8% carrier ampholytes (pH 3-10) at 20mg/0.4ml. Aliquots of 20 $\mu$ l of each extract were diluted x4 in the same buffer and applied to the 3-10 pH Immobiline DryStrips for the 1st dimensional separation by isoelectric focusing (IEF). The 2nd dimensional separation was performed using ExcelGel SDS, gradient 8-18% gels. All procedures were performed using appropriate reagents and pre-cast gels, together with the Multiphor electrophoresis unit (all from GE Healthcare). Gels were stained with colloidal Coomassie Blue stain (TES-CM-0033). 2D PAGE was carried out at Campden BRI. Images were analysed with SameSpots software from Non-Linear Dynamics.

### *5.2.15 Brabender farinograph*

A flour sample of 300.0g was allowed to equilibrate to 25.0  $\pm$  5.0°C. The flour sample was placed in the farinograph bowl and the lid was closed, thereby engaging the safety switch. The farinograph

was turned on and the pen placed on the recording chart at 8 minutes. The farinograph was then allowed to run with the bowl empty for 1 minute with the pen on the zero line then stopped when the pen reached 9 minutes. The burette including the tip was filled with water at  $30.0 \pm 2.0^{\circ}\text{C}$ . The pen was set on the chart paper, so that the pen is on a 9-minute line. Mixing of the dry flour was then started with the motor running at  $63 \pm 2$  rpm. As the pen crossed the zero minute line, addition of water from the burette was started through the front end of the right hand slot in the lid. A volume of water was added close to that expected to bring the curve to a maximum consistency of 600BU (Brabender units). Water addition was completed within 30 seconds. When the dough formed, a plastic scraper was used to carefully push any flour particles or dough adhering to the mixing bowl walls down into the dough being mixed.

The chart output is called a farinogram. Farinogram characteristics (except water absorption) were measured relative to the line on which the peak of the curve actually centred. If, for example, the curve centres at 610BU measurements were made along this line. Water absorption is the volume in millilitres of water added to achieve a consistency of 600BU expressed as a percentage of the weight in grams of flour used. If the peak consistency was exactly on the 600 BU line, then the water absorption percentage was that read directly from the burette. When the peak consistency varied from 600BU by up to  $\pm 20$ BU, a correction was made to the reading from the burette. The correction was 0.6% per 20BU difference. If the peak value was greater than 600BU the calculated

correction was added to the burette reading and if the peak value was lower than 600BU the calculated correction was subtracted from the burette reading. Water absorption is given to 1 decimal place. Development time is the time in minutes from the start of mixing to the point on the curve immediately before the first signs of weakening. Development time is given to the nearest 0.5 minute. Stability is the difference in time (in minutes) between the point where the top of the curve first intercepts the centre line at the maximum consistency and the point where the top of the curve leaves this line. Stability is given to the nearest 0.5 minute. Degree of softening is the difference in height (in BU) between the centre of the curve immediately before the first signs of weakening and the centre of the curve 12 minutes later. Degree of softening is given to the nearest 5BU.

#### *5.2.16 Brabender extensograph*

Before use, the temperature of the extensograph cabinet was checked to ensure that it was  $30 \pm 0.5$  °C. The dough-holders were lightly greased with vegetable oil. Water was placed in the troughs of the dough-holder cradles and they were returned to the dough cabinets at least 15 minutes before use. The chart paper was correctly aligned on the sprockets of the chart recorder to ensure that the pen followed the arcs on the chart paper when the extensograph balance arm was moved. The pen was placed on the zero line before a dough-holder with clamps and 150g weight are placed in position on the extensograph balance arm.



**Fig. 5.6 – Extensograph apparatus**

A piece of dough that has been mixed, balled, moulded and incubated is placed onto the balance arm of the extensograph before a hook is used to stretch the dough to breaking point while the dough's resistance to stretching is recorded.

A mixed dough sample was removed from the farinograph with the minimum of handling, taking care that it was not pulled or deformed unnecessarily in the process. Scissors were used to scale off a 150g dough-piece as near as possible in one piece. The 150g dough-piece was placed in the balling unit and moulded (twenty revolutions of the plate). It was then removed from the balling unit and passed once through the moulder ensuring that the dough-piece entered the moulder centrally positioned and base first. A dough-holder was taken from a cradle in the cabinet and the clamps were removed. The test piece from the moulder was placed into the centre of the holder and clamped in position. The dough-holder was replaced in the cradle in the cabinet and the door was shut. A timer was set to 45 minutes. A second dough-piece was weighed, balled and moulded. The second holder was removed from the cradle and the dough-piece was clamped. The dough-holder was replaced in the cradle in the cabinet and the door was shut.

Forty five minutes after clamping the first dough-piece, the first dough-holder was placed in position on the balance arm of the extensograph, ensuring that the pen tip was on the extensograph chart paper. The bridge between the two halves of the dough-holder was on the left hand side to avoid impeding the hook. The hook descent was started immediately (Fig. 5.6). Once the dough-piece had broken, the dough-holder was removed from the balance arm and the dough was collected from the dough-holder and hook. The hook was returned to the start position. The chart paper was turned back to the same start position as for the first dough and the

stretching procedure was carried out on the second dough-piece.

Resistance is the mean maximum height of the curves from the two dough-pieces at each test time of 45 minutes. Resistance is given to the nearest 5BU (Brabender units). Extensibility is the mean distance travelled by the chart paper from the moment the hook touches the dough-piece until the dough-piece breaks. Extensibility is given to the nearest millimetre.

## **5.3 Results**

### *5.3.1 Protein analysis of grain from T0 plants*

An SDS-PAGE was performed to determine the types of seed storage proteins being expressed in T1 seeds (i.e. seeds harvested from T0 parents). Three mature seeds of each T0 plant were run across four gels; however two of the gels did not run well including that containing the control line. In the two successful gels some differences between lines could be observed although these were not consistent between replicates in the same line and could be due to differing levels of protein in each sample (Fig. 8.1). This suggests that there was little or no difference in the ratio of gluten proteins between lines, although further study was required to confirm this.

### *5.3.2 T2 grain size and shape analysis*

In order to help determine which lines should be selected to be grown in the next generation, an analysis of the size and shape of the T2 grain was performed. Photographs were taken of grain belonging to 41 T2 lines, including 6 lines from the L24 bar-only control parent. The photographs were analysed to give values for plan area, perimeter, length, width and circularity of each grain image (circularity =  $4\pi \times \text{plan area}/\text{perimeter}^2$ ). A circularity value of 1 indicates a perfect circle and increasingly elongated shapes give values approaching 0. The number of grains analysed for each line ranged from 76 to 703 but was mostly in the range 150-200. The mean of each of the values was determined for each T2 line (Fig. 5.7-Fig. 5.11). While L05.6 apparently had the highest mean

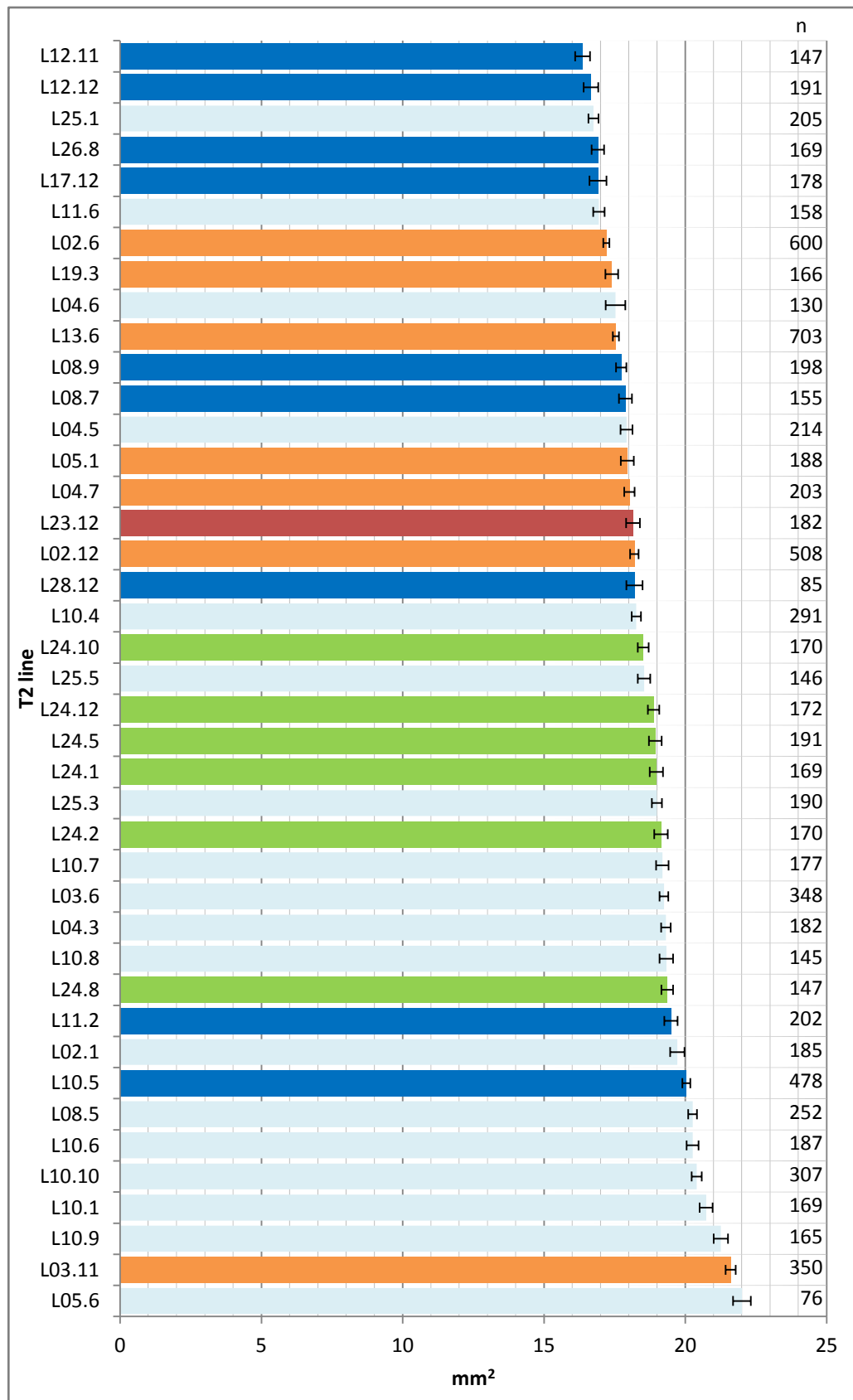


**Fig. 5.7 – Plan area of grain from T2 lines.**

Green bars: bar-only control lines, orange bars: appear hemizygous, blue bars: appear homozygous, pale blue bars: zygosity unknown, red bar: appears null segregant. Error bars indicate standard error. Numbers on the right represent number of grains analysed in each line (n).

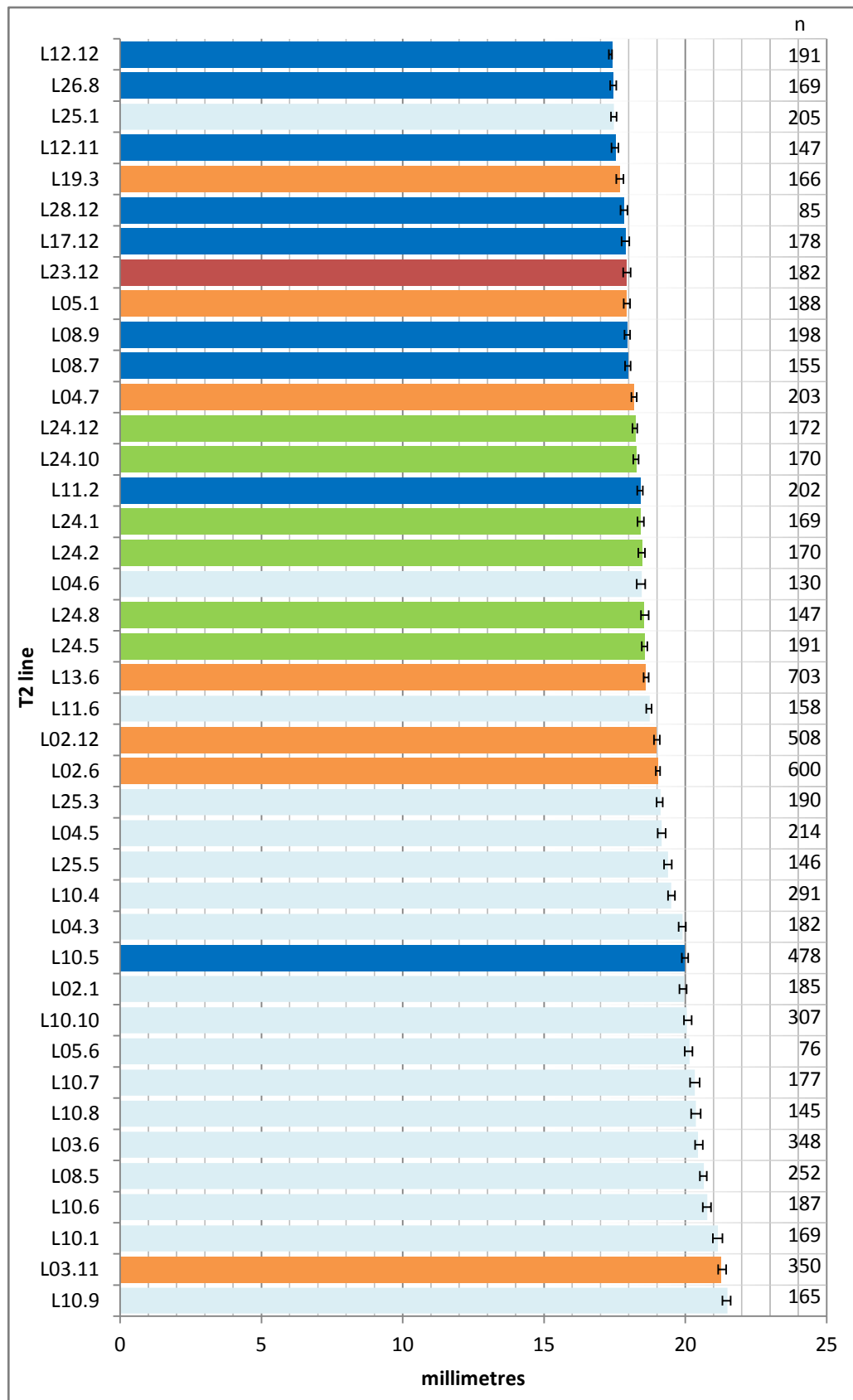


**Fig. 5.8 – Perimeter of grain from T2 lines.**

Green bars: bar-only control lines, orange bars: appear hemizygous, blue bars: appear homozygous, pale blue bars: zygosity unknown, red bar: appears null segregant. Error bars indicate standard error. Numbers on the right represent number of grains analysed in each line (n).

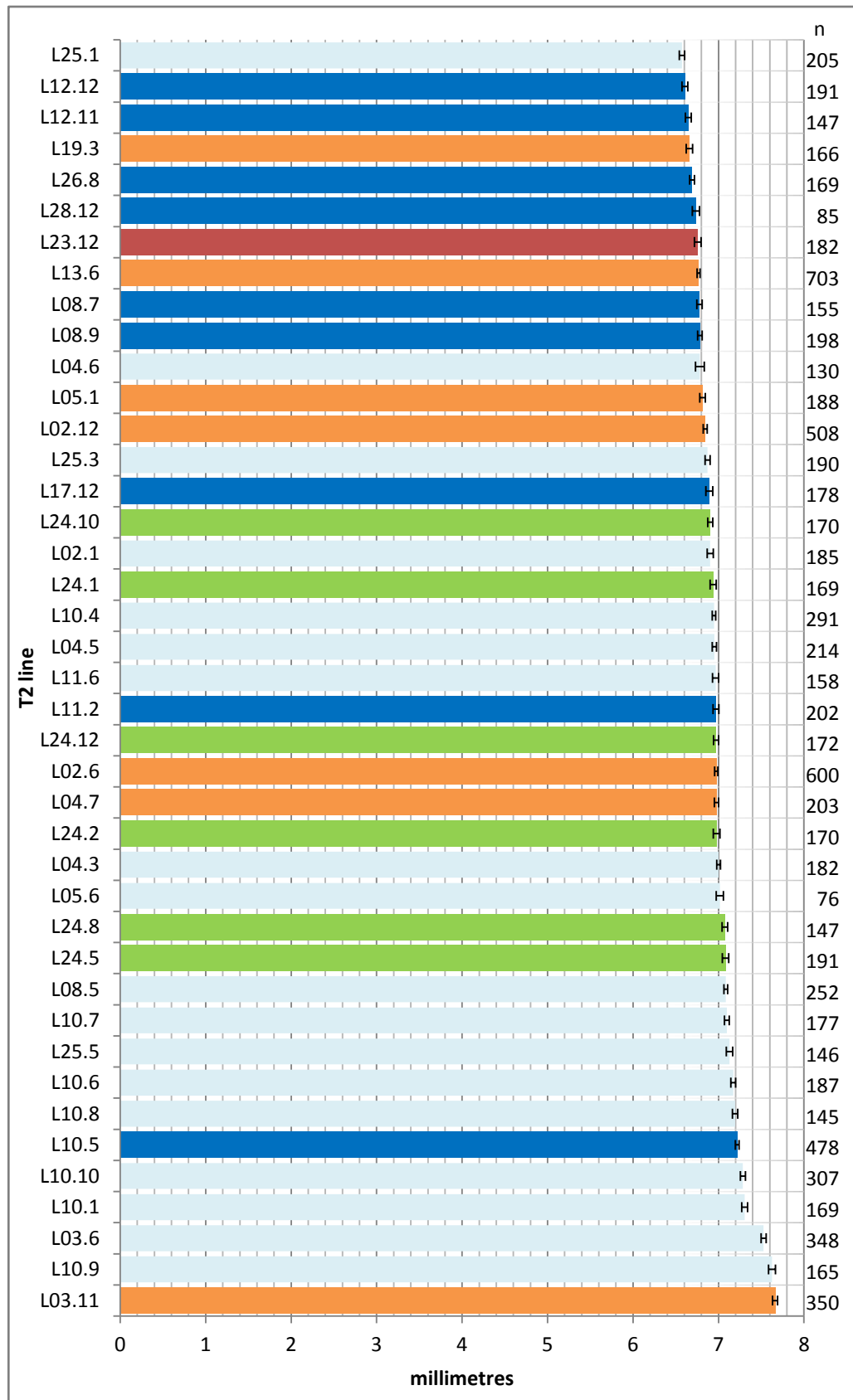


**Fig. 5.9 – Length of grain from T2 lines.**

Green bars: bar-only control lines, orange bars: appear hemizygous, blue bars: appear homozygous, pale blue bars: zygosity unknown, red bar: appears null segregant. Error bars indicate standard error. Numbers on the right represent number of grains analysed in each line (n).

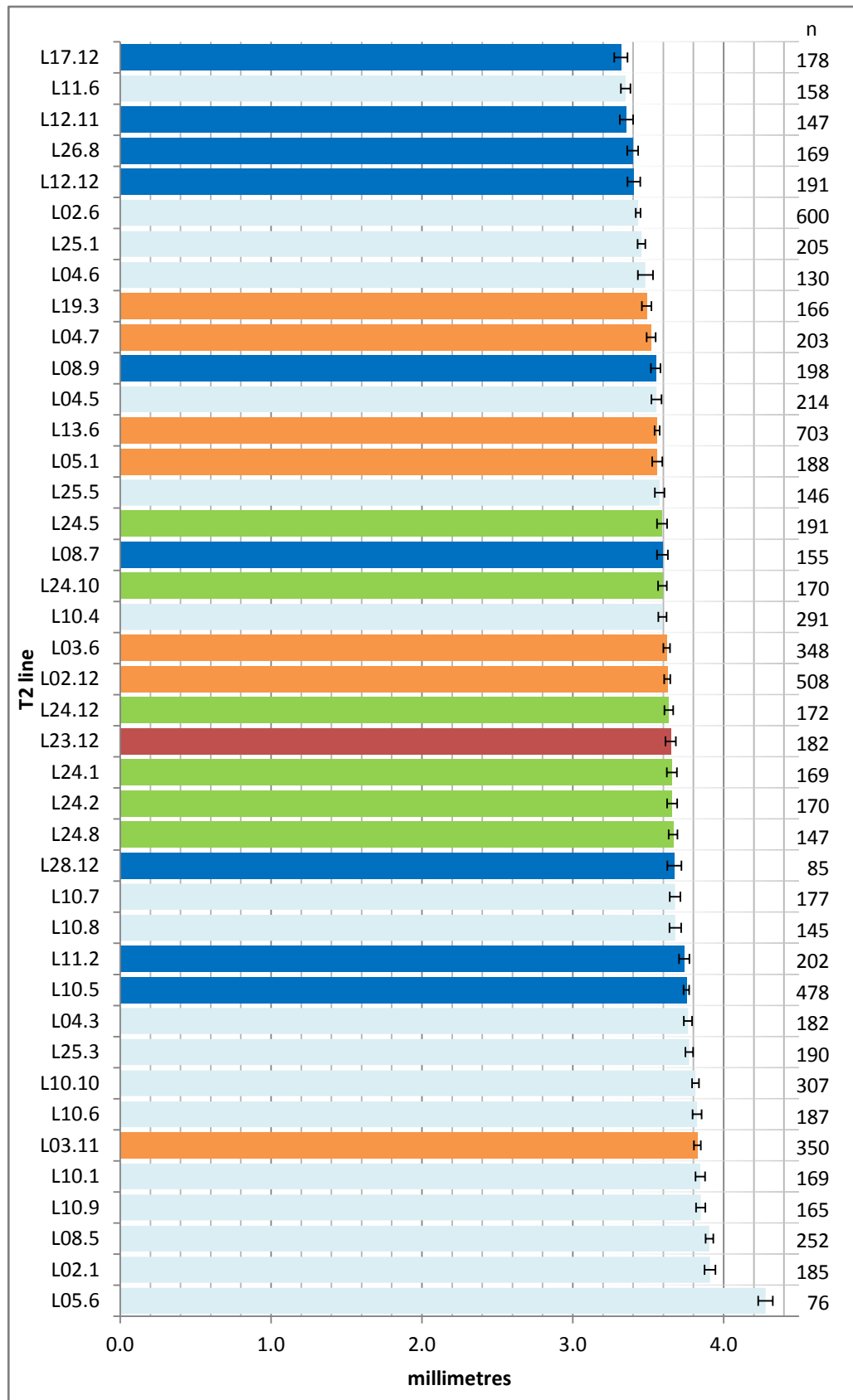


**Fig. 5.10 – Width of grain from T2 lines.**

Green bars: bar-only control lines, orange bars: appear hemizygous, blue bars: appear homozygous, pale blue bars: zygosity unknown, red bar: appears null segregant. Error bars indicate standard error. Numbers on the right represent number of grains analysed in each line (n).

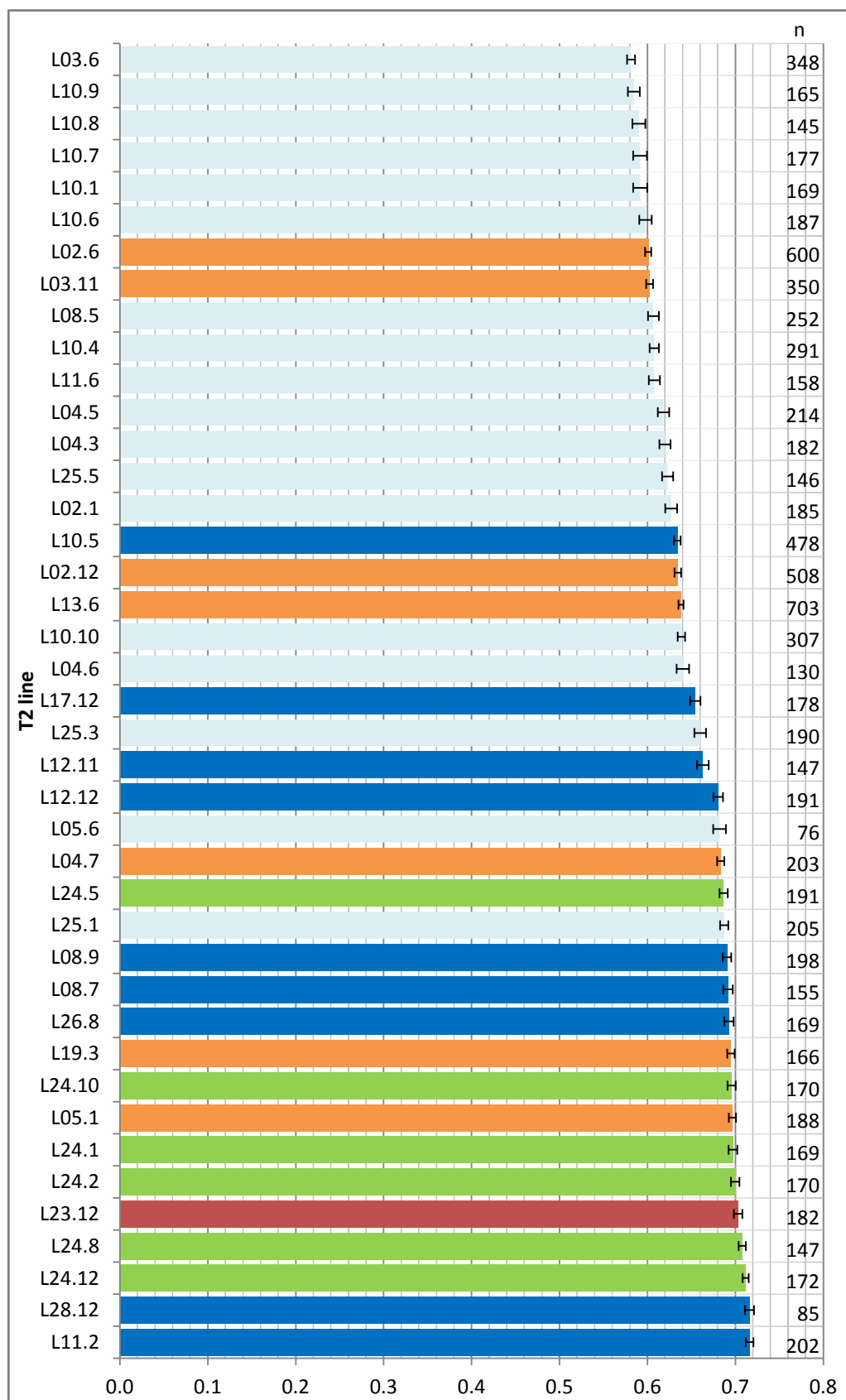


**Fig. 5.11 – Circularity of grain from T2 lines.**

Green bars: bar-only control lines, orange bars: appear hemizygous, blue bars: appear homozygous, pale blue bars: zygosity unknown, red bar: appears null segregant. Error bars indicate standard error. Numbers on the right represent number of grains analysed in each line (n).

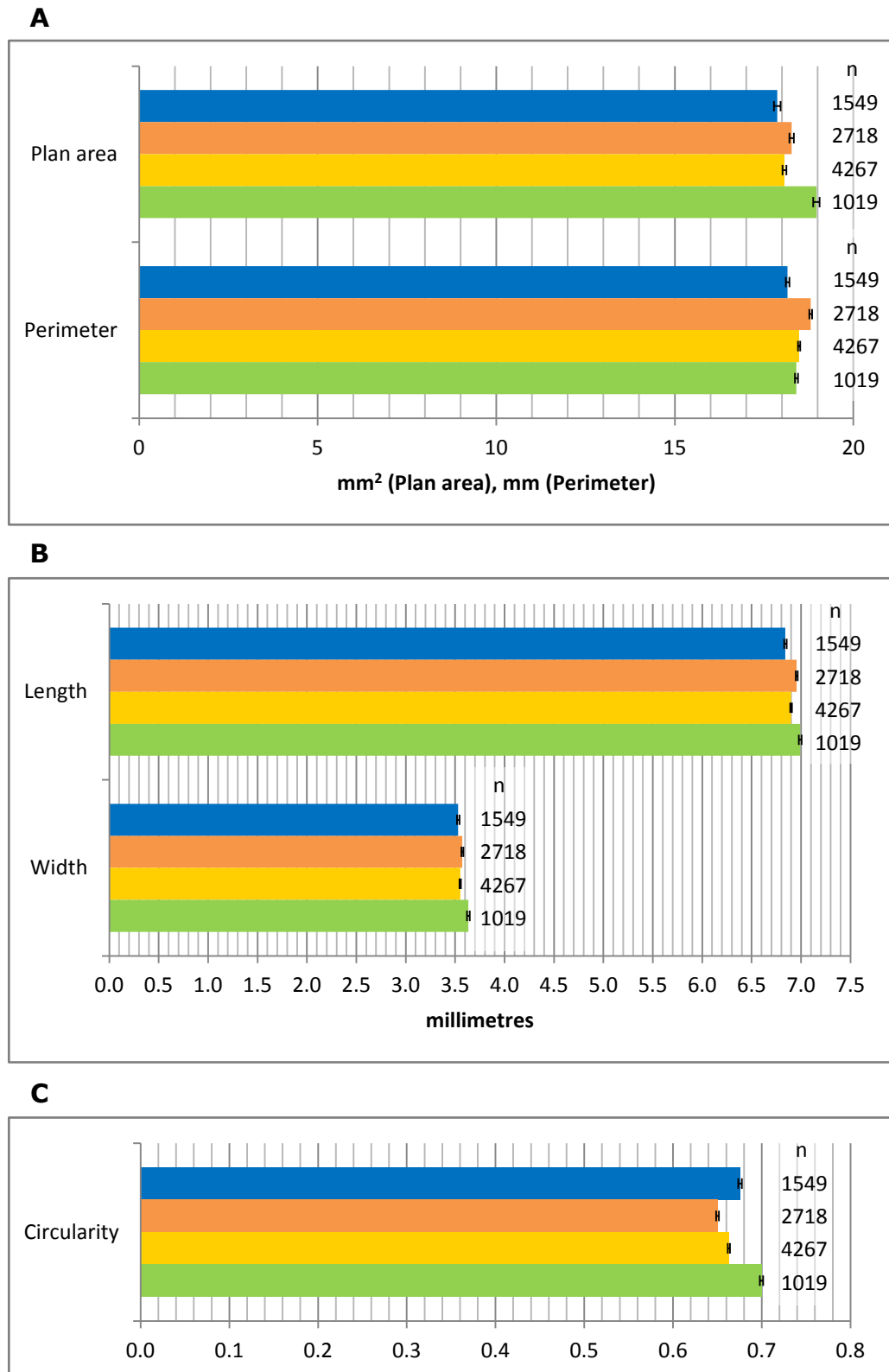


**Fig. 5.12 – Mean size and shape values of grain from T2 lines.**

A: Plan area and Perimeter; B: Length and Width; C: Circularity. Blue bars indicate mean of lines that appear homozygous in PCR, orange bars indicate mean of lines that appear hemizygous in PCR, yellow bars indicate mean of lines that are positive for the transgene in PCR (homozygous + hemizygous), green bars indicate mean of bar-only control lines. Error bars indicate standard error. Numbers on the right represent number of grains analysed in each category (n).

perimeter and width, it had the lowest number of grains analysed (76) therefore its mean values are the least reliable.

The control lines tend towards the mid-range in most of the properties, with a slight leaning towards the higher range in plan area and the lower range in perimeter, and with a wide spread in length. This implies that the transgene has little effect on these grain properties. However, the control lines appeared to have greater circularity than most of the other lines (Fig. 5.11), which would suggest that the transgene reduces grain circularity (i.e. causes a more elongated grain shape). Upon analysis of mean values for PCR homozygous lines, hemizygous lines, transgenic lines (both homozygous and hemizygous) and bar-only control lines, the transgene appears to reduce plan area and circularity (Fig. 5.12).

### *5.3.3 T2 grain protein analysis*

To better understand protein deposition in the T2 grain, SDS-PAGE experiments were carried out on the mature seeds of 30 lines selected by PCR and seed bag weight (Fig. 8.2-Fig. 8.6). Controls used included bar-only and gold-only T1 lines (Fig. 8.2-Fig. 8.4), and a bar-only T2 line (Fig. 5.13-Fig. 8.6). Densitometry was performed by the Cereals and Milling Department at Campden BRI on 5 of the gels. Only very small differences were found between the intensity of the bands in transgenic lines compared to the controls (Fig. 5.14). This indicates that the transgene has little, if any, effect on the ratio of different seed storage proteins, which was suggested by the first SDS-PAGE results.

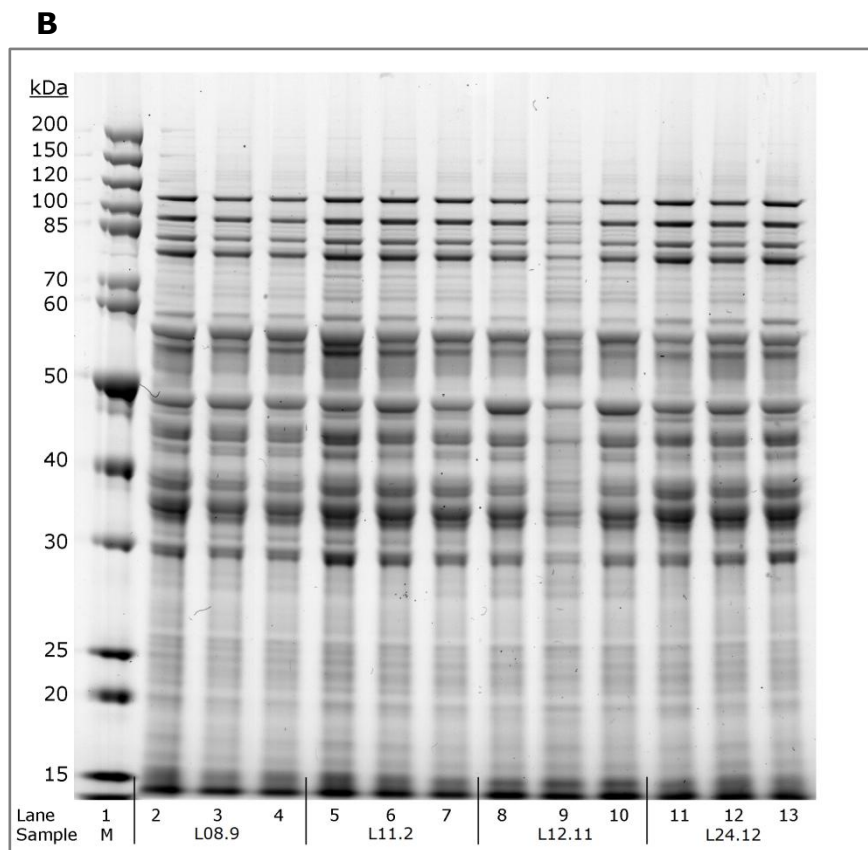
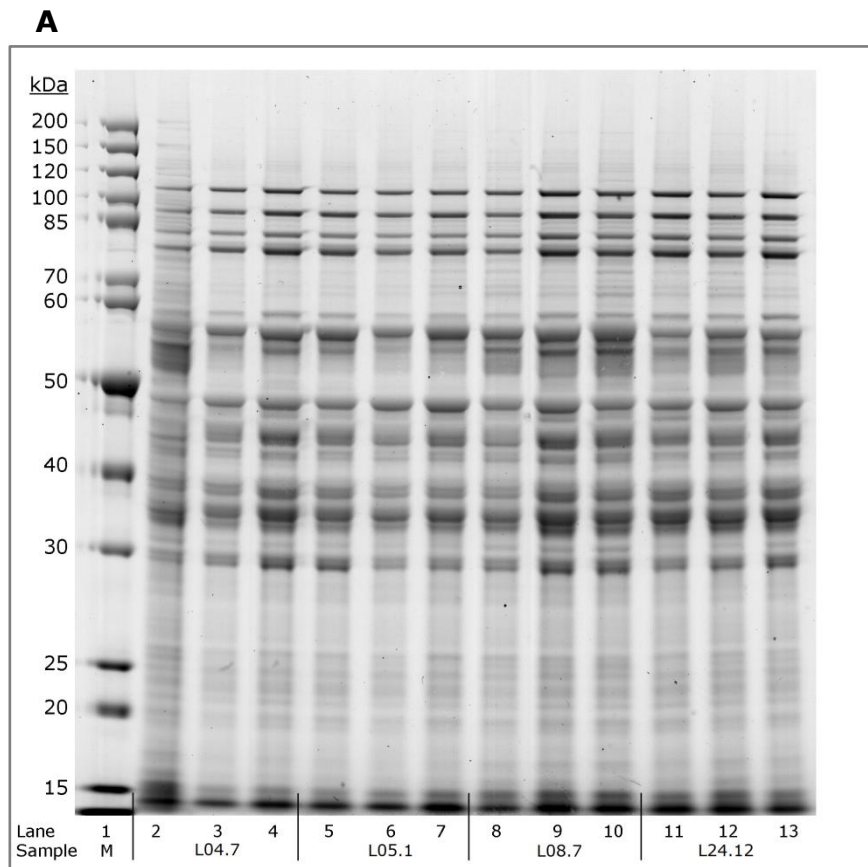


**Fig. 5.13 – SDS-PAGE of mature T2 seeds.**  
 Sizes of marker proteins are indicated on the left in kDa. Lane numbers and line names are displayed below the gels. L24.12 = T2 bar-only control line. M indicates a lane containing protein marker.

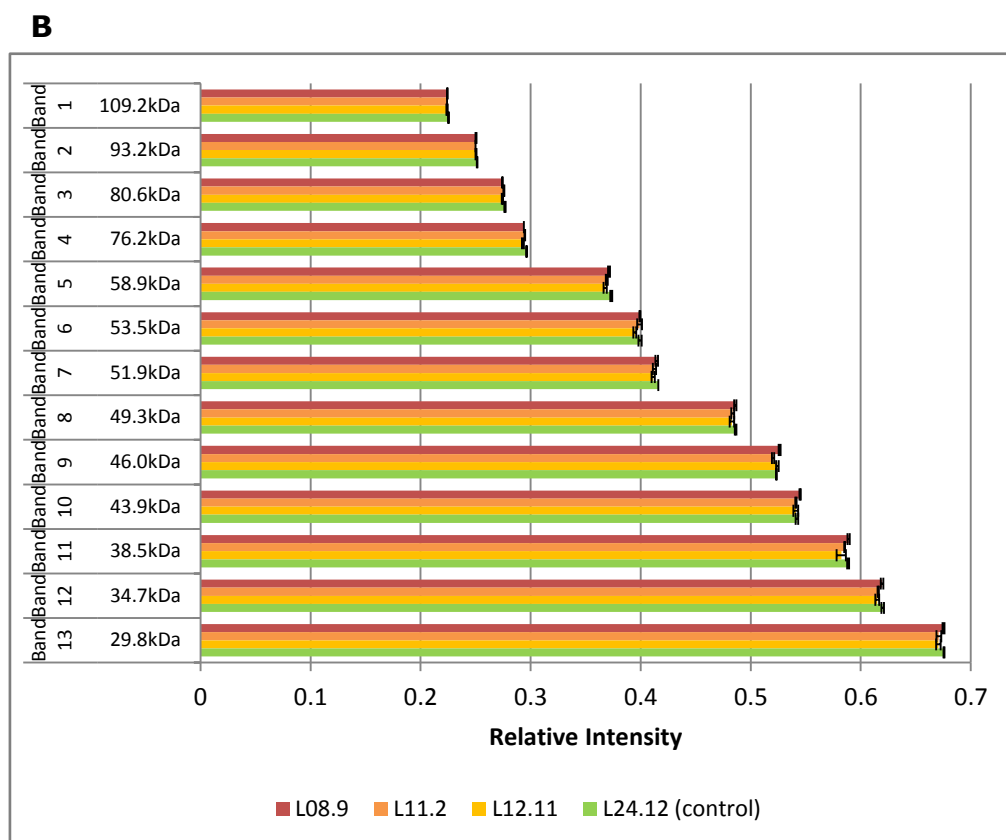
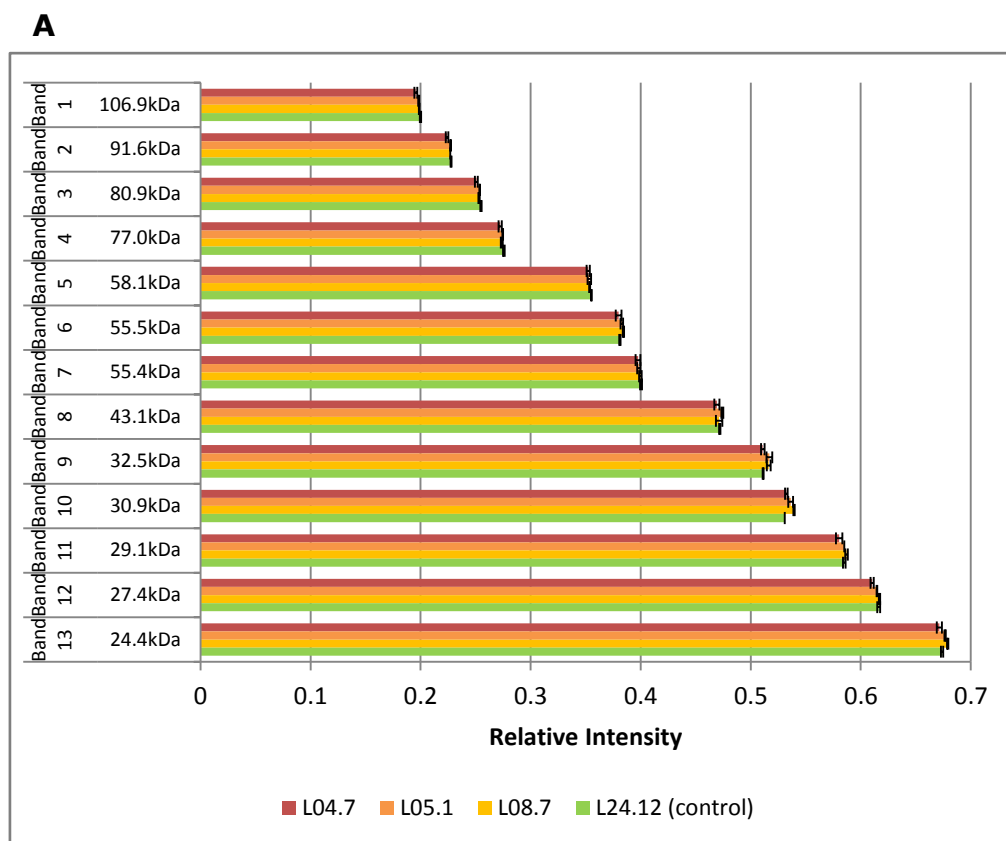


**Fig. 5.14 – Examples of densitometry analysis of T2 SDS-PAGE.**  
 A: Densitometry analysis of Fig. 5.13 A; B: Densitometry analysis of Fig. 5.13 B. Molecular weights of 13 bands are indicated on the left in kDa. Error bars indicate standard error.

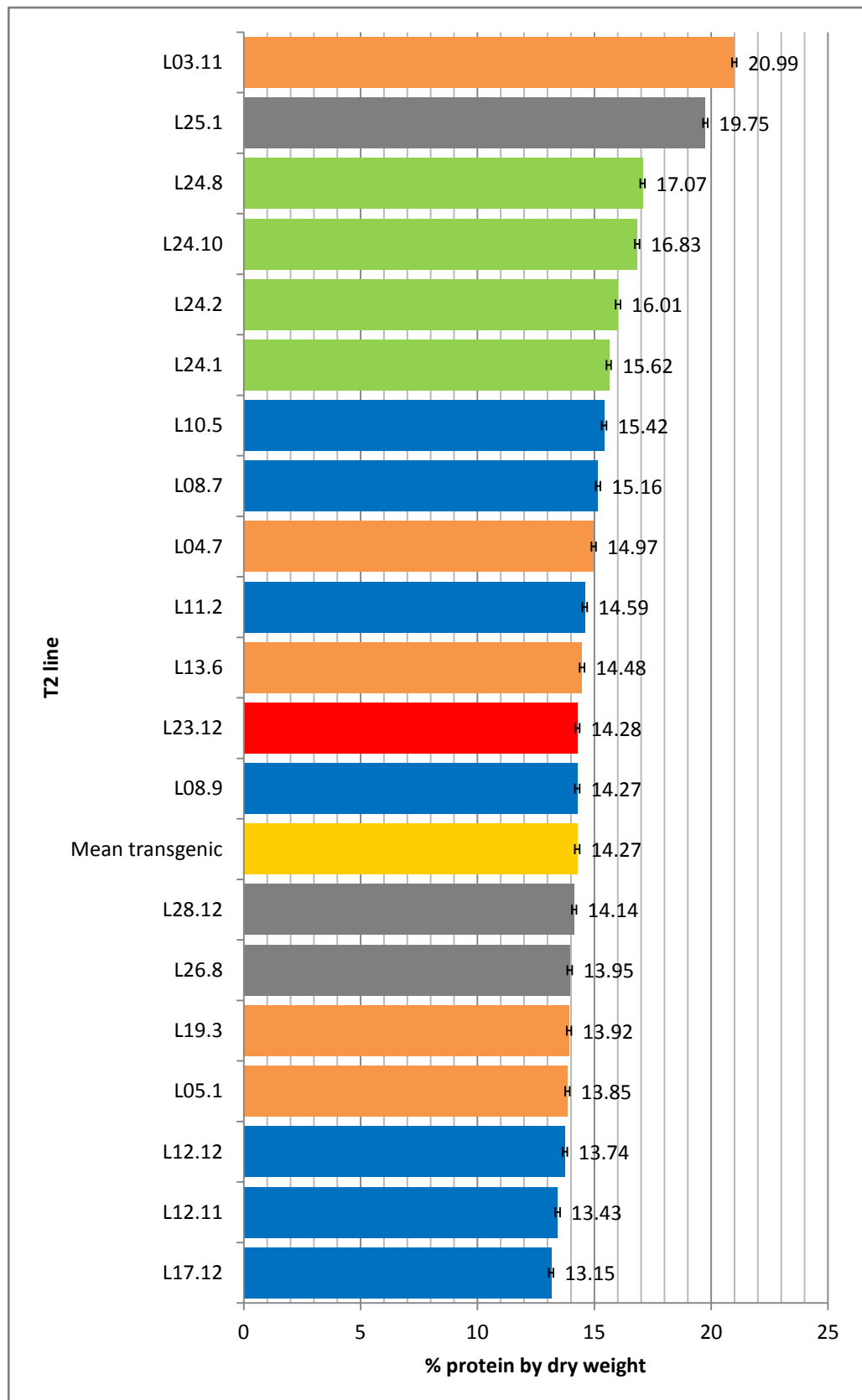


**Fig. 5.15 – Protein content of flour from 20 shortlisted T2 lines as a percentage of dry weight.**

Green bars: bar-only control lines; orange bars: appear hemizygous; blue bars: appear homozygous; grey bars: zygosity unknown; red bar: appears null segregant; yellow bar: mean of transgenic lines (excluding high protein line L03.11). Error bars indicate predicted error of protein and moisture measuring techniques (0.1% dry weight).

After milling, a protein content analysis was carried out on the T2 flour to compare the total levels of protein in the 20 selected lines (Fig. 5.15). The mean protein content of the control T2 lines on a dry weight basis was 16.38% while that of all the T2 lines found to contain the transgene was 14.83% - a proportional drop of 9.5%. If the anomalous high protein transgenic line L03.11 is discounted the proportional difference is a 12.9% reduction in the mean protein content of the transgenic lines.

#### *5.3.4 T2 dough rheology*

The main factor in deciding which homozygous T2 lines to grow on in the next generation was a study of the processing properties of the dough. Twenty lines were chosen to be milled based on transgene PCR and grain weight. Once milled, the flour samples were tested for moisture and protein content (Fig. 5.15) and mixed into dough using reomixer apparatus. The reomixer produced traces of resistance to mixing over the course of 10 minutes, measured in arbitrary units of torque from 0 to 10 (Fig. 5.16). The important features of the trace are peak torque, dough development time (time at peak torque), breakdown amount/angle (reduction in dough strength after peak torque) and trace width.

The high protein line L25.1 showed a high peak torque of 9V but a thin trace and short development time of 130s. On the other hand, homozygous T2 lines L10.5, L12.11 and L17.12 had substantially lower peak torques of around 7 but somewhat longer development times (150-190s). Trace width varied between them -

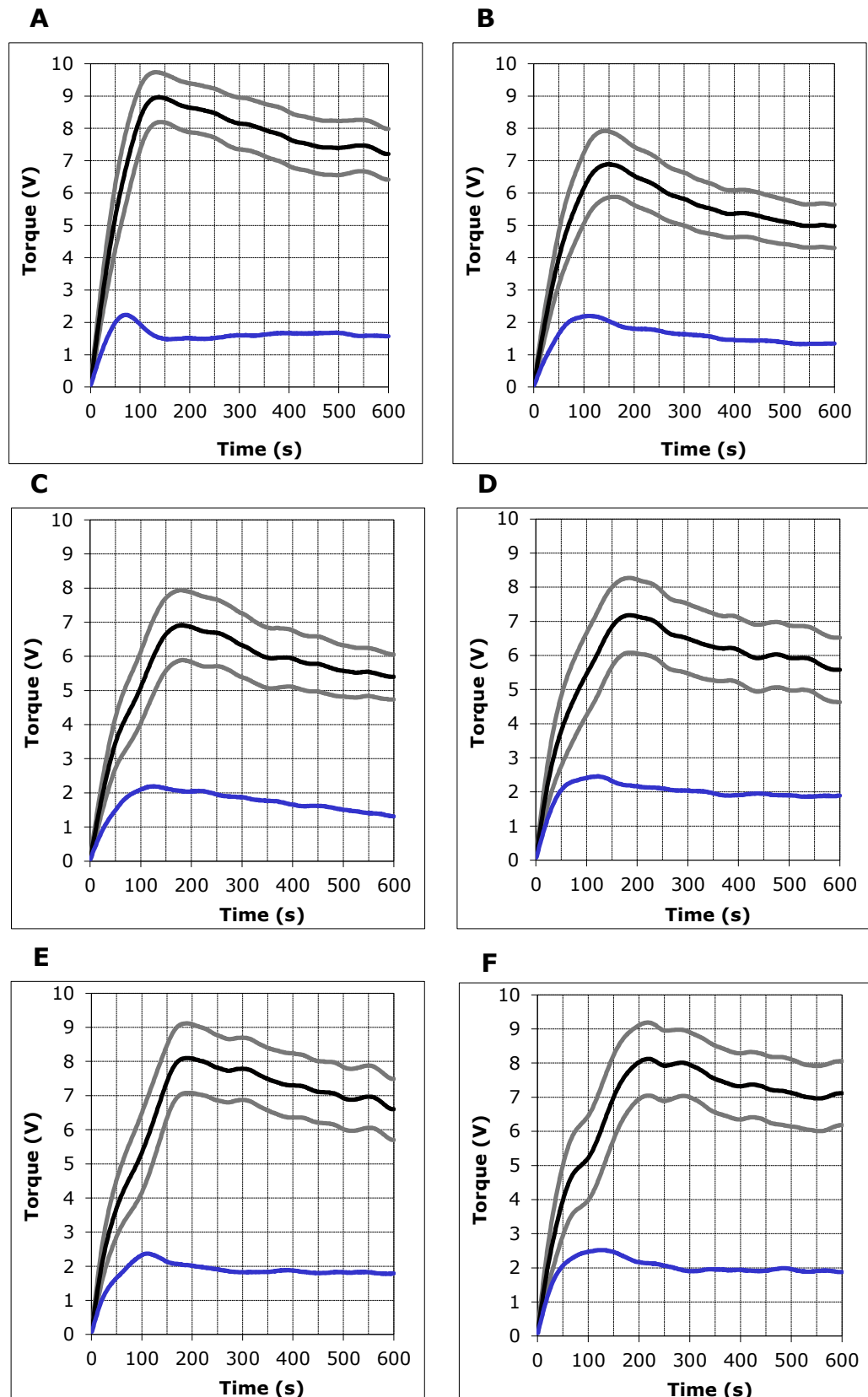


**Fig. 5.16 – Six examples of torque traces during mixing of dough made with flour from T2 lines.**

A: High protein line L25.1; B: Homozygous line L10.5; C: Homozygous line L12.11; D: Homozygous line L17.12; E: Control line L24.2; F: Control line L24.10. Black line indicates middle of trace, grey lines indicate edges of trace, blue line indicates trace width.

L17.12 had the widest trace (similar to the controls) and the trace of the other two lines appeared to gradually narrow after peak torque. The peak torque of the four control lines was in the range 8.1-8.4 and occurred after 195-225s. Trace width was greater than most of the transgenic lines.

Certain variables from the traces of the twenty lines were fed into two dough quality indicators – PC1 and PC2. PC1 increases as peak torque and dough development time decrease, therefore weak biscuit-like flours have a higher PC1 and strong bread-like flours give a lower PC1. PC2 is determined by breakdown – greater breakdown gives a higher PC2 value – so a more stable dough will have a lower PC2. The PC values were calculated for each line and plotted on a quality map (Fig. 5.17).

Not including the anomalous high protein line L03.11, transgenic T2 lines had higher PC1 values and lower PC2 values than the control lines, and homozygous lines more so than hemizygous lines. A null segregant included in the experiment showed similar PC1 to the controls but somewhat decreased PC2, although only one hemizygous line had a PC2 value between the null segregant and the control lines. These results indicate that presence of the transgene in the grain significantly altered the processing properties of the dough.

### *5.3.5 Expression of RabD genes in T3 RabD knockdown line*

In order to support that case that any differences discovered in the T3 line L10.5 were due to the successful knockdown of the

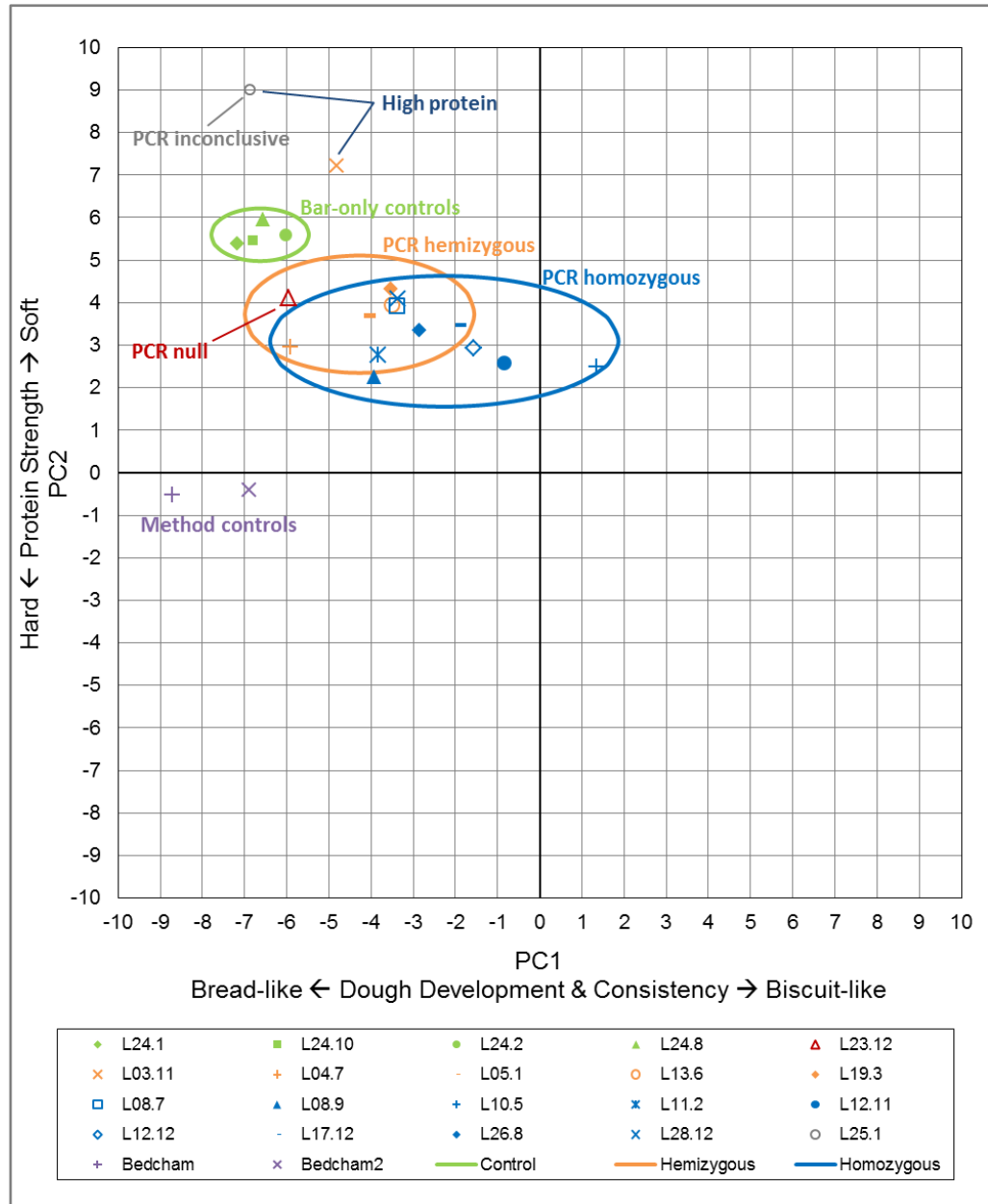


**Fig. 5.17 – Quality map of T2 flour reomixer data.**

Green points: bar-only control lines, orange points: appear hemizygous, blue points: appear homozygous, purple points: method control, red point: appears null segregant, grey point: zygosity unknown. Ellipses are calculated from a group of coordinates based on genotype (control, hemizygous or homozygous) at  $\pm 2.45$  standard deviation from the mean. The high protein line L03.11 was not included in the ellipse calculations.

target *RabD* gene Ta.54382 it was necessary to confirm that expression was reduced in the developing endosperm compared to the T3 control line L24.2. Additionally, it would also be useful to learn whether the RNAi had affected other *RabD* genes due to sequence similarity. To these ends, a quantitative real-time PCR was performed looking at the RNA concentration of four *RabD* genes in the endosperm of T3 lines L10.5 (knockdown) and L24.2 (control) at 14 and 21dpa (Fig. 5.18).

Three other genes were also included as potential normalisation genes and calibrations curves were set up as in the previous qPCR experiment (Expression of *RabD* genes in developing wheat endosperm). RNA concentration data for the *RabD* genes were normalised using the Ta.54227 gene (for primers see Table 2).

All four *RabD* genes were found to some extent to have lower transcript levels at 14dpa in the transgenic line compared to the control. The *RabD1* genes Ta.35418 and Ta.47209 had 49% and 22% reductions in RNA concentration respectively. The *RabD2a* target gene Ta.54382 saw a 60% reduction and its closest relative Ta.54881 had 50% lower expression than in the control. At 21dpa the RNA concentrations of *RabD2* genes Ta.54382 and Ta.54881 again showed similar drops in the transgenic line compared to the control line of 58% and 60% respectively. However, at 21dpa the RNAi effect on the *RabD1* genes was larger in Ta.47209 (51% transcript reduction compared to control) than Ta.35418 (appeared to be slightly reduced but the difference was not statistically significant), which contrasts with the *RabD1* expression drops at

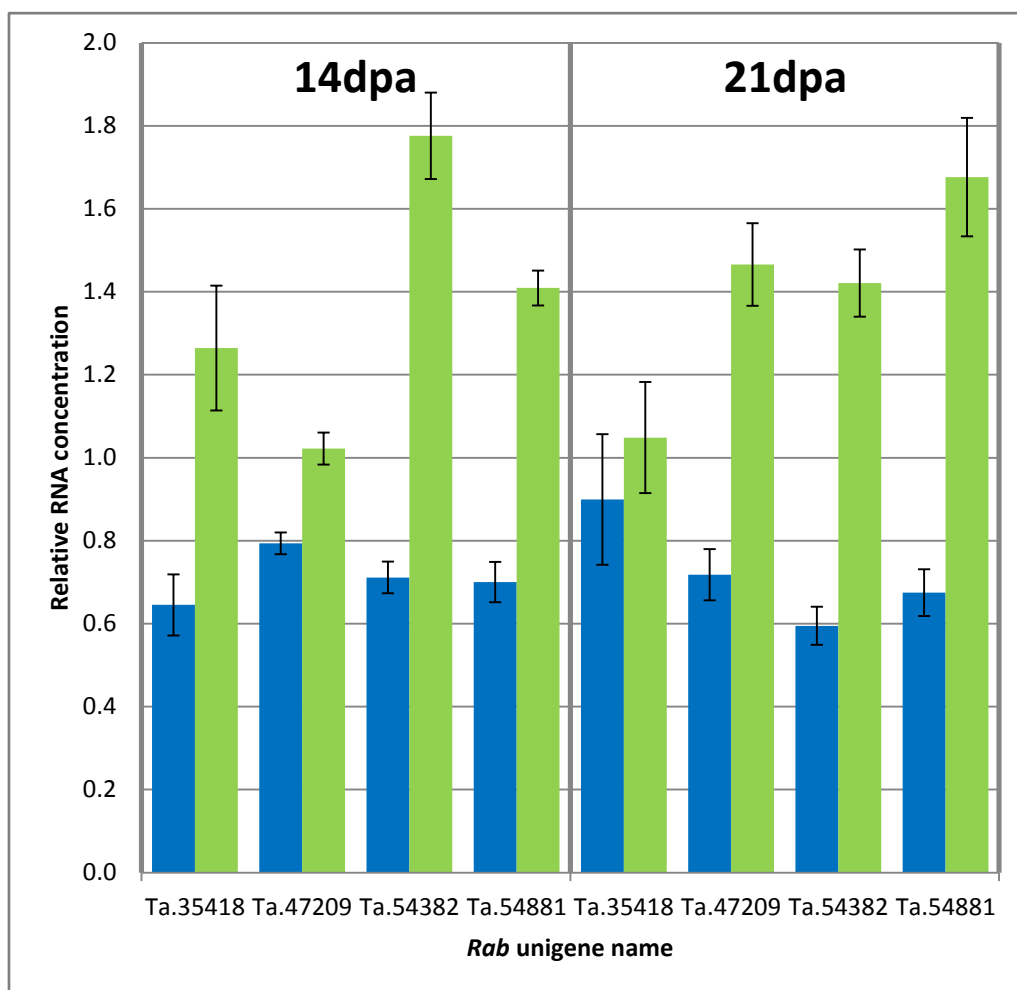


**Fig. 5.18 - Expression of *RabD* genes at 14 and 21 days post anthesis in the developing endosperm of T3 wheat.**

Blue bars: L10.5 (GM), green bars: L24.2 (control). Expression normalised with Ta.54227 gene (cell division control). Error bars indicate standard error. *RabD1a* = Ta.35418, *RabD1b* = Ta.47209, *RabD2a* = Ta.54382, *RabD2b* = Ta.54881.

14dpa where Ta.35418 appeared to be affected more. The transgene clearly had a large effect on RNA concentration of *RabD* genes in the developing endosperm, with *RabD2* genes knocked down by 50-60% at 14 and 21dpa.

### *5.3.6 T3 grain size and shape analysis*

An analysis of the size and shape of the T3 grain was performed in order to reveal any differences between the knockdown and control lines and to determine whether or not differences seen in the T2 generation were also present between T3 lines (Fig. 5.19). Photographs were taken of grain belonging to the T3 knockdown line L10.5 and the T3 control line L24.2. The photographs were analysed to give values for plan area, perimeter, length, width and circularity of each grain image (as T2 grain size and shape analysis). The data set for L10.5 was produced through analysis of 1329 grains and that for L24.2 from 984 grains.

There is a slightly greater perimeter and smaller plan area in the grains of the T3 knockdown line compared to the control line (Fig. 5.19 A). Additionally, the knockout grains are slightly longer and thinner (Fig. 5.19 B). These combined small differences result in a significant reduction in circularity of the knockdown line compared to the control (Fig. 5.19 C). This finding agrees with the results from the T2 generation (Fig. 5.11), which further indicates that the changes seen are caused by the transgene.

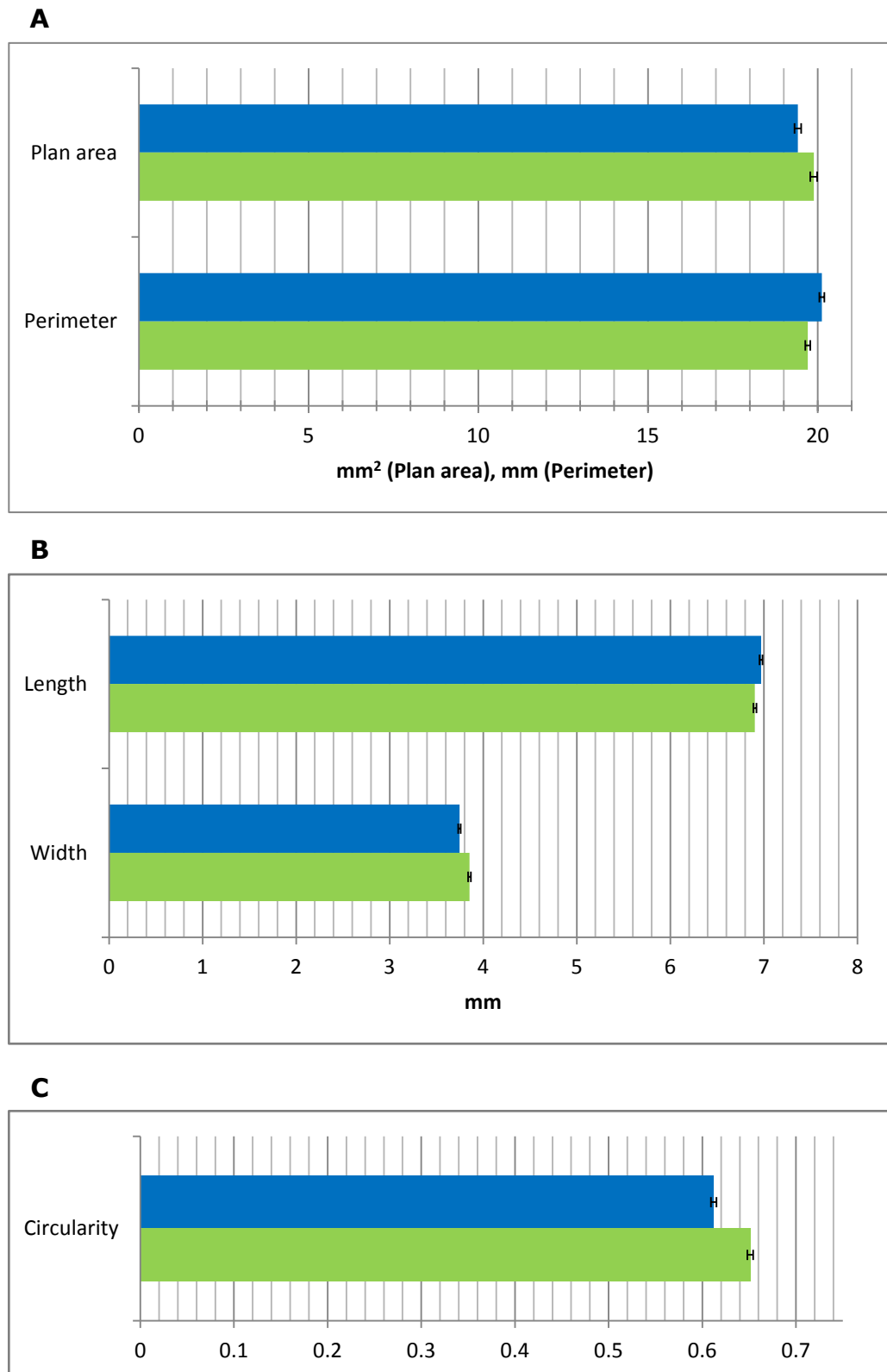


**Fig. 5.19 – Mean size and shape values of grain from T3 lines.**

A: Plan area and Perimeter; B: Length and Width; C: Circularity. Blue bars indicate T3 knockdown line L10.5 (1329 grains analysed), green bars indicate T3 bar-only control line L24.2 (984 grains analysed). Error bars indicate standard error.

### *5.3.7 Yield of T3 grain harvest*

Mature grain was harvested from 100 T2 wheat plants of each line (L10.5 and L24.2) and threshed before undergoing size and shape analysis. The grain was conditioned to 16.3% moisture before milling at which point the grain weight of the T3 knockdown line L10.5 was 1822g and that of the T3 control line L24.2 was 1615g, a proportional difference of 12.8% more in the transgenic line. In the previous generation, grain was harvested from individual T1 plants. In that generation the L10.5 T1 plant produced 20.03g of grain and the L24.2 plant produced 23.67g (15.4% less in the transgenic line). As the transgenic line produced more T3 grain but less T2 grain compared to the control, it cannot be determined whether any difference in yield is caused by the transgene.

### *5.3.8 Analysis of T3 grain protein content*

An analysis of protein content determined that there was a 1.37% reduction in total protein in the T3 transgenic line L10.5 compared to the control line L24.2, a proportional difference of 9.2% (Fig. 5.20 A). This finding concurs with the differences in protein content of T2 transgenic lines compared to the T2 controls (Fig. 5.15), and specifically the difference between T2 lines L10.5 and L24.2. No significant difference in starch content was found between the T3 knockdown and control lines (Fig. 5.20 B).

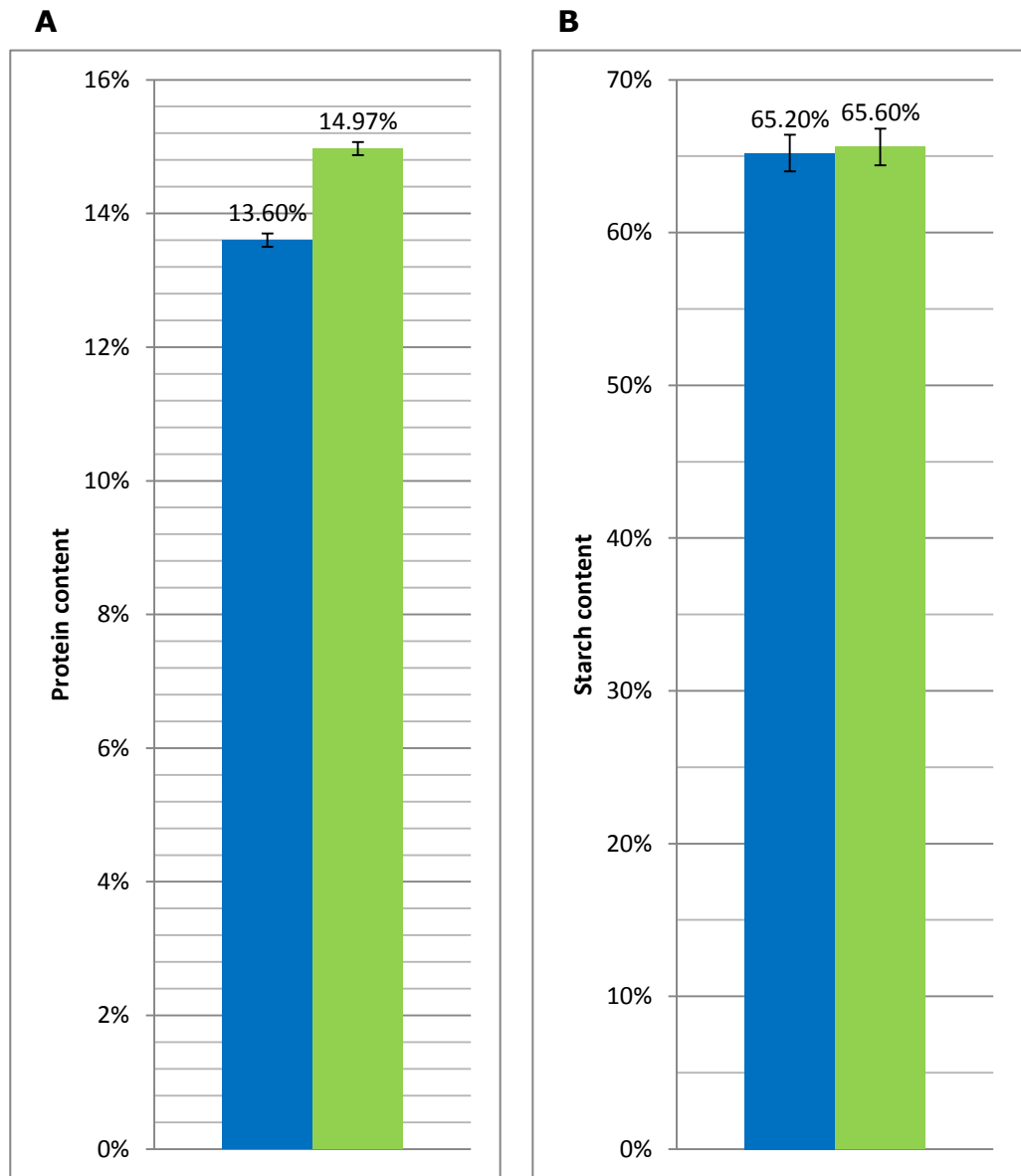


**Fig. 5.20 – Protein and starch content of flour from knockdown and control T3 lines as a percentage of dry weight.**

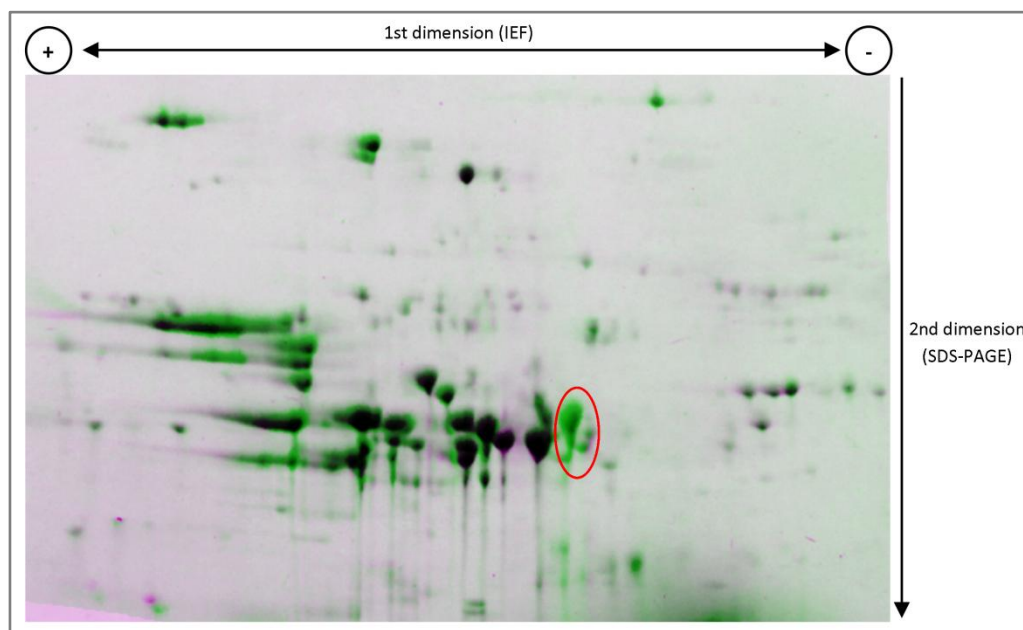
A: Protein content of T3 lines on dry weight basis; B: starch content of T3 lines. The blue bars represent T3 knockdown line L10.5, the green bars represent T3 bar-only control line L24.2. Error bars indicate predicted error of measuring techniques.

### *5.3.9 Two-dimensional gel analysis of T3 lines*

No substantial changes in levels of different protein subunits were previously found when SDS-PAGE was performed on mature seeds from 29 T2 lines (Fig. 8.2-Fig. 8.6). In order to confirm the levels of subunits were unchanged between the transgenic and control T3 lines a two dimensional PAGE was performed by Doug Smith at Campden BRI using flour from the knockdown and control lines (Fig. 5.21). There appeared to be more protein loaded onto the transgenic gel than the control gel, which makes identification of differences largely speculative. Additionally, only one gel of each line was run, which rules out calculation of statistical significance of spots using 2D gel software. However, taken as a preliminary experiment there are some promising features which hint at differences in a few seed storage proteins.

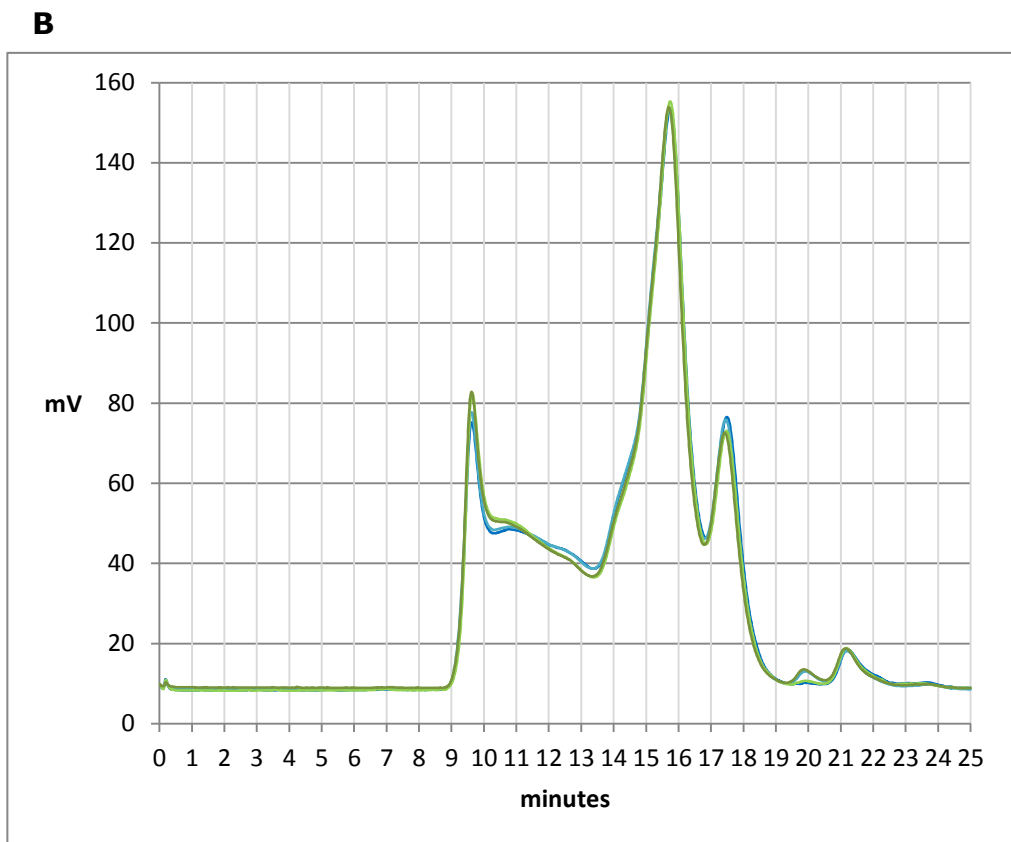
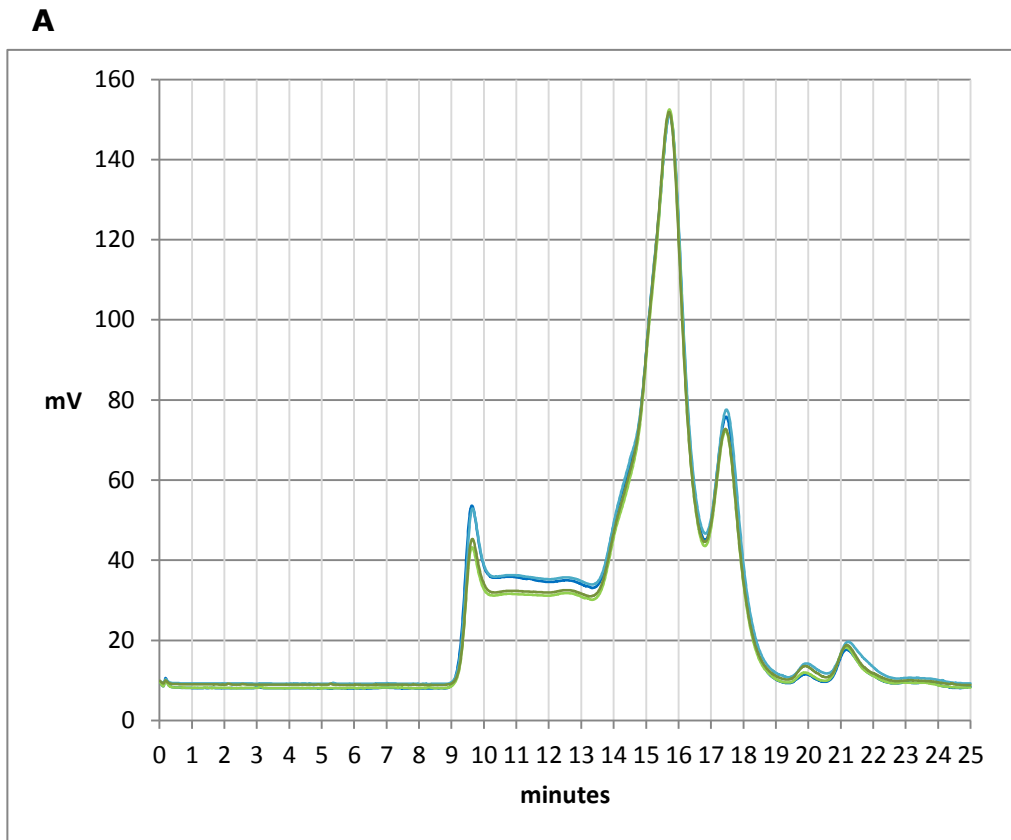
### *5.3.10 Analysis of glutenin macropolymer composition in T3 dough*

As the difference in protein content was relatively small compared to the alteration of dough rheology in the T2 generation (Fig. 5.15-Fig. 5.17) and the relative levels of gluten subunits were very similar (Fig. 5.14), it was hypothesised that other factors were contributing to the processing properties of the dough. To investigate bonding strength of subunits in the glutenin macropolymer that gives dough its elastic properties, a size exclusion high performance liquid chromatography (SE-HPLC) experiment was carried out (Fig. 5.22). Two replicates of each T3



**Fig. 5.21 – Aligned and overlaid images of 2D gels from T3 flour.**

Protein from T3 transgenic line L10.5 shown in green. Protein from T3 control line L24.2 shown in pink. The first dimension run (horizontal) was isoelectric focussing (IEF) and second dimension (vertical) was SDS-PAGE. Possible increased protein in transgenic line circled in red.

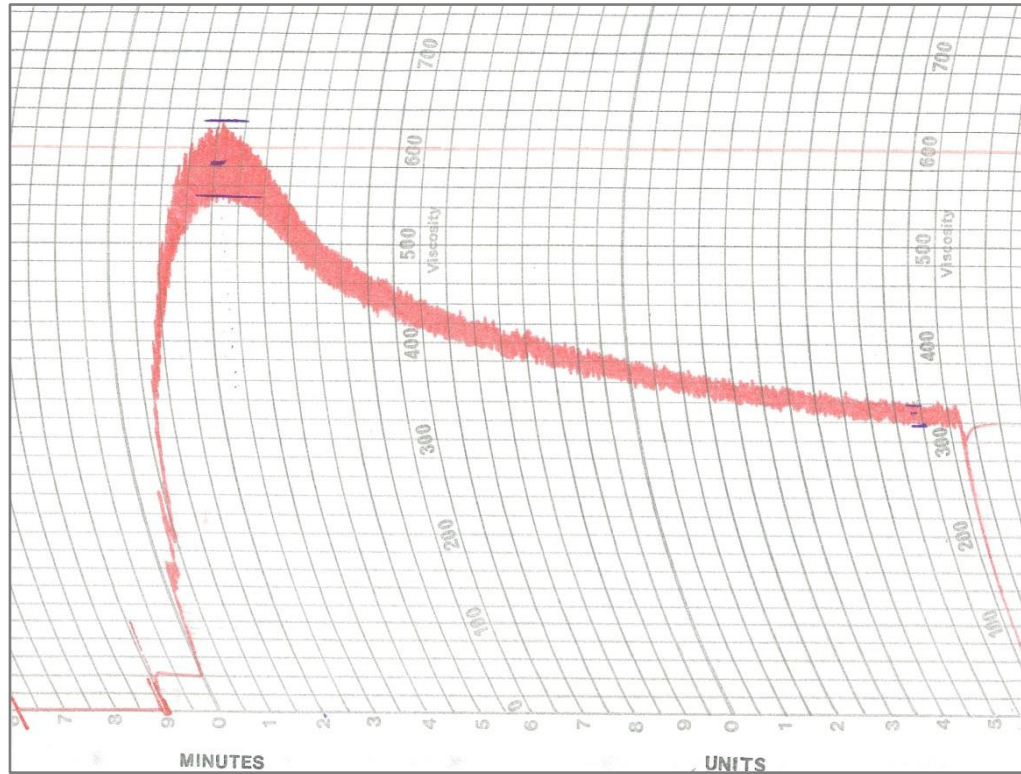
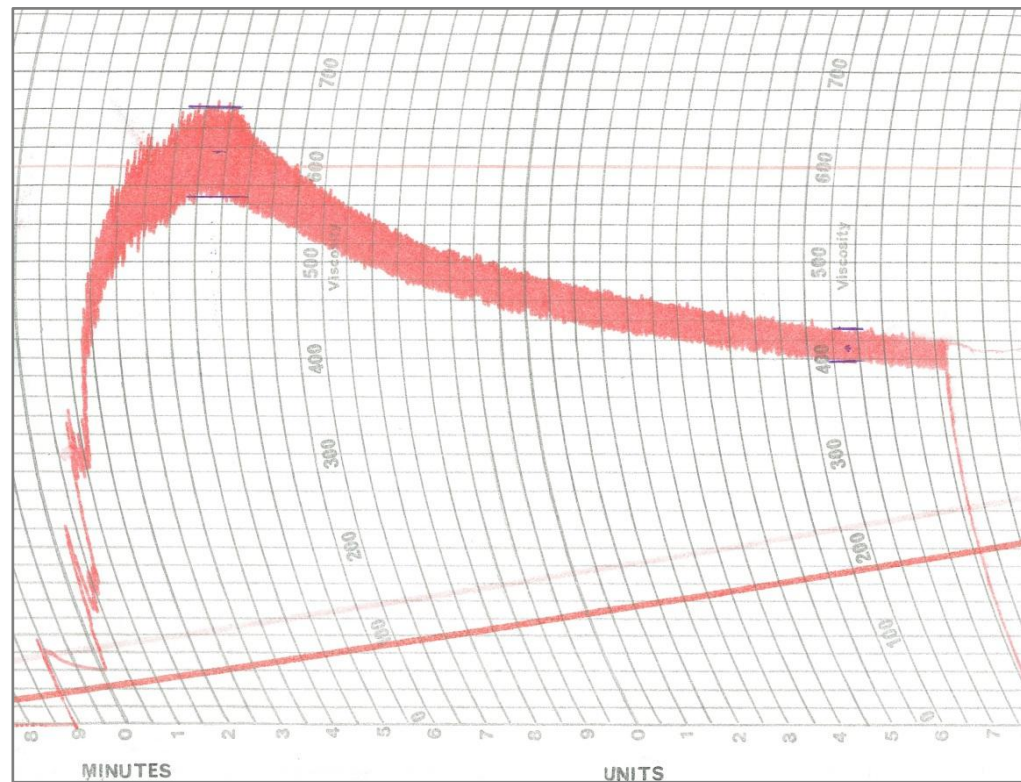


**Fig. 5.22 – SE-HPLC traces of protein from T3 flour samples.**

A: Untreated flour sample. B: Sonicated flour sample. The two replicates of T3 line L10.5 are in light and dark blue; the two replicates of T3 bar-only control line L24.2 are in light and dark green.

line were run untreated and sonicated. Proteins with a higher molecular weight run through the column faster and are on the left of the plot while smaller proteins take longer to pass through the column and are on the right. The purpose of the sonication was to disrupt bonding in the glutenin macropolymer, which has a very high molecular weight and is excluded from the column. Proteins present in the untreated samples consist of monomers, oligomers and glutenin subunits which were only weakly bound to the glutenin macropolymer. The sonicated samples should contain the same proteins as the equivalent untreated samples plus the glutenin subunits that have been released from the macropolymer.

The plot of untreated samples shows that there is visibly more protein in the whole glutenin subunit range between 9m and 13m40s in the T3 knockdown line L10.5 than the T3 control line L24.2 (Fig. 5.22). There is also a smaller difference in the globulin/albumin fraction between 16m50s and 19m, with the transgenic line again showing more protein. The two lines appear similar in the 13m40s-14m45s fraction, though with a slightly higher protein level in the transgenic, while the 14m45s-16m50s  $\alpha$ -/ $\gamma$ -gliadin fraction appears identical between lines. In the plot of sonicated samples the 14m45s-16m50s  $\alpha$ -/ $\gamma$ -gliadin and 16m50s-19m globulin/albumin fractions appear unchanged from the untreated samples, while the 13m40s-14m45s  $\omega$ -gliadin fraction appears to increase slightly in both T3 lines compared to the untreated samples. The 9m-13m40s glutenin subunit range is where the sonication has had the most effect with both lines showing more

**A****B**

**Fig. 5.23 – Farinograph traces of dough made with flour from T3 lines.**

X-axis = time (minutes); y-axis = resistance to mixing (Brabender units). A: T3 knockdown line L10.5 (Development time 2 minutes, Stability 1.5 minutes, Degree of softening 250BU). B: T3 bar-only control line L24.2 (Development time 3.5 minutes, Stability 2.5 minutes, Degree of softening 200BU).

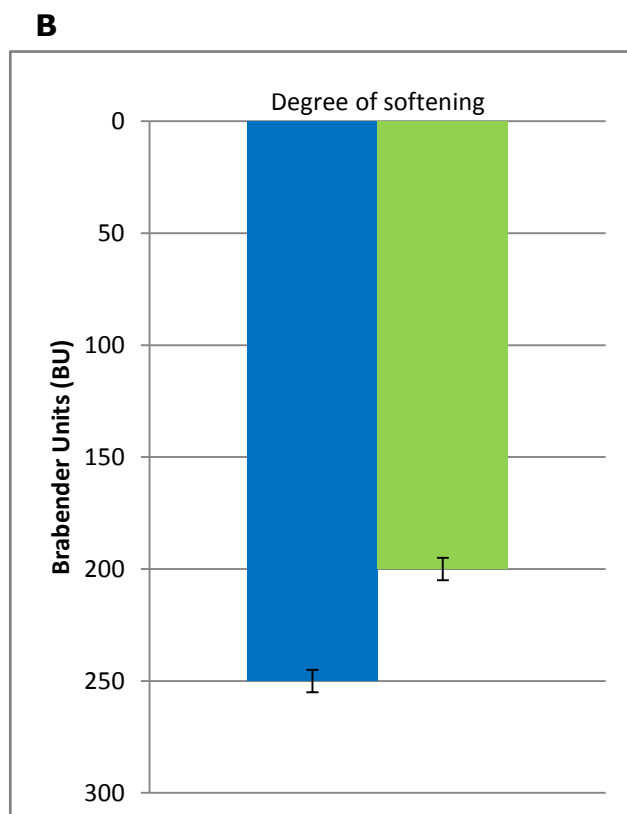
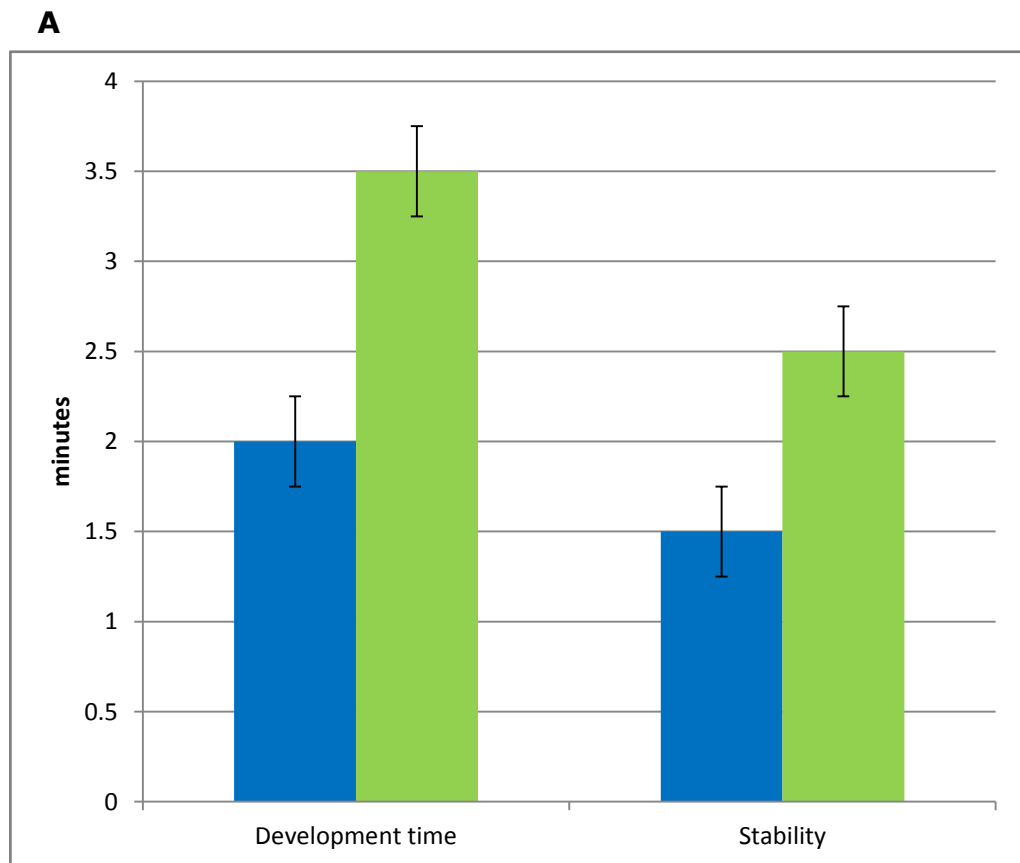
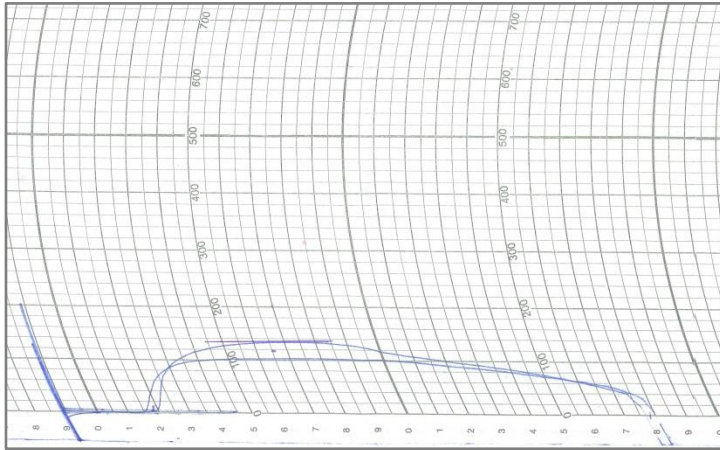


**Fig. 5.24 – Results from farinograph mixing of T3 dough.**

A: Development time (time until peak resistance) and Stability (amount of time during which the top of the trace is above the centre of peak resistance) - times were rounded to the nearest 0.5 minutes, indicated by error bars. B: Degree of softening (drop in resistance between peak resistance and 12 minutes after peak resistance) - values are given to the nearest 10 BU, indicated by error bars. The blue bars represent T3 knockdown line L10.5, the green bars represent T3 bar-only control line L24.2.

**A**



**B**

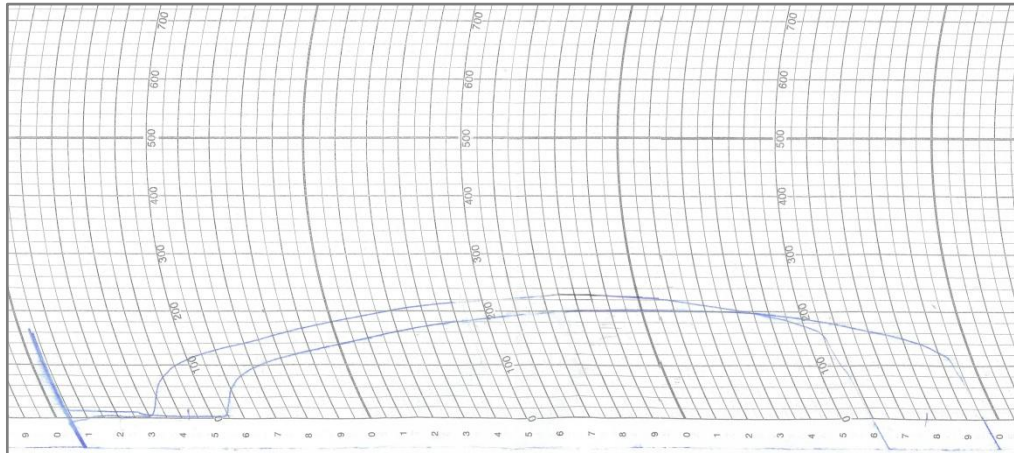


**Fig. 5.25 – Extensograph traces of dough made with flour from T3 lines.**

X-axis = time (min); y-axis = resistance to stretching (Brabender units). A: T3 knockdown line L10.5 (Resistance 120BU, Extensibility 16cm). B: T3 bar-only control line L24.2 (Resistance 210BU, Extensibility 23.5cm)

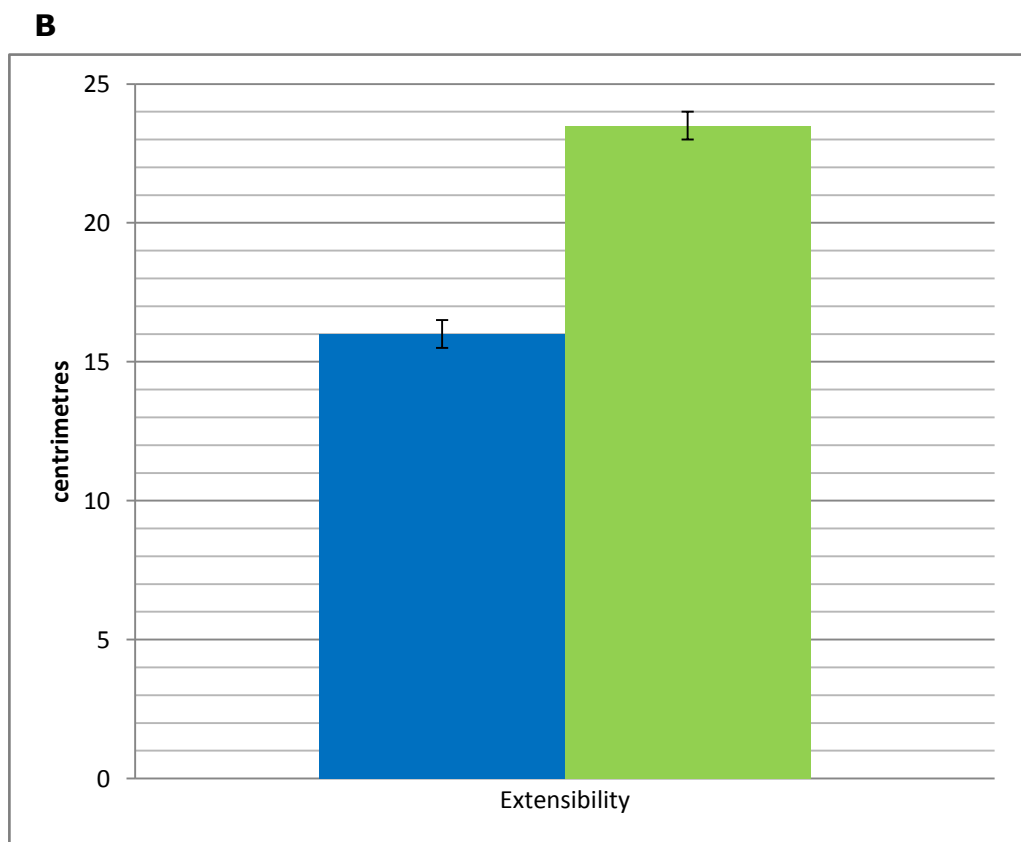
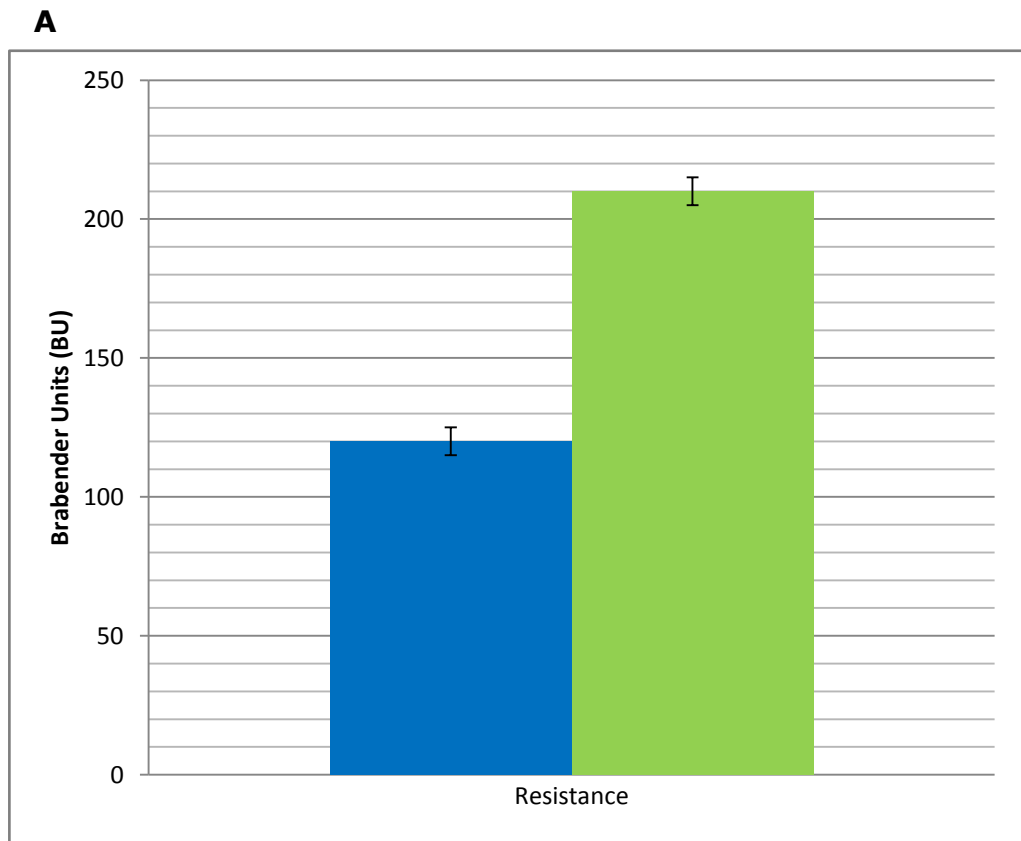


**Fig. 5.26 – Measurement of T3 dough processing properties by extensograph.**  
 A: Resistance (peak resistance during stretching) – values are given to the nearest 10 BU, indicated by error bars. B: Extensibility (time until dough breaks) – values are given to the nearest 0.5 minutes, indicated by error bars. The blue bars represent T3 knockdown line L10.5, the green bars represent T3 bar-only control line L24.2.

protein compared to the untreated samples, though the fractions increase by varying amounts. In the 9m-10m10s HMW-GS and 10m10s-11m20s LMW-GS fractions the knockdown line displays a lower level of protein compared to the control, whereas in the 11m20s-13m40s LMW-GS fraction the knockdown shows more protein than the control.

### *5.3.11 T3 dough rheology*

The small-scale rheology results from the T2 generation (Fig. 5.16-Fig. 5.17) showed substantial changes in the processing characteristics of the dough of transgenic lines. In order to demonstrate the specific changes in gluten quality on a larger scale, farinograph and extensograph tests were carried out (Fig. 5.23-Fig. 5.26). The Brabender farinograph measures and records the resistance of a dough to mixing as it is formed from flour and water, is developed and is broken down. While similar to the reomixer test performed on T2 flour (see 5.3.4 T2 dough rheology), the farinograph is better established and more reliable. The dough mixed by the farinograph is moulded on the Brabender extensograph into a standard shape and rested for 45 minutes before being stretched to breaking point on the extensograph and a curve drawn recording the extensibility of the dough and its resistance to stretching. The dough is immediately remoulded and, after a further rest period, is re-stretched.

In the traces produced by the farinograph, there are clear differences between the T3 knockdown line L10.5 and the T3 control

line L24.2 (Fig. 5.23). The dough development time (time until peak resistance) is noticeably shorter in the knockdown line and the dough starts to break down more quickly after peak resistance. Additionally, the width of the trace in the knockdown line is smaller than in the control throughout the mixing and the resistance drops to a lower level compared to the control. The specific measurements made by the farinograph back up these observations (Fig. 5.24). The knockout line had a 43% reduction in development time, 40% reduction in stability (time during which the top edge of the trace is above the centre of the peak resistance) and 25% increase in degree of softening (difference in resistance between peak resistance and 12 minutes after peak resistance) compared to the control line.

The extensograph traces show that dough made from the T3 knockdown line was less resistant to extension and also broke much earlier than dough made from the control line (Fig. 5.25). This is reflected by the resistance (peak resistance during stretching) and extensibility (time until dough breaks) figures which were respectively 43% lower and 32% lower in the knockout line compared to the control (Fig. 5.26).

## **5.4 Discussion**

### *5.4.1 Protein content of transgenic wheat*

In both T2 and T3 generations the knockdown lines had a lower protein content than the control lines. This could be due to limits in ER to Golgi trafficking causing a bottleneck in the process of protein production, transport and storage. As such this may have led to negative feedback in the expression of seed storage proteins or a reduction in ribosome efficiency due to either large glutenin aggregates in the ER lumen or higher levels of transport directly from the ER to protein bodies, leading to depletion of the rough ER membrane. Alternatively, excess protein destined to be transported to the Golgi may have been targeted to a lytic compartment for degradation instead, reducing the efficiency of protein production. Another hypothesis is that lower expression of *RabD* genes in the developing endosperm may have affected cell growth, division, organisation or other cell processes, which could have adversely affected seed storage protein production.

In fact, RabD2b was found to be involved in growth and development in *Arabidopsis*, with lines overexpressing a mutant *RabD2b* gene exhibiting two different phenotypes showing growth and development abnormalities (Wang *et al*, 2012). The authors also agreed with earlier suggestions by Pinheiro *et al* (2009) that RabD1 and RabD2 members may be functionally redundant, or at least overlapping, due to similar Golgi-associated localisation in *Arabidopsis* and lack of phenotype in *RabD2b* or *RabD2c* knockout plants. This evidence lends itself to the idea that endosperm

development was adversely affected in the knockout line. However, this effect may be limited by the fact that the HMW-GS promoter present in the vector construct used doesn't become active until around 10dpa, by which time syncytium formation and cellularisation are usually complete (Fineran *et al*, 1982; Mares *et al*, 1975; Mares *et al*, 1977).

#### 5.4.2 Gluten bonding strength

The SE-HPLC results show visible differences between the knockdown and control lines, which may shed light on bonding strength between glutenin subunits. The fractions that do not increase between untreated and sonicated samples (14m45s-19m -  $\alpha$ -/ $\gamma$ -gliadin and globulin/albumin) are likely to be almost exclusively composed of monomers that do not bond inter-molecularly and do not form part of the glutenin fraction. Those fractions that are higher in the untreated knockdown line samples than the untreated controls and which rise equally in both lines when sonicated (11m20s-14m45s - smaller LMW-GS and  $\omega$ -gliadin) would appear to have similar proportions of subunits incorporated in the glutenin macropolymer in both lines but more unincorporated subunits in the knockdown line. On the other hand, the larger glutenin fractions (9m-11m20s - HMW-GS and larger LMW-GS) appear to show greater levels of unincorporated glutenin subunits in the knockdown line but during sonication significantly more macropolymer-incorporated subunits are released from the control line and the total levels of protein after sonication are also greater in the control

line.

These findings provide evidence that the *RabD* knockdown transgene has markedly affected bonding between glutenin subunits in the gluten macropolymer of dough. Bonding strength appears most reduced in HMW-GS and some of the larger LMW-GS. As these subunits are probably the most important in giving gluten its elastic properties (Anjum *et al*, 2007) the transgenic dough would be expected to have weaker gluten strength when processed. This correlates with the results of the rheology experiments, in which the knockdown lines exhibited considerable reductions in gluten strength and extensibility compared to controls.

#### *5.4.3 Potential post-translation modification differences in storage proteins of transgenic wheat*

Based on the SDS-PAGE, SE-HPLC and rheology results, there appears to be a reduction in the bonding ability of the gluten proteins. A significant contributing factor to this may be the likelihood that fewer gluten proteins in the transgenic lines than in the control lines go through important post-translational modifications that occur in the Golgi.

A number of studies on glycosylation of gluten proteins have yielded results indicating that a significant proportion of wheat storage proteins are glycosylated (Gujska & Khan, 1999; Lauriere *et al*, 1996; Tilley, 1997; Tilley *et al*, 1993). One study found that gliadins and glutenins were both glycosylated and aggregated LMW-GS showed N-glycans with xylose, thought to indicate processing in

the Golgi (Lauriere *et al*, 1996). Meanwhile, other studies describe finding little or no glycosylation of HMW-GS and  $\alpha$ -gliadins using mostly mass spectrometric approaches such as GC-MS, RP-HPLC/ESI-MS and MALDI-TOF-MS (Bollecker *et al*, 1998; Cunsolo *et al*, 2002; Cunsolo *et al*, 2003; Cunsolo *et al*, 2004; Foti *et al*, 2000; Roels & Delcour, 1996; Turner *et al*, 2002; Zhang *et al*, 2008). Additionally, some of these studies also discovered false positive results when using other techniques including periodate-digoxigenin glycan detection assay and acid PAGE (Bollecker *et al*, 1998; Roels & Delcour, 1996).

N-glycosylation in plants begins in the ER and continues in the Golgi where further modifications to the glycan take place (Song *et al*, 2011). In contrast, the majority of O-glycosylation occurs in the Golgi, though O-glycosylation can also occur in the ER (Webster & Thomas, 2012). While evidence has built up that HMW-GS are probably not commonly glycosylated, LMW-GS and gliadins are less well studied and there is still uncertainty about whether or not they undergo glycosylation (Li *et al*, 2008). If any LMW-GS or gliadins are glycosylated, then it is likely that reducing ER-to-Golgi vesicle traffic would have a profound effect on this process.

Based on results produced, it is likely that post-translational modifications occur in the Golgi that affect bonding ability of gluten proteins. These modifications could be in the form of disulphide and/or hydrogen bonding, or folding into a structure able to produce the loop and chain arrangement thought to give gluten its elasticity in dough (Belton, 1999). Protein disulphide isomerase (PDI) is

located in the ER and protein bodies, and though this glycoprotein is thought to catalyse inter-molecular covalent bonding between glutenin subunits, it is not known whether it has a role in folding of the subunits (Shimoni *et al*, 1995).

## 6 General Discussion

### 6.1.1 Expression of *RabD* genes in developing wheat endosperm of wild type and transgenic Cadenza wheat

Each of the four *RabD* protein sequences available in wheat has high sequence similarity to one of the four *RabD* proteins present in *Brachypodium*, the most closely related species studied. This implies that while there may be other *RabD* genes present in the wheat genome, the *RabD* sequences collected for wheat may represent all of those that are actually expressed, or at least one of each homeologue present. As such, the qPCR assessing the expression of four wheat *RabD* genes in developing wheat endosperm may represent all those expressed. Alternatively, mRNA from multiple homeologues may have been amplified by a given primer pair, in which case the RNA concentration seen would be the result of the expression of multiple genes. However, if the homeologous sequences are well conserved enough with the targeted mRNA to bind with the same primers, it is likely that the RNAi mechanism would also target those sequences. Either way, the qPCR confirming the knockdown of *RabD* genes in the T3 endosperm gives a valid representation of relative transcript levels of members of the *RabD* clade between the transgenic and control lines.

Transcript levels of all four wheat *RabD* genes studied were reduced in the transgenic line at 14dpa, and all but Ta.35418 (*RabD1*) were knocked down at 21dpa. The transgenic effect is thought to have been a result of an RNAi vector containing a 270bp

sequence taken from a single *Rab* gene, Ta.54382 (*RabD2a*) with a 21nt match with Ta.54881 (*RabD2b*). A recent study by Wang *et al* (2012) found that overexpression of a YFP-associated mutant *RabD2b* gene in *Arabidopsis* led to cosuppression of the native *RabD2b* gene along with down-regulation of *RabD1* and *RabD2c* genes, though *RabD2a* appeared unaffected. A similar down-regulation mechanism might help account for the expression pattern seen in the developing T3 seeds, where aside from the target gene, three other genes of the same subfamily showed reduced transcript levels. Alternatively, the fact that this strategy appeared to affect a number of similar genes regardless of whether or not there was a perfect 21nt match between them could be due to cleavage of mRNA sequences that are highly conserved with the siRNA incorporated into RISC, in addition to those that are fully identical.

Ta.2291 (Class I ARF), Ta.2776 (RNase L inhibitor-like protein) and Ta.54227 (AAA-superfamily ATPase involved in cell division control) were selected as normalising genes for qPCR based on work identifying reference genes in wheat by Paolacci *et al* (2009). Ta.54227 appeared to have the most stable expression in both qPCR experiments and Ta.2776 also appeared to be an acceptable reference gene in the wild type qPCR. For the first qPCR on wild type endosperm, Ta.2776 and Ta.54227 were used to normalise the RabD RNA concentration data, whereas for the second qPCR investigating expression in transgenic endosperm Ta.54227 was the only reference gene used. However, using any combination of reference genes, including no normalisation, still produces a

significant reduction in expression of *RabD2a* and *RabD2b* in the transgenic line compared to the control at both 14dpa and 21dpa.

Ta.2291 (Class I ARF) seemed to be unsuitable as a reference gene in both qPCR experiments and in fact appeared to be significantly up-regulated in the transgenic line compared to the control by 79% at 14dpa and 120% at 21dpa (based on normalisation with Ta.54227). This is an interesting result as ARF proteins are small GTPases involved in endosomal vesicle trafficking and are part of the same Ras superfamily as Rab GTPases (Wennerberg *et al*, 2005). It would appear that reduced translation of *RabD* mRNA affected some equilibrium or feedback mechanism in the vesicle transport system leading to increased expression of at least one ARF gene, perhaps to compensate for reduced ER-to-Golgi vesicle traffic.

### 6.1.2 Effect of RNAi on Rab gene expression

The chosen RNAi strategy targeted one gene – Ta.54382 (*RabD2a*) – though there was also a match with Ta.54881 (*RabD2b*) of 21nt, which is thought to be the minimum size of siRNAs incorporated into RISC (Hirai & Kodama, 2008). Nevertheless, there appeared to be a knockdown effect on the *RabD1* genes despite the fact they had no matches with the target sequence of 21nt or more. Additionally, the proportional RNA reduction for *RabD2b* was similar to that for *RabD2a* at 21dpa. These non-specific effects may be explained by a number of studies in the last decade which showed that RNAi does not necessarily require perfect identity with the

siRNA incorporated into RISC. Identity in certain regions of the siRNA or a very high overall homology is sufficient to produce mRNA cleavage (Birmingham *et al*, 2006; Fedorov *et al*, 2006; Haley & Zamore, 2004; Sigoillot *et al*, 2012). These off-target effects can be exploited to target multiple genes for knockdown, as in this work, to avoid an absence of phenotype due to gene redundancy. On the other hand, off-target effects can cause a problem in large-scale RNAi screens, which require high specificity (Sigoillot *et al*, 2012). Based on the idea that knockdown of *RabD* genes other than the target gene was due to non-specificity of RNAi, it is likely that if any *RabD* genes other than those studied in qPCR were expressed in the wheat endosperm, they would also have been knocked down in the transgenic line due to sequence similarity.

An alternative RNAi strategy suggested involved a target sequence containing a region of a consensus sequence based on the four wheat *RabD* coding sequences available. This approach might have shown a more uniform knockdown of the four *RabD* genes, though some regions of the sequence may have been generic and conserved between *Rab* genes in general, which could have caused knockdown of non-target *Rab* genes (Birmingham *et al*, 2006; Fedorov *et al*, 2006; Haley & Zamore, 2004). While there were no  $\geq 21$ nt matches of this *RabD* consensus target region with wheat *Rab* coding sequences outside the RabD clade, general homology with other *Rab* CDS was not taken into account. Care should be taken when using a similar consensus-based RNAi strategy that off-targeting does not affect results. This type of strategy is probably

best suited to studies that aim to knock down a large group of genes with high homology.

### 6.1.3 Trafficking of gluten proteins

There is disagreement as to whether or not glutenins and gliadins are transported differentially through two alternate trafficking routes in the endosperm. No differences in gluten protein distribution were noted in one study by Loussert *et al* (2008). However, although differential use of trafficking routes by gluten proteins is uncertain, segregation of gluten proteins within and between protein bodies has been described in various other studies (Rubin *et al*, 1992; Tosi *et al*, 2011; Tosi *et al*, 2009). Rubin *et al* (1992) suggested that high density protein bodies originated from aggregation of glutenins in the ER while low density bodies contained gliadins trafficked via the Golgi. A study of fluorescent protein-tagged  $\gamma$ -gliadins expressed in tobacco showed accumulation and retention of the  $\gamma$ -gliadins within protein body-like structures in the ER and in addition to this most did not co-localise with the Golgi (Francin-Allami *et al*, 2011). Alternatively, Tosi *et al* (2009) followed a tagged LMW-GS throughout endosperm development and, based on their results, put forward the idea that a given gluten protein was more likely to take one trafficking route over the other depending on development stage. During early development a greater proportion of the LMW-GS was trafficked via the Golgi compared to transport from the ER directly to protein bodies. However, later in development, during increased protein production, aggregation in

the ER was more frequent.

Based on SE-HPLC results of this study, the reduction of *RabD* expression in wheat endosperm appears to reduce the bonding ability of HMW-GS and larger LMW-GS while smaller LMW-GS are visibly less affected. This may point towards different glutenin subunits favouring different trafficking routes or alternatively that smaller glutenins are not as dependant on processing in the Golgi to retain their ability to bond in the glutenin macropolymer. However, if there is a difference in the ratio of proteins trafficked via the Golgi compared to ER aggregation and it remained the same in the knockdown line, it is not apparent in the SDS-PAGE results, which do not show any differences in subunit proportions present in the mature seed between the knockdown and control lines.

#### *6.1.4 Gluten quality in transgenic wheat*

The T3 rheology results clearly indicate a reduction in dough strength and extensibility in the knockdown line compared to the control. It is likely that altered inter-molecular bonding in the glutenin macropolymer contributed to this effect, combined with a drop in total protein content. These findings are at odds with a study by Di Luccia *et al* (2005) on durum wheat expressing a trans-dominant mutant *RabD2* gene thought to limit ER to Golgi traffic. They also saw a reduction in protein content in the transgenic but also an apparent increase in gluten strength in a 10g mixing test as well as a higher gluten index. The expression of the mutant gene itself was confirmed in the transgenic line by RT-PCR, though it was

not shown what effect the mutant gene had on native *RabD* gene expression. A 10g mixograph on one transgenic line compared to one control line using wholemeal flour was the main demonstration of improved gluten quality, alongside a gluten index test which demonstrates the cohesiveness of the dough. Using wholemeal flour in small-scale mixing tests has been shown to give results that are unrepresentative of actual dough and baking quality unless specific precautions are taken, including ensuring low particle size (Lai *et al*, 1989; Steinfurth *et al*, 2012). Use of different mills was also shown to have a large effect on the mixing quality of wholemeal flours (Rakszegi *et al*, 2010).

The difference in ploidy between durum wheat and bread wheat is the cause of a difference in the number of subunits produced. For instance, bread wheat has 6 HMW-GS genes (2 on each genome), though 5 is the actual maximum number expressed in any one variety (Payne *et al*, 1981), while durum wheat also has 2 genes on each genome (4 in total) with a maximum of 3 expressed subunits. The D genome found in bread wheat is not present in durum wheat which may mean that there is a significant difference in the trafficking and processing of gluten protein between the two species. An increase in the gluten strength of durum wheat may be easier to achieve than in bread wheat as it naturally has a lower gluten strength than bread wheat. The disparity in results with this study may be due to genetic or other differences between species studied, in addition to the fact that the mutant *Rab* gene was from tobacco rather than wheat. Alternatively,

some difference in the methods used for knockdown or analysis of the transgenic flour could account for the different outcomes of these studies.

As it has been confirmed that the *RabD* genes are knocked down in the developing endosperm in the T3 transgenic line relative to the control line, it is reasonable to conclude that the expression of one or more of these genes has an effect on gluten quality.

#### *6.1.5 Future prospects*

This work has provided a considerable insight into the cellular environment of the developing endosperm of wheat and its key role in dough characteristics. The knowledge gained about the sequence and function of Rab GTPases in the endosperm of hexaploid wheat can be further exploited to better understand, and possibly improve, the technological properties of flour.

While it has been confirmed that the transgenic line had reduced transcript levels of *RabD* genes, no comparison of actual ER-to-Golgi vesicle traffic between knockdown and control lines was performed. To make this easier to achieve, production of a line containing the transgene along with fluorescence-tagged ER and Golgi compartments would be carried out, possibly by hybridisation with existing wheat lines with similar features to that used by Sparkes *et al* (2009) in *Arabidopsis*. This approach could reveal specific differences in the behaviour of the endomembrane system in the transgenic endosperm as well as the way the gluten proteins are produced, transported, processed, sorted and stored.

Based on the results of this work, it would appear that *RabD* expression is linked to dough processing quality in bread wheat – at least in that gluten quality appears reduced when *RabD* expression is reduced. It may be inferred therefore that an increased level of *RabD* expression might improve gluten quality. However, overexpression of native *RabD* genes has met with a lack of phenotype in studies on durum wheat and *Arabidopsis* (Di Luccia *et al*, 2005; Wang *et al*, 2012). When no phenotype was found in transgenic *Arabidopsis* overexpressing RAC/ROP small GTPases, the authors of the study suggested that interactors including GAPs and GDIs could be responsible for keeping GTPase activity stable despite a greater quantity of protein present (Brembu *et al*, 2005). It is reasonable to conclude that the wide range of Rab interaction partners could prove problematic to efforts to up-regulate vesicle trafficking from ER to Golgi by genetic modification.

The RNAi strategy used to reduce *RabD2a* and *RabD2b* RNA levels appeared to target a wider range of transcripts than was originally expected, also including those belonging to *RabD1* genes. To determine whether or not the transgene had affected members of other Rab clades, it would be prudent in future to include a closely related *Rab* outside of the RabD clade in any qPCR experiment assessing knockdown success. For example, a selection of *RabE* genes as practised by Wang *et al* (2012) due to the RabE clade being most closely related to the RabD subfamily.

SDS-PAGE experiments appeared to show very little change in ratio of seed storage protein subunits between transgenic and

control grains. To gain a deeper insight into the types and quantities of different proteins present, further experiments such as Western blot and native 2D PAGE could be performed with the transgenic grain.

The evidence presented here, particularly from the SE-HPLC and rheology work, suggests that processing in the Golgi could be responsible for important post-translational modifications that improve the breadmaking potential of the gluten proteins. With this in mind, an increased proportion of seed storage proteins trafficked through the Golgi in the developing endosperm could be beneficial to gluten quality. While the transgenic approach to higher *RabD* expression may be difficult to achieve, native levels of RabD activity may vary between different varieties and lines of wheat. With the bioinformatics and expression data produced in this study as a starting point, *RabD* expression could be analysed in a set of wheat varieties and lines. Of particular interest might be varieties that show predictors for poor breadmaking quality such as low protein and HMW-GS associated with low gluten strength, yet demonstrate good breadmaking quality. For comparison, it may be useful to include varieties with the opposite condition – good quality predictors but low quality real-life characteristics. It is worth investigating whether as yet unexplained gluten quality of these varieties could be attributed to differences in trafficking in the endosperm.

PCR, RT-PCR and qPCR of wheat deletion lines with individual chromosomes missing could shed light on the locations of the *RabD*

genes and reveal silenced genes. Additionally, a PCR experiment to obtain the full genomic sequences of the *RabD* genes would be simple to complete using the sequence data produced in this project and would support further investigation of *Rab* genes in wheat, as well as aiding in PCR primer design.

In order to obtain more information about the regulation of ER-to-Golgi vesicle trafficking, an analysis of possible transcription factors of *RabD* genes and their interactors and effectors may be useful. A gene network could perhaps provide details of transcription factors that affect a wide range of proteins active in the endomembrane system. This information could then potentially be used in designing later transformation experiments, with a greater likelihood of producing a phenotype than *RabD* overexpression alone.

Most attempts to alter breadmaking quality in bread wheat using biotechnology have targeted the gluten proteins themselves, particularly the HMW glutenin subunits. This study represents a novel approach to this area of work by altering the transport of these important proteins in the endosperm. The resulting effects reported on grain shape, protein content, bonding in the glutenin macropolymer and dough rheology have considerably added to the understanding of factors that contribute towards gluten quality.

## 7 References

Allan, B. B., Moyer, B. D. & Balch, W. E. (2000). Rab1 recruitment of p115 into a cis-SNARE complex: Programming budding COPII vesicles for fusion. *Science*, 289(5478), 444-448.

Allen, A. M., Barker, G. L. A., Berry, S. T., Coghill, J. A., Gwilliam, R., Kirby, S., Robinson, P., Brenchley, R. C., D'amore, R., Mckenzie, N., Waite, D., Hall, A., Bevan, M., Hall, N. & Edwards, K. J. (2011). Transcript-specific, single-nucleotide polymorphism discovery and linkage analysis in hexaploid bread wheat (*Triticum aestivum* L.). *Plant Biotechnology Journal*, 9(9), 1086-1099.

Anjum, F. M., Khan, M. R., Din, A., Saeed, M., Pasha, I. & Arshad, M. U. (2007). Wheat gluten: High molecular weight glutenin subunits - Structure, genetics, and relation to dough elasticity. *Journal of Food Science*, 72(3), R56-R63.

Antonin, W., Fasshauer, D., Becker, S., Jahn, R. & Schneider, T. R. (2002). Crystal structure of the endosomal SNARE complex reveals common structural principles of all SNAREs. *Nature Structural Biology*, 9(2), 107-111.

Bahk, J. D., Bang, W. Y. & Heo, J. B. (2009). Plant PRA plays an important role in intracellular vesicular trafficking between compartments as GDF. *Plant Signal Behav*, 4(11), 1094-5.

Balandin, M., Royo, J., Gomez, E., Muniz, L., Molina, A. & Hueros, G. (2005). A protective role for the embryo surrounding region of the maize endosperm, as evidenced by the characterisation of ZmESR-6, a defensin gene specifically expressed in this region. *Plant Molecular Biology*, 58(2), 269-282.

Baluska, F., Menzel, D., Barlow, P. W. (2006). Cytokinesis in plant and animal cells: Endosomes 'shut the door'. *Developmental Biology*, 294(1), 1-10.

Bartels, D. & Thompson, R. D. (1986). Synthesis of messenger-RNAs coding for abundant endosperm proteins during wheat-grain development. *Plant Science*, 46(2), 117-125.

Bate, N. J., Niu, X. P., Wang, Y. W., Reimann, K. S. & Helentjaris, T. G. (2004). An invertase inhibitor from maize localizes to the embryo surrounding region during early kernel development. *Plant Physiology*, 134(1), 246-254.

Batoko, H., Zheng, H. Q., Hawes, C. & Moore, I. (2000). A Rab1 GTPase is required for transport between the endoplasmic reticulum and Golgi apparatus and for normal Golgi movement in plants. *Plant Cell*, 12(11), 2201-2217.

- Baulcombe, D. (2004). RNA silencing in plants. *Nature*, 431(7006), 356-363.
- Baulcombe, D. (2005). RNA silencing. *Trends in Biochemical Sciences*, 30(6), 290-293.
- Baumberger, N. & Baulcombe, D. C. (2005). *Arabidopsis* ARGONAUTE1 is an RNA Slicer that selectively recruits microRNAs and short interfering RNAs. *Proceedings of the National Academy of Sciences of the United States of America*, 102(33), 11928-11933.
- BCE (2011). *Growing quality wheat for export 2012*. London, UK: Home Grown Cereals Authority.
- Belton, P. S. (1999). On the elasticity of wheat gluten. *Journal of Cereal Science*, 29(2), 103-107.
- Bennett, M. D., Smith, J. B. & Barclay, I. (1975). Early seed development in Triticeae. *Philosophical Transactions of the Royal Society of London Series B-Biological Sciences*, 272(916), 199.
- Bietz, J. A., Huebner, F. R., Sanderson, J. E. & Wall, J. S. (1977). Wheat gliadin homology revealed through N-terminal amino-acid sequence-analysis. *Cereal Chemistry*, 54(5), 1070-1083.
- Birmingham, A., Anderson, E. M., Reynolds, A., Ilsley-Tyree, D., Leake, D., Fedorov, Y., Baskerville, S., Maksimova, E., Robinson, K., Karpilow, J., Marshall, W. S. & Khvorova, A. (2006). 3' UTR seed matches, but not overall identity, are associated with RNAi off-targets. *Nature Methods*, 3(3), 199-204.
- Blechl, A., Lin, J., Nguyen, S., Chan, R., Anderson, O. D. & Dupont, F. M. (2007). Transgenic wheats with elevated levels of Dx5 and/or Dy10 high-molecular-weight glutenin subunits yield doughs with increased mixing strength and tolerance. *Journal of Cereal Science*, 45(2), 172-183.
- Bollecker, S. S. J., Kaiser, K. P., Kohler, P., Wieser, H. & Schofield, J. D. (1998). Re-examination of the glycosylation of high M-r subunits of wheat glutenin. *Journal of Agricultural and Food Chemistry*, 46(12), 4814-4823.
- Bonello, J. F., Sevilla-Lecoq, S., Berne, A., Risueno, M. C., Dumas, C. & Rogowsky, P. M. (2002). ESR proteins are secreted by the cells of the embryo surrounding region. *Journal of Experimental Botany*, 53(374), 1559-1568.
- Bouche, N., Lauressergues, D., Gascioli, V. & Vaucheret, H. (2006). An antagonistic function for *Arabidopsis* DCL2 in development and a new function for DCL4 in generating viral siRNAs. *EMBO Journal*, 25(14), 3347-3356.

- Brembu, T., Winge, P. & Bones, A. M. (2005). The small GTPase AtRAC2/ROP7 is specifically expressed during late stages of xylem differentiation in *Arabidopsis*. *Journal of Experimental Botany*, 56(419), 2465-2476.
- Brodersen, P. & Voinnet, O. (2006). The diversity of RNA silencing pathways in plants. *Trends in Genetics*, 22(5), 268-280.
- Burgess, S. R. & Shewry, P. R. (1986). Identification of homologous globulins from embryos of wheat, barley, rye and oats. *Journal of Experimental Botany*, 37(185), 1863-1871.
- Burgoyne, R. D. & Morgan, A. (2007). Membrane trafficking: Three steps to fusion. *Current Biology*, 17, R255-R258.
- Bushuk, W. & Zillman, R. R. (1978). Wheat cultivar identification by gliadin electrophoregrams .1. Apparatus, method and nomenclature. *Canadian Journal of Plant Science*, 58(2), 505-515.
- Cai, H. Q., Reinisch, K. & Ferro-Novick, S. (2007). Coats, tethers, Rabs, and SNAREs work together to mediate the intracellular destination of a transport vesicle. *Developmental Cell*, 12(5), 671-682.
- Cao, X. C., Ballew, N. & Barlowe, C. (1998). Initial docking of ER-derived vesicles requires Uso1p and Ypt1p but is independent of SNARE proteins. *EMBO Journal*, 17(8), 2156-2165.
- Cassidy, B. G., Dvorak, J. & Anderson, O. D. (1998). The wheat low-molecular-weight glutenin genes: characterization of six new genes and progress in understanding gene family structure. *Theoretical and Applied Genetics*, 96(6-7), 743-750.
- Chang, S., Puryear, J. & Cairney, J. (1993). A Simple and Efficient Method for Isolating RNA from Pine Trees. *Plant Molecular Biology Reporter*, 11(2), 113-116.
- Cheung, A. Y., Chen, C. Y. H., Glaven, R. H., De Graaf, B. H. J., Vidali, L., Hepler, P. K. & Wu, H. M. (2002). Rab2 GTPase regulates vesicle trafficking between the endoplasmic reticulum and the Golgi bodies and is important to pollen tube growth. *Plant Cell*, 14(4), 945-962.
- Chow, C.-M., Neto, H., Foucart, C., Moore, I. (2008). Rab-A2 and Rab-A3 GTPases define a trans-Golgi endosomal membrane domain in *Arabidopsis* that contributes substantially to the cell plate. *Plant Cell*, 20(1).
- Chuang, C. F. & Meyerowitz, E. M. (2000). Specific and heritable genetic interference by double-stranded RNA in *Arabidopsis thaliana*. *Proceedings of the National Academy of Sciences of the United States of America*, 97(9), 4985-4990.

Cock, J. M. & McCormick, S. (2001). A large family of genes that share homology with CLAVATA3. *Plant Physiology*, 126(3), 939-942.

Colot, V., Robert, L. S., Kavanagh, T. A., Bevan, M. W. & Thompson, R. D. (1987). Localization of sequences in wheat endosperm protein genes which confer tissue-specific expression in tobacco. *EMBO Journal*, 6(12), 3559-3564.

Cossegal, M., Vernoud, V., Depege, N. & Rogowsky, P. M. (2007). The embryo surrounding region. *Plant Cell Monographs*, 57-71.

Cunsolo, V., Foti, S., Saletti, R., Gilbert, S., Tatham, A. S. & Shewry, P. R. (2002). Investigation and correction of the gene-derived sequence of glutenin subunit 1Dx2 by matrix-assisted laser desorption/ionisation mass spectrometry. *Rapid Communications in Mass Spectrometry*, 16(20), 1911-1918.

Cunsolo, V., Foti, S., Saletti, R., Gilbert, S., Tatham, A. S. & Shewry, P. R. (2003). Structural studies of glutenin subunits 1Dy10 and 1Dy12 by matrix-assisted laser desorption/ionisation mass spectrometry and high-performance liquid chromatography/electrospray ionisation mass spectrometry. *Rapid Communications in Mass Spectrometry*, 17(5), 442-454.

Cunsolo, V., Foti, S., Saletti, R., Gilbert, S., Tatham, A. S. & Shewry, P. R. (2004). Structural studies of the allelic wheat glutenin subunits 1Bx7 and 1Bx20 by matrix-assisted laser desorption/ionization mass spectrometry and high-performance liquid chromatography/electrospray ionization mass spectrometry. *Journal of Mass Spectrometry*, 39(1), 66-78.

Curtin, S. J., Watson, J. M., Smith, N. A., Eamens, A. L., Blanchard, C. L. & Waterhouse, P. M. (2008). The roles of plant dsRNA-binding proteins in RNAi-like pathways. *Febs Letters*, 582(18), 2753-2760.

de Graaf, B. H. J., Cheung, A. Y., Andreyeva, T., Levasseur, K., Kieliszewski, M., Wu, H. M. (2005). Rab11 GTPase-regulated membrane trafficking is crucial for tip-focused pollen tube growth in tobacco. *Plant Cell*, 17(9).

Delcour, J. A., Joye, I. J., Pareyt, B., Wilderjans, E., Brijs, K. & Lagrain, B. (2012). Wheat gluten functionality as a quality determinant in cereal-based food products. In Doyle, M. P. & Klaenhammer, T. R. (Eds.), *Annual Review of Food Science and Technology*, Vol 3. Palo Alto: Annual Reviews.

Dhonukshe, P., Baluska, F., Schlicht, M., Hlavacka, A., Samaj, J., Friml, J., Gadella, T. W. J. (2006). Endocytosis of cell surface material mediates cell plate formation during plant cytokinesis. *Developmental Cell*, 10(1): 137-150.

Di Luccia, A., Lamacchia, C., Fares, C., Padalin, L., Mamone, G., La Gatta, B., Gambacorta, G., Faccia, M., Di Fonzo, N. & La Notte, E. (2005). A proteomic approach to study protein variation in GM durum wheat in relation to technological properties of semolina. *Annali Di Chimica*, 95(6), 405-414.

Diekmann, Y., Seixas, E., Gouw, M., Tavares-Cadete, F., Seabra, M. C. & Pereira-Leal, J. B. (2011). Thousands of Rab GTPases for the Cell Biologist. *Plos Computational Biology*, 7(10).

Diracsvejstrup, A. B., Sumizawa, T. & Pfeffer, S. R. (1997). Identification of a GDI displacement factor that releases endosomal Rab GTPases from Rab-GDI. *EMBO Journal*, 16(3), 465-472.

D'Ovidio, R. & Masci, S. (2004). The low-molecular-weight glutenin subunits of wheat gluten. *Journal of Cereal Science*, 39(3), 321-339.

Drummond, A., Ashton, B., Buxton, S., Cheung, M., Cooper, A., Heled, J., Kearse, M., Moir, R., Stones-Havas, S., Sturrock, S., Thierer, T. & Wilson, A. (2010). Geneious v5.1. Biomatters Ltd.

Ebine, K. & Ueda, T. (2009). Unique mechanism of plant endocytic/vacuolar transport pathways. *Journal of Plant Research*, 122(1), 21-30.

Ecker, J. R. & Davis, R. W. (1986). Inhibition of gene-expression in plant-cells by expression of antisense RNA. *Proceedings of the National Academy of Sciences of the United States of America*, 83(15), 5372-5376.

Fasshauer, D., Sutton, R. B., Brunger, A. T. & Jahn, R. (1998). Conserved structural features of the synaptic fusion complex: SNARE proteins reclassified as Q- and R-SNAREs. *Proceedings of the National Academy of Sciences of the United States of America*, 95(26), 15781-15786.

Fedorov, Y., Anderson, E. M., Birmingham, A., Reynolds, A., Karpilow, J., Robinson, K., Leake, D., Marshall, W. S. & Khvorova, A. (2006). Off-target effects by siRNA can induce toxic phenotype. *Rna-a Publication of the Rna Society*, 12(7), 1188-1196.

Felsenstein, J. (1985). Confidence-limits on phylogenies - an approach using the bootstrap. *Evolution*, 39(4), 783-791.

Fineran, B. A., Wild, D. J. C. & Ingerfeld, M. (1982). Initial wall formation in the endosperm of wheat, *Triticum aestivum*: a re-evaluation. *Canadian Journal of Botany-Revue Canadienne De Botanique*, 60(9), 1776-1795.

Fire, A., Xu, S. Q., Montgomery, M. K., Kostas, S. A., Driver, S. E. & Mello, C. C. (1998). Potent and specific genetic interference by double-stranded RNA in *Caenorhabditis elegans*. *Nature*, 391(6669),

806-811.

Foti, S., Maccarrone, G., Saletti, R., Roepstorff, P., Gilbert, S., Tatham, A. S. & Shewry, P. R. (2000). Verification of the cDNA deduced sequence of glutenin subunit 1Dx5 and an M-r 58 000 repetitive peptide by matrix-assisted laser desorption/ionisation mass spectrometry (MALDI-MS). *Journal of Cereal Science*, 31(2), 173-183.

Francin-Allami, M., Saumonneau, A., Lavenant, L., Boudier, A., Sparkes, I., Hawes, C. & Popineau, Y. (2011). Dynamic trafficking of wheat gamma-gliadin and of its structural domains in tobacco cells, studied with fluorescent protein fusions. *Journal of Experimental Botany*, 62(13), 4507-4520.

Graybosch, R. A., Seabourn, B., Chen, Y. H. R. & Blechl, A. E. (2011). Quality and agronomic effects of three high-molecular-weight glutenin subunit transgenic events in winter wheat. *Cereal Chemistry*, 88(1), 95-102.

Grewal, S. I. S. & Moazed, D. (2003). Heterochromatin and epigenetic control of gene expression. *Science*, 301(5634), 798-802.

Grosshans, B. L., Ortiz, D. & Novick, P. (2006). Rabs and their effectors: Achieving specificity in membrane traffic. *Proceedings of the National Academy of Sciences of the United States of America*, 103(32), 11821-11827.

Gujaska, E. & Khan, K. (1999). Characterization of the carbohydrates of nonreduced glutenin fractionated by multistacking SDS-PAGE from two hard red spring wheat flours. *Cereal Chemistry*, 76(2), 198-203.

Gupta, R. B. & Shepherd, K. W. (1990). 2-step one-dimensional SDS-PAGE analysis of LMW subunits of glutelin .1. Variation and genetic-control of the subunits in hexaploid wheats. *Theoretical and Applied Genetics*, 80(1), 65-74.

Gupta, R. B. & Shepherd, K. W. (1993). Production of multiple wheat-rye 1RS translocation stocks and genetic-analysis of LMW subunits of glutenin and gliadins in wheats using these stocks. *Theoretical and Applied Genetics*, 85(6-7), 719-728.

Gurkan, C., Lapp, H., Alory, C., Su, A. I., Hogenesch, J. B. & Balch, W. E. (2005). Large-scale profiling of Rab GTPase trafficking networks: The membrome. *Molecular Biology of the Cell*, 16(8), 3847-3864.

Hagberg, S. (1960). A rapid method for determining alpha-amylase activity. *Cereal Chemistry*, 37(2), 218-222.

Haley, B. & Zamore, P. D. (2004). Kinetic analysis of the RNAi

enzyme complex. *Nature Structural & Molecular Biology*, 11(7), 599-606.

Hamilton, A. J., Lycett, G. W. & Grierson, D. (1990). Antisense gene that inhibits synthesis of the hormone ethylene in transgenic plants. *Nature*, 346(6281), 284-287.

Hammond-Kosack, M. C. U., Holdsworth, M. J. & Bevan, M. W. (1993). In vivo footprinting of a low-molecular-weight glutenin gene (LMWG-1D1) in wheat endosperm. *EMBO Journal*, 12(2), 545-554.

Heid, C. A., Stevens, J., Livak, K. J. & Williams, P. M. (1996). Real time quantitative PCR. *Genome Research*, 6(10), 986-994.

Heo, J. B., Rho, H. S., Kim, S. W., Hwang, S. M., Kwon, H. J., Nahm, M. Y., Bang, W. Y., Bahk, J. D. (2005). OsGAP1 functions as a positive regulator of OSRab11-mediated TGN to PM or vacuole trafficking. *Plant and Cell Physiology*, 46(12).

HGCA (2012). *HGCA Recommended Lists 2012/13 for cereals and oilseeds*. Coventry, UK: Home Grown Cereals Authority.

Hirai, S. & Kodama, H. (2008). RNAi vectors for manipulation of gene expression in higher plants. *The Open Plant Science Journal*, 2, 21-30.

Hong, W. J. (2005). SNARES and traffic. *Biochimica et Biophysica Acta-Molecular Cell Research*, 1744(2), 120-144.

Horgan, C. P., McCaffrey, M. W. (2011). Rab GTPases and microtubule motors. *Biochemical Society Transactions*, 39: 1202-1206.

Ikeda, T. M., Araki, E., Fujita, Y. & Yano, H. (2006). Characterization of low-molecular-weight glutenin subunit genes and their protein products in common wheats. *Theoretical and Applied Genetics*, 112(2), 327-334.

Jackson, E. A., Holt, L. M. & Payne, P. I. (1983). Characterization of high molecular-weight gliadin and low-molecular-weight glutenin subunits of wheat endosperm by two-dimensional electrophoresis and the chromosomal localization of their controlling genes. *Theoretical and Applied Genetics*, 66(1), 29-37.

Jones, H. D. & Sparks, C. A. (2009). Transgenic Wheat, Barley and Oats: Production and Characterization. In Jones, H. D. & Shewry, P. R. (Eds.), *Methods in Molecular Biology*. Totowa, NJ: Humana Press Inc.

Kasarda, D. D. (1989). Glutenin structure in relation to wheat quality. In Pomeranz, Y. (Ed.), *Wheat is Unique*. St Paul, MN: American Association of Cereal Chemistry

Kasarda, D. D., Autran, J. C., Lew, E. J. L., Nimmo, C. C. & Shewry, P. R. (1983). N-terminal amino-acid-sequences of omega-gliadins and omega-secalins - implications for the evolution of prolamin genes. *Biochimica et Biophysica Acta*, 747(1-2), 138-150.

Kato, A., Endo, M., Kato, H. & Saito, T. (2005). The antisense promoter of AtRE1, a retrotransposon in *Arabidopsis thaliana*, is activated in pollens and calluses. *Plant Science*, 168(4), 981-986.

Katoh, K. & Toh, H. (2010). Parallelization of the MAFFT multiple sequence alignment program. *Bioinformatics*, 26(15), 1899-1900.

Kermode, A. & Bewley, J. (1999). Synthesis, processing and deposition of seed proteins: The pathway of protein synthesis and deposition of the cell. In Shewry, P. & Casey, R. (Eds.), *Seed Proteins*. Kluwer Academic.

Kreis, M., Forde, B. G., Rahman, S., Mifflin, B. J. & Shewry, P. R. (1985). Molecular evolution of the seed storage proteins of barley, rye and wheat. *Journal of Molecular Biology*, 183(3), 499-502.

Lai, C. S., Hosney, R. C. & Davis, A. B. (1989). Effects of wheat bran in breadmaking. *Cereal Chemistry*, 66(3), 217-219.

Lamacchia, C., Shewry, P. R., Di Fonzo, N., Forsyth, J. L., Harris, N., Lazzeri, P. A., Napier, J. A., Halford, N. G. & Barcelo, P. (2001). Endosperm-specific activity of a storage protein gene promoter in transgenic wheat seed. *Journal of Experimental Botany*, 52(355), 243-250.

Lauriere, M., Bouchez, I., Doyen, C. & Eynard, L. (1996). Identification of glycosylated forms of wheat storage proteins using two-dimensional electrophoresis and blotting. *Electrophoresis*, 17(3), 497-501.

Lee, G. J., Sohn, E. J., Lee, M. H. & Hwang, I. (2004). The *Arabidopsis* Rab5 homologs Rha1 and Ara7 localize to the prevacuolar compartment. *Plant and Cell Physiology*, 45(9), 1211-1220.

Leon, E., Marin, S., Gimenez, M. J., Piston, F., Rodriguez-Quijano, M., Shewry, P. R. & Barro, F. (2009). Mixing properties and dough functionality of transgenic lines of a commercial wheat cultivar expressing the 1Ax1, 1Dx5 and 1Dy10 HMW glutenin subunit genes. *Journal of Cereal Science*, 49(1), 148-156.

Leon, E., Piston, F., Aouni, R., Shewry, P. R., Rosell, C. M., Martin, A. & Barro, F. (2010). Pasting properties of transgenic lines of a commercial bread wheat expressing combinations of HMW glutenin subunit genes. *Journal of Cereal Science*, 51(3), 344-349.

Levanony, H., Rubin, R., Altschuler, Y. & Galili, G. (1992). Evidence for a novel route of wheat storage proteins to vacuoles. *Journal of Cell Biology*, 119(5), 1117-1128.

Lew, E. J. L., Kuzmicky, D. D. & Kasarda, D. D. (1992). Characterization of low-molecular-weight glutenin subunits by reversed-phase high-performance liquid-chromatography, sodium dodecyl sulfate-polyacrylamide gel-electrophoresis, and N-terminal amino-acid sequencing. *Cereal Chemistry*, 69(5), 508-515.

Li, X. H., Wang, A. L., Xiao, Y. H., Yan, Y. M., He, Z. H., Appels, R., Ma, W. J., Hsam, S. L. K. & Zeller, F. J. (2008). Cloning and characterization of a novel low molecular weight glutenin subunit gene at the Glu-A3 locus from wild emmer wheat (*Triticum turgidum* L. var. *dicoccoides*). *Euphytica*, 159(1-2), 181-190.

Lid, S. E., Al, R. H., Krekling, T., Meeley, R. B., Ranch, J., Opsahl-Ferstad, H. G. & Olsen, O. A. (2004). The maize disorganized aleurone layer 1 and 2 (*dil1*, *dil2*) mutants lack control of the mitotic division plane in the aleurone layer of developing endosperm. *Planta*, 218(3), 370-378.

Loussert, C., Popineau, Y. & Mangavel, C. (2008). Protein bodies ontogeny and localization of prolamin components in the developing endosperm of wheat caryopses. *Journal of Cereal Science*, 47(3), 445-456.

Lu, C. G., Zainal, Z., Tucker, G. A. & Lycett, G. W. (2001). Developmental abnormalities and reduced fruit softening in tomato plants expressing an antisense Rab11 GTPase gene. *Plant Cell*, 13(8), 1819-1833.

Lycett, G. (2008). The role of Rab GTPases in cell wall metabolism. *Journal of Experimental Botany*, 59(15), 4061-4074.

Mares, D. J., Norstog, K. & Stone, B. A. (1975). Early stages in development of wheat endosperm. 1. Change from free nuclear to cellular endosperm. *Australian Journal of Botany*, 23(2), 311-326.

Mares, D. J., Stone, B. A., Jeffery, C. & Norstog, K. (1977). Early stages in development of wheat endosperm. 2. Ultrastructural observations on cell-wall formation. *Australian Journal of Botany*, 25(6), 599-613.

Masci, S., D'ovidio, R., Lafiandra, D. & Kasarda, D. D. (1998). Characterization of a low-molecular-weight glutenin subunit gene from bread wheat and the corresponding protein that represents a major subunit of the glutenin polymer. *Plant Physiology*, 118(4), 1147-1158.

Masci, S., Rovelli, L., Kasarda, D. D., Vensel, W. H. & Lafiandra, D. (2002). Characterisation and chromosomal localisation of C-type

low-molecular-weight glutenin subunits in the bread wheat cultivar Chinese Spring. *Theoretical and Applied Genetics*, 104(2-3), 422-428.

Mazel, A., Leshem, Y., Tiwari, B. S. & Levine, A. (2004). Induction of salt and osmotic stress tolerance by overexpression of an intracellular vesicle trafficking protein AtRab7 (AtRabG3e). *Plant Physiology*, 134(1), 118-128.

Metakovsky, E. V., Branlard, G., Chernakov, V. M., Upelniek, V. P., Redaelli, R. & Pogna, N. E. (1997). Recombination mapping of some chromosome 1A-, 1B-, 1D- and 6B-controlled gliadins and low-molecular-weight glutenin subunits in common wheat. *Theoretical and Applied Genetics*, 94(6-7), 788-795.

Miki, D., Itoh, R. & Shimamoto, K. (2005). RNA silencing of single and multiple members in a gene family of rice. *Plant Physiology*, 138(4), 1903-1913.

Morel, M. H., Dehlon, P., Autran, J. C., Leygue, J. P. & Bar-L'helgouac'h, C. (2000). Effects of temperature, sonication time, and power settings on size distribution and extractability of total wheat flour proteins as determined by size-exclusion high-performance liquid chromatography. *Cereal Chemistry*, 77(5), 685-691.

Moyer, B. D., Allan, B. B. & Balch, W. E. (2001). Rab1 interaction with a GM130 effector complex regulates COPII vesicle cis-Golgi tethering. *Traffic*, 2(4), 268-276.

Muller, S. & Wieser, H. (1997). The location of disulphide bonds in monomeric gamma-type gliadins. *Journal of Cereal Science*, 26(2), 169-176.

Nabim (2011). *Nabim Wheat Guide 2011*. London, UK: National Association of British & Irish Millers.

Nakano, M., Nobuta, K., Vemaraju, K., Tej, S. S., Skogen, J. W. & Meyers, B. C. (2006). Plant MPSS databases: signature-based transcriptional resources for analyses of mRNA and small RNA. *Nucleic Acids Research*, 34, D731-D735.

Napier, J. A., Richard, G., Turner, M. F. P. & Shewry, P. R. (1997). Trafficking of wheat gluten proteins in transgenic tobacco plants: gamma-gliadin does not contain an endoplasmic reticulum retention signal. *Planta*, 203(4), 488-494.

Nemeth, C., Freeman, J., Jones, H. D., Sparks, C., Pellny, T. K., Wilkinson, M. D., Dunwell, J., Andersson, A. a. M., Aman, P., Guillon, F., Saulnier, L., Mitchell, R. a. C. & Shewry, P. R. (2010). Down-regulation of the CSLF6 gene results in decreased (1,3;1,4)-beta-D-glucan in endosperm of wheat. *Plant Physiology*, 152(3), 1209-1218.

Olsen, O. A. (2004). Nuclear endosperm development in cereals and *Arabidopsis thaliana*. *Plant Cell*, 16, S214-S227.

Paolacci, A. R., Tanzarella, O. A., Porceddu, E. & Ciaffi, M. (2009). Identification and validation of reference genes for quantitative RT-PCR normalization in wheat. *Bmc Molecular Biology*, 10, 27.

Park, M., Kim, S. J., Vitale, A. & Hwang, I. (2004). Identification of the protein storage vacuole and protein targeting to the vacuole in leaf cells of three plant species. *Plant Physiology*, 134(2), 625-639.

Parker, R. & Sheth, U. (2007). P bodies and the control of mRNA translation and degradation. *Molecular Cell*, 25(5), 635-646.

Parr, T., Bardsley, R. G., Gilmour, R. S. & Buttery, P. J. (1992). Changes in calpain and calpastatin messenger-RNA induced by beta-adrenergic stimulation of bovine skeletal-muscle. *European Journal of Biochemistry*, 208(2), 333-339.

Payne, P. I. (1987). Genetics of wheat storage proteins and the effect of allelic variation on bread-making quality. *Annual Review of Plant Physiology and Plant Molecular Biology*, 38, 141-153.

Payne, P. I. & Corfield, K. G. (1979). Subunit composition of wheat glutenin proteins, isolated by gel-filtration in a dissociating medium. *Planta*, 145(1), 83-88.

Payne, P. I., Holt, L. M. & Law, C. N. (1981). Structural and genetic studies on the high-molecular-weight subunits of wheat glutenin .1. Allelic variation in subunits amongst varieties of wheat (*Triticum aestivum*). *Theoretical and Applied Genetics*, 60(4), 229-236.

Payne, P. I., Jackson, E. A., Holt, L. M. & Law, C. N. (1984). Genetic-linkage between endosperm storage protein genes on each of the short arms of chromosome-1A and chromosome-1B in wheat. *Theoretical and Applied Genetics*, 67(2-3), 235-243.

Payne, P. I., Law, C. N. & Mudd, E. E. (1980). Control by homoeologous group-1 chromosomes of the high-molecular-weight subunits of glutenin, a major protein of wheat endosperm. *Theoretical and Applied Genetics*, 58(3-4), 113-120.

Pereira-Leal, J. B. & Seabra, M. C. (2001). Evolution of the Rab family of small GTP-binding proteins. *Journal of Molecular Biology*, 313(4), 889-901.

Pfeffer, S. & Aivazian, D. (2004). Targeting RAB GTPases to distinct membrane compartments. *Nature Reviews Molecular Cell Biology*, 5(11), 886-896.

Pinheiro, H., Samalova, M., Geldner, N., Chory, J., Martinez, A. &

- Moore, I. (2009). Genetic evidence that the higher plant Rab-D1 and Rab-D2 GTPases exhibit distinct but overlapping interactions in the early secretory pathway. *Journal of Cell Science*, 122(20), 3749-3758.
- Plutner, H., Cox, A. D., Pind, S., Khosravifar, R., Bourne, J. R., Schwaninger, R., Der, C. J. & Balch, W. E. (1991). Rab1b regulates vesicular transport between the endoplasmic-reticulum and successive Golgi compartments. *Journal of Cell Biology*, 115(1), 31-43.
- Pontier, D., Yahubyan, G., Vega, D., Bulski, A., Saez-Vasquez, J., Hakimi, M. A., Lerbs-Mache, S., Colot, V. & Lagrange, T. (2005). Reinforcement of silencing at transposons and highly repeated sequences requires the concerted action of two distinct RNA polymerases IV in *Arabidopsis*. *Genes & Development*, 19(17), 2030-2040.
- Popineau, Y., Deshayes, G., Lefebvre, J., Fido, R., Tatham, A. S. & Shewry, P. R. (2001). Prolamin aggregation, gluten viscoelasticity, and mixing properties of transgenic wheat lines expressing 1Ax and 1Dx high molecular weight glutenin subunit transgenes. *Journal of Agricultural and Food Chemistry*, 49(1), 395-401.
- Preuss, M. L., Schmitz, A. J., Thole, J. M., Bonner, H. K. S., Otegui, M. S., Nielsen, E. (2006). A role for the RabA4b effector protein PI-4K beta 1 in polarized expansion of root hair cells in *Arabidopsis thaliana*. *Journal of Cell Biology*, 172(7).
- Qi, P. F., Wei, Y. M., Yue, Y. W., Yan, Z. H. & Zheng, Y. L. (2006). Biochemical and molecular characterization of gliadins. *Molecular Biology*, 40(5), 713-723.
- Rakszegi, M., Bogнар, Z., Li, Z., Bekes, F., Lang, L. & Bedo, Z. (2010). Effect of milling on the starch properties of winter wheat genotypes. *Starch-Starke*, 62(2), 115-122.
- Rakszegi, M., Pastori, G., Jones, H. D., Bekes, F., Butow, B., Lang, L., Bedo, Z. & Shewry, P. R. (2008). Technological quality of field grown transgenic lines of commercial wheat cultivars expressing the 1Ax1 HMW glutenin subunit gene. *Journal of Cereal Science*, 47(2), 310-321.
- Rehman, R. U., Stigliano, E., Lycett, G. W., Sticher, L., Sbrano, F., Faraco, M., Dalessandro, G. & Di Sansebastiano, G. P. (2008). Tomato Rab11a characterization evidenced a difference between SYP121-dependent and SYP122-dependent exocytosis. *Plant and Cell Physiology*, 49(5), 751-766.
- Rho, H. S., Heo, J. B., Bang, W. Y., Hwang, S. M., Nahm, M. Y., Kwon, H. J., Kim, S. W., Lee, B. H. & Bahk, J. D. (2009). The role of OsPRA1 in vacuolar trafficking by OsRab GTPases in plant system.

*Plant Science*, 177(5), 411-417.

Roels, S. P. & Delcour, J. A. (1996). Evidence for the non-glycoprotein nature of high molecular weight glutenin subunits of wheat. *Journal of Cereal Science*, 24(3), 227-239.

Rojas, A. M., Fuentes, G., Rausell, A. & Valencia, A. (2012). The Ras protein superfamily: Evolutionary tree and role of conserved amino acids. *Journal of Cell Biology*, 196(2), 189-201.

Rubin, R., Levanony, H. & Galili, G. (1992). Evidence for the presence of 2 different types of protein bodies in wheat endosperm. *Plant Physiology*, 99(2), 718-724.

Rutherford, S. & Moore, I. (2002). The *Arabidopsis* Rab GTPase family: another enigma variation. *Current Opinion in Plant Biology*, 5(6), 518-528.

Sabelli, P. A. & Larkins, B. A. (2009). The development of endosperm in grasses. *Plant Physiology*, 149(1), 14-26.

Saiki, R. K., Gelfand, D. H., Stoffel, S., Scharf, S. J., Higuchi, R., Horn, G. T., Mullis, K. B. & Erlich, H. A. (1988). Primer-directed enzymatic amplification of DNA with a thermostable DNA-polymerase. *Science*, 239(4839), 487-491.

Saito, C. & Ueda, T. (2009). Functions of Rab and SNARE proteins in plant life. *International Review of Cell and Molecular Biology*, Vol 274, 274, 183-233.

Saitou, N. & Nei, M. (1987). The Neighbor-Joining method - a new method for reconstructing phylogenetic trees. *Molecular Biology and Evolution*, 4(4), 406-425.

Sambrook, J., Fritsch, E. F. & Maniatis, T. (1989). Transformation of Plasmids/Cosmids into *E. coli*. In Sambrook, J., Fritsch, E. F. & Maniatis, T. (Eds.), *Molecular Cloning: A Laboratory Manual*. Second ed. Long Island, NY: Cold Spring Harbor Laboratory Press.

Schwarz, D. S., Hutvagner, G., Du, T., Xu, Z. S., Aronin, N. & Zamore, P. D. (2003). Asymmetry in the assembly of the RNAi enzyme complex. *Cell*, 115(2), 199-208.

Shapter, F. M., Henry, R. J. & Lee, L. S. (2008). Endosperm and starch granule morphology in wild cereal relatives. *Plant Genetic Resources Characterization and Utilization*, 6(2).

She, M. Y., Ye, X. G., Yan, Y. M., Howit, C., Belgard, M. & Ma, W. J. (2011). Gene networks in the synthesis and deposition of protein polymers during grain development of wheat. *Functional & Integrative Genomics*, 11(1), 23-35.

- Shewry, P.R., D'ovidio, R., Lafiandra, D., Jenkins, J., Mills, E. & Békés, F. (2009). Wheat grain proteins. In Khan K, S. P. (Ed.), *Wheat: Chemistry and Technology*. St. Paul, MN: AACC Int.
- Shewry, P. R. & Halford, N. G. (2002). Cereal seed storage proteins: structures, properties and role in grain utilization. *Journal of Experimental Botany*, 53(370), 947-958.
- Shewry, P. R., Halford, N. G. & Tatham, A. S. (1992). High-molecular-weight subunits of wheat glutenin. *Journal of Cereal Science*, 15(2), 105-120.
- Shewry, P. R. & Tatham, A. S. (1997). Disulphide bonds in wheat gluten proteins. *Journal of Cereal Science*, 25(3), 207-227.
- Shewry, P. R., Tatham, A. S., Barro, F., Barcelo, P. & Lazzeri, P. (1995). Biotechnology of breadmaking - unraveling and manipulating the multi-protein gluten complex. *Bio-Technology*, 13(11), 1185-1190.
- Shimoni, Y., Zhu, X. Z., Levanony, H., Segal, G. & Galili, G. (1995). Purification, characterization, and intracellular-localization of glycosylated protein disulfide-isomerase from wheat grains. *Plant Physiology*, 108(1), 327-335.
- Sigoillot, F. D., Lyman, S., Huckins, J. F., Adamson, B., Chung, E., Quattrochi, B. & King, R. W. (2012). A bioinformatics method identifies prominent off-targeted transcripts in RNAi screens. *Nature Methods*, 9(4), 363-U66.
- Singh, N. K., Shepherd, K. W., Langridge, P., Gruen, L. C., Skerritt, J. H. & Wrigley, C. W. (1988). Identification of legumin-like proteins in wheat. *Plant Molecular Biology*, 11(5), 633-639.
- Sivars, U., Aivazian, D. & Pfeffer, S. R. (2003). Yip3 catalyses the dissociation of endosomal Rab-GDI complexes. *Nature*, 425(6960), 856-859.
- Smith, C. J. S., Watson, C. F., Ray, J., Bird, C. R., Morris, P. C., Schuch, W. & Grierson, D. (1988). Antisense RNA inhibition of polygalacturonase gene-expression in transgenic tomatoes. *Nature*, 334(6184), 724-726.
- Song, W., Henquet, M. G. L., Mentink, R. A., Van Dijk, A. J., Cordewener, J. H. G., Bosch, D., America, A. H. P. & Van Der Krol, A. R. (2011). N-glycoproteomics in plants: Perspectives and challenges. *Journal of Proteomics*, 74(8), 1463-1474.
- Sparkes, I. A., Hawes, C. & Baker, A. (2005). AtPEX2 and AtPEX10 are targeted to peroxisomes independently of known endoplasmic reticulum trafficking routes. *Plant Physiology*, 139(2), 690-700.

Sparkes, I. A., Ketelaar, T., De Ruijter, N. C. A. & Hawes, C. (2009). Grab a Golgi: laser trapping of Golgi bodies reveals in vivo interactions with the endoplasmic reticulum. *Traffic*, 10(5), 567-571.

Steinfurth, D., Koehler, P., Seling, S. & Muhling, K. H. (2012). Comparison of baking tests using wholemeal and white wheat flour. *European Food Research and Technology*, 234(5), 845-851.

Stenmark, H. (2009). Rab GTPases as coordinators of vesicle traffic. *Nature Reviews Molecular Cell Biology*, 10(8), 513-525.

Suh, H. Y., Lee, D. W., Lee, K. H., Ku, B., Choi, S. J., Woo, J. S., Kim, Y. G. & Oh, B. H. (2010). Structural insights into the dual nucleotide exchange and GDI displacement activity of SidM/DrrA. *EMBO Journal*, 29(2), 496-504.

Svoboda, P. (2004). Long dsRNA and silent genes strike back : RNAi in mouse oocytes and early embryos. *Cytogenetic and Genome Research*, 105(2-4), 422-434.

Tamura, K., Peterson, D., Peterson, N., Stecher, G., Nei, M. & Kumar, S. (2011). MEGA5: molecular evolutionary genetics analysis using maximum likelihood, evolutionary distance, and maximum parsimony methods. *Molecular Biology and Evolution*, 28(10), 2731-2739.

Tanaka, T., Antonio, B. A., Kikuchi, S., Matsumoto, T., Nagamura, Y., Numa, H., Sakai, H., Wu, J., Itoh, T., Sasaki, T., Aono, R., Fujii, Y., Habara, T., Harada, E., Kanno, M., Kawahara, Y., Kawashima, H., Kubooka, H., Matsuya, A., Nakaoka, H., Saichi, N., Sanbonmatsu, R., Sato, Y., Shinso, Y., Suzuki, M., Takeda, J. I., Tanino, M., Todokoro, F., Yamaguchi, K., Yamamoto, N., Yamasaki, C., Imanishi, T., Okido, T., Tada, M., Ikeo, K., Tateno, Y., Gojobori, T., Lin, Y. C., Wei, F. J., Hsing, Y. I., Zhao, Q., Han, B., Kramer, M. R., McCombie, R. W., Lonsdale, D., O'donovan, C. C., Whitfield, E. J., Apweiler, R., Koyanagi, K. O., Khurana, J. P., Raghuvanshi, S., Singh, N. K., Tyagi, A. K., Haberer, G., Fujisawa, M., Hosokawa, S., Ito, Y., Ikawa, H., Shibata, M., Yamamoto, M., Bruskiwich, R. M., Hoen, D. R., Bureau, T. E., Namiki, N., Ohyanagi, H., Sakai, Y., Nobushima, S., Sakata, K., Barrero, R. A., Souvorov, A., Smith-White, B., Tatusova, T., An, S., An, G., Oota, S., Fuks, G., Messing, J., Christie, K. R., Lieberherr, D., Kim, H., Zuccolo, A., Wing, R. A., Nobuta, K., Green, P. J., Lu, C., Meyers, B. C., Chaparro, C., Piegu, B., Panaud, O. & Echeverria, M. (2008). The rice annotation project database (RAP-DB): 2008 update. *Nucleic Acids Research*, 36, D1028-D1033.

Tatham, A. S., Drake, A. F. & Shewry, P. R. (1990). Conformational studies of synthetic peptides corresponding to the repetitive regions of the high-molecular-weight (HMW) glutenin subunits of wheat. *Journal of Cereal Science*, 11(3), 189-200.

Tatham, A. S. & Shewry, P. R. (1985). The conformation of wheat gluten proteins - the secondary structures and thermal stabilities of alpha-gliadins, beta-gliadins, gamma-gliadins and omega-gliadins. *Journal of Cereal Science*, 3(2), 103-113.

Tatham, A. S. & Shewry, P. R. (1995). The S-poor prolamins of wheat, barley and rye. *Journal of Cereal Science*, 22(1), 1-16.

Tilley, K. A. (1997). Detection of O-glycosidically linked mannose within the structure of a highly purified glutenin subunit isolated from Chinese Spring wheat. *Cereal Chemistry*, 74(4), 371-374.

Tilley, K. A., Lookhart, G. L., Hosney, R. C. & Mawhinney, T. P. (1993). Evidence for glycosylation of the high-molecular-weight glutenin subunit-2, subunit-7, subunit-8, and subunit-12 from chinese spring and tam-105 wheats. *Cereal Chemistry*, 70(5), 602-606.

Toonen, R. F. G. & Verhage, M. (2007). Munc18=1 in secretion: lonely Munc joins SNARE team and takes control. *Trends in Neurosciences*, 30(11), 564-572.

Tosi, P., Gritsch, C. S., He, J. B. & Shewry, P. R. (2011). Distribution of gluten proteins in bread wheat (*Triticum aestivum*) grain. *Annals of Botany*, 108(1), 23-35.

Tosi, P., Parker, M., Gritsch, C. S., Carzaniga, R., Martin, B. & Shewry, P. R. (2009). Trafficking of storage proteins in developing grain of wheat. *Journal of Experimental Botany*, 60(3), 979-991.

Turner, J. B., Garner, G. V., Gordon, D. B., Brookes, S. J. & Smith, C. A. (2002). Are alpha-gliadins glycosylated? *Protein and Peptide Letters*, 9(1), 23-29.

Ueda, T., Matsuda, N., Anai, T., Tsukaya, H., Uchimiya, H. & Nakano, A. (1996). An *Arabidopsis* gene isolated by a novel method for detecting genetic interaction in yeast encodes the GDP dissociation inhibitor of Ara4 GTPase. *Plant Cell*, 8(11), 2079-2091.

Ueda, T., Uemura, T., Sato, M. H. & Nakano, A. (2004). Functional differentiation of endosomes in *Arabidopsis* cells. *Plant Journal*, 40(5), 783-789.

Ueda, T., Yoshizumi, T., Anai, T., Matsui, M., Uchimiya, H. & Nakano, A. (1998). AtGDI2, a novel *Arabidopsis* gene encoding a Rab GDP dissociation inhibitor. *Gene*, 206(1), 137-143.

Van Der Krol, A. R., Lenting, P. E., Veenstra, J., Van Der Meer, I. M., Koes, R. E., Gerats, A. G. M., Mol, J. N. M. & Stuitje, A. R. (1988). An anti-sense chalcone synthase gene in transgenic plants inhibits flower pigmentation. *Nature (London)*, 333(6176), 866-869.

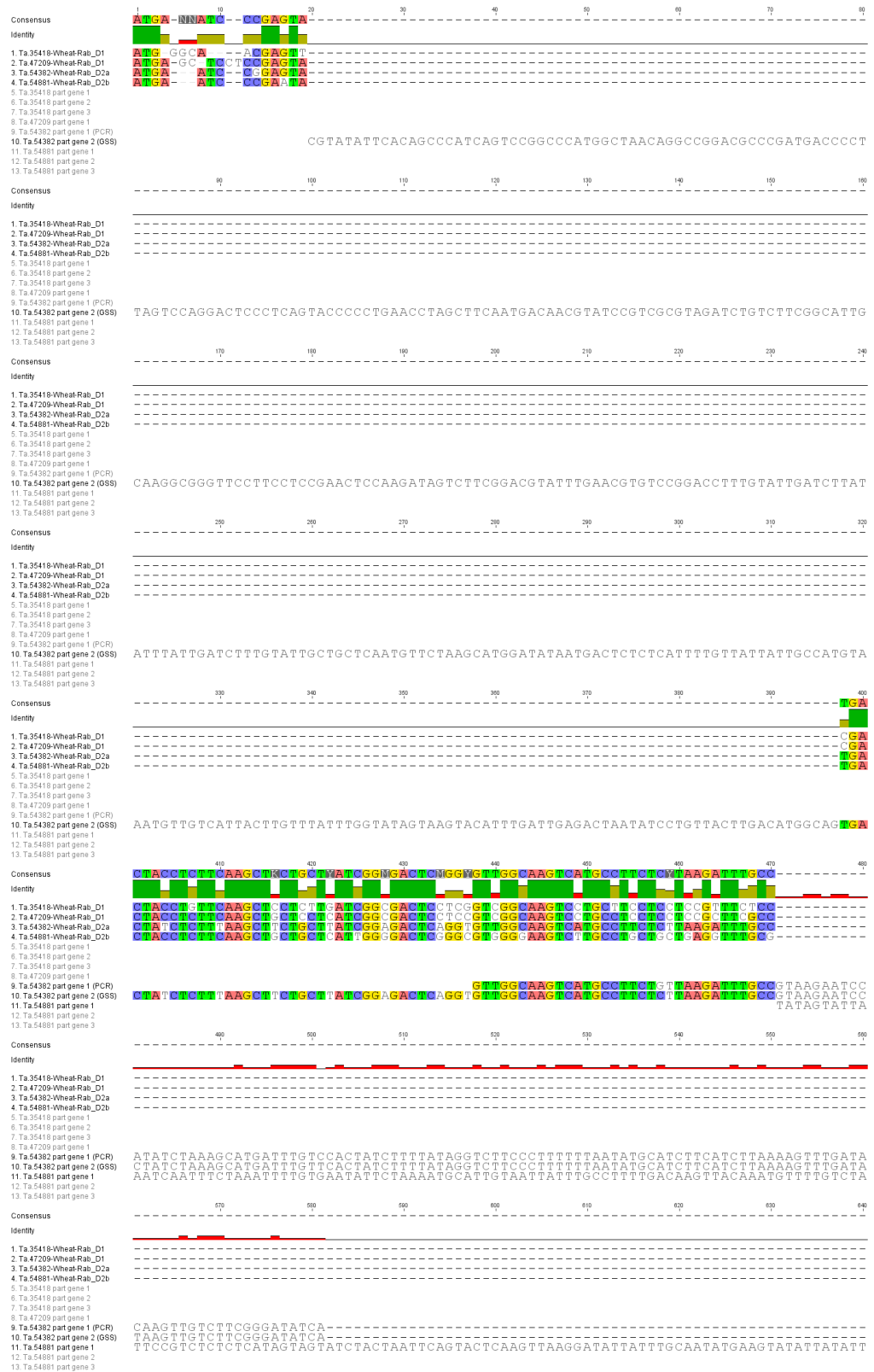
- Vernoud, V., Horton, A. C., Yang, Z. B. & Nielsen, E. (2003). Analysis of the small GTPase gene superfamily of *Arabidopsis*. *Plant Physiology*, 131(3), 1191-1208.
- Wang, F., Liu, C., Wei, C., Cui, Y. H., Zheng, Q., Zhang, J. M., Wu, J. S. & Liu, K. D. (2012). AtRabD2b, a functional ortholog of the yeast ypt1, controls various growth and developmental processes in *Arabidopsis*. *Plant Molecular Biology Reporter*, 30(2), 275-285.
- Webster, D. E. & Thomas, M. C. (2012). Post-translational modification of plant-made foreign proteins; glycosylation and beyond. *Biotechnology Advances*, 30(2), 410-418.
- Wennerberg, K., Rossman, K. L. & Der, C. J. (2005). The Ras superfamily at a glance. *Journal of Cell Science*, 118(5), 843-846.
- Wickner, W. & Schekman, R. (2008). Membrane fusion. *Nature Structural & Molecular Biology*, 15(7), 658-664.
- Woollard, A. A. D. & Moore, I. (2008). The functions of Rab GTPases in plant membrane traffic. *Current Opinion in Plant Biology*, 11(6), 610-619.
- Woychik, J. H., Dimler, R. J. & Boundy, J. A. (1961). Starch gel electrophoresis of wheat gluten proteins with concentrated urea. *Archives of Biochemistry and Biophysics*, 94(3), 477.
- Xu, P., Zhang, Y. J., Kang, L., Roossinck, M. J. & Mysore, K. S. (2006). Computational estimation and experimental verification of off-target silencing during posttranscriptional gene silencing in plants. *Plant Physiology*, 142(2), 429-440.
- Yue, S. J., Li, H., Li, Y. W., Zhu, Y. F., Guo, J. K., Liu, Y. J., Chen, Y. & Jia, X. (2008). Generation of transgenic wheat lines with altered expression levels of 1Dx5 high-molecular weight glutenin subunit by RNA interference. *Journal of Cereal Science*, 47(2), 153-161.
- Zadoks, J. C., Chang, T. T. & Konzak, C. F. (1974). Decimal code for growth stages of cereals. *Weed Research*, 14(6), 415-421.
- Zarsky, V., Cvrckova, F., Bischoff, F. & Palme, K. (1997). At-GDI1 from *Arabidopsis thaliana* encodes a Rab-specific GDP dissociation inhibitor that complements the sec19 mutation of *Saccharomyces cerevisiae*. *Febs Letters*, 403(3), 303-308.
- Zerial, M. & McBride, H. (2001). Rab proteins as membrane organizers. *Nature Reviews Molecular Cell Biology*, 2(2), 107-117.
- Zhang, J. M., Hill, D. R. & Sylvester, A. W. (2007). Diversification of the RAB guanosine triphosphatase family in dicots and monocots. *Journal of Integrative Plant Biology*, 49(8), 1129-1141.

Zhang, Q., Dong, Y. M., An, X. L., Wang, A. L., Zhang, Y. Z., Li, X. H., Gao, L. Y., Xia, X. C., He, Z. H. & Yan, Y. M. (2008). Characterization of HMW glutenin subunits in common wheat and related species by matrix-assisted laser desorption/ionization time-of-flight mass spectrometry (MALDI-TOF-MS). *Journal of Cereal Science*, 47(2), 252-261.

Zheng, H. Q., Camacho, L., Wee, E., Henri, B. A., Legen, J., Leaver, C. J., Malho, R., Hussey, P. J. & Moore, I. (2005). A Rab-E GTPase mutant acts downstream of the Rab-D subclass in biosynthetic membrane traffic to the plasma membrane in tobacco leaf epidermis. *Plant Cell*, 17(7), 2020-2036.

# 8 Appendix

## 8.1 Alignment of wheat RabD nucleotide sequences





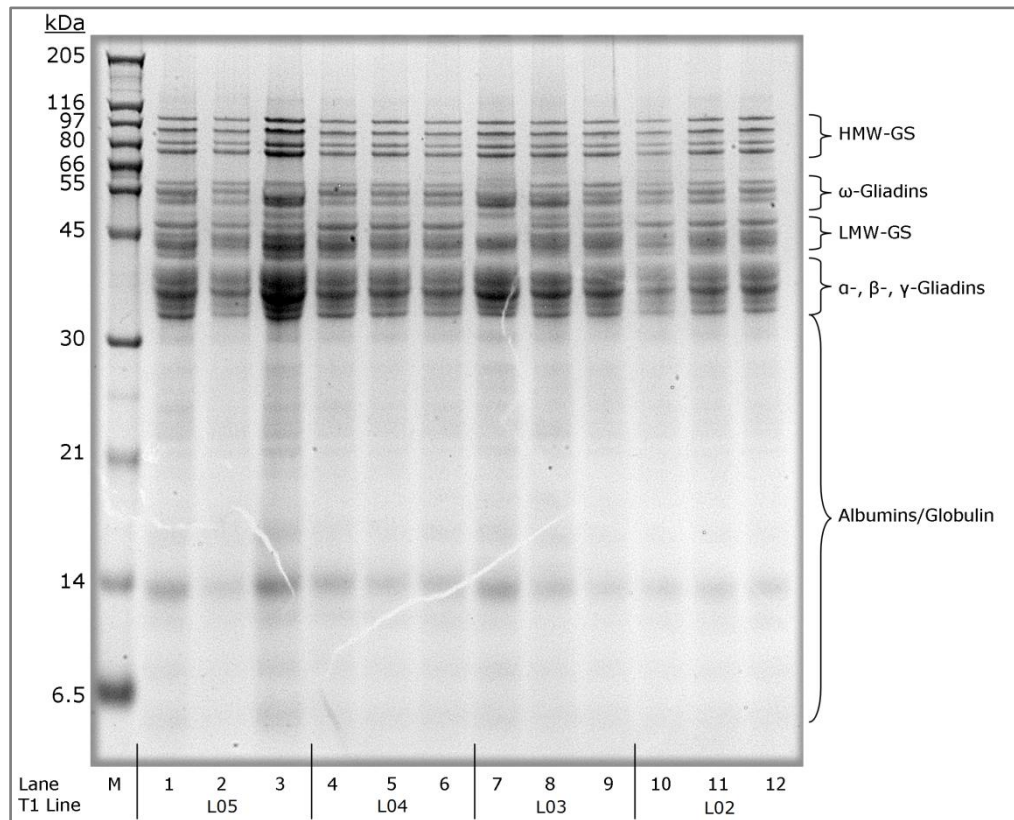






## 8.2 SDS-PAGE gels

**A**



**B**

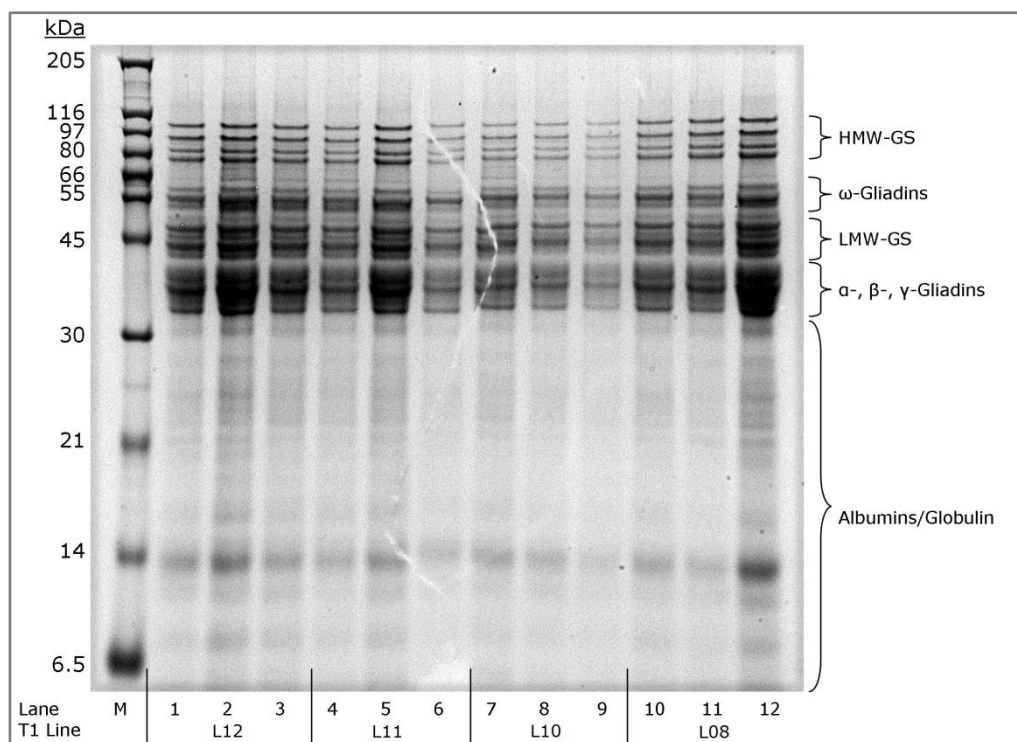


**Fig. 8.1 – SDS-PAGE of mature T1 seeds.**

Sizes of marker proteins are indicated on the left in kDa. Lane numbers and T1 lines are displayed below the gels. Categories of seed storage proteins are indicated on the right. M indicates a lane containing protein marker.

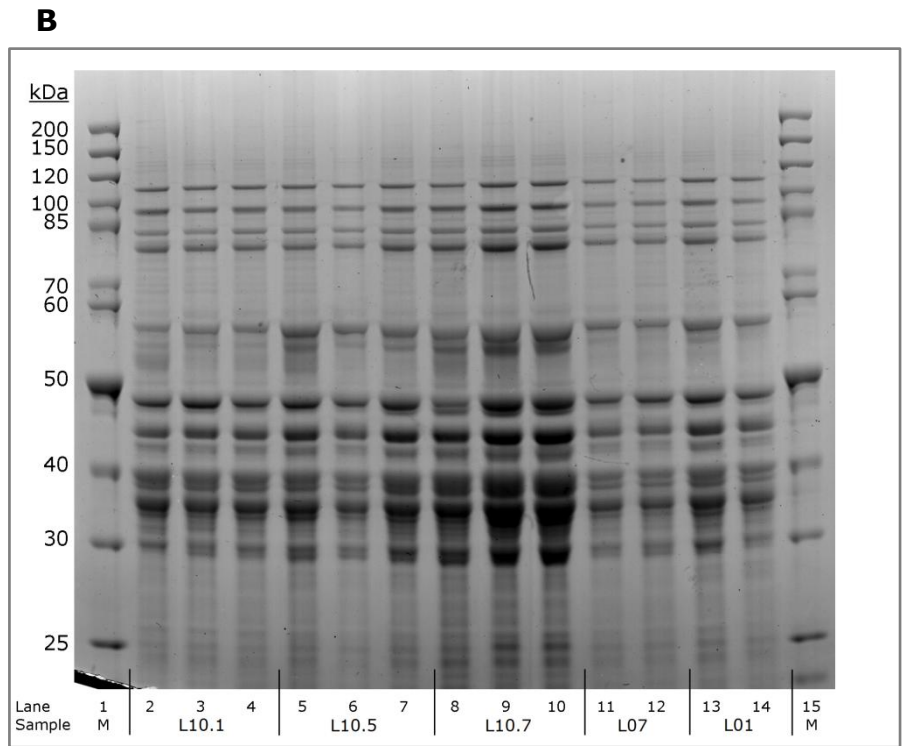
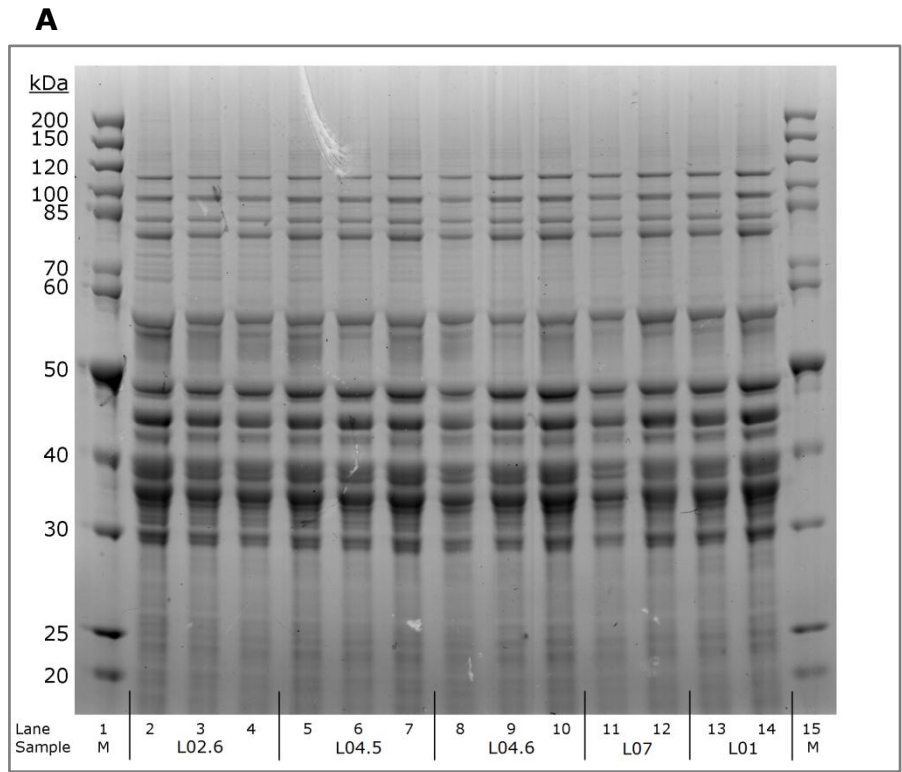
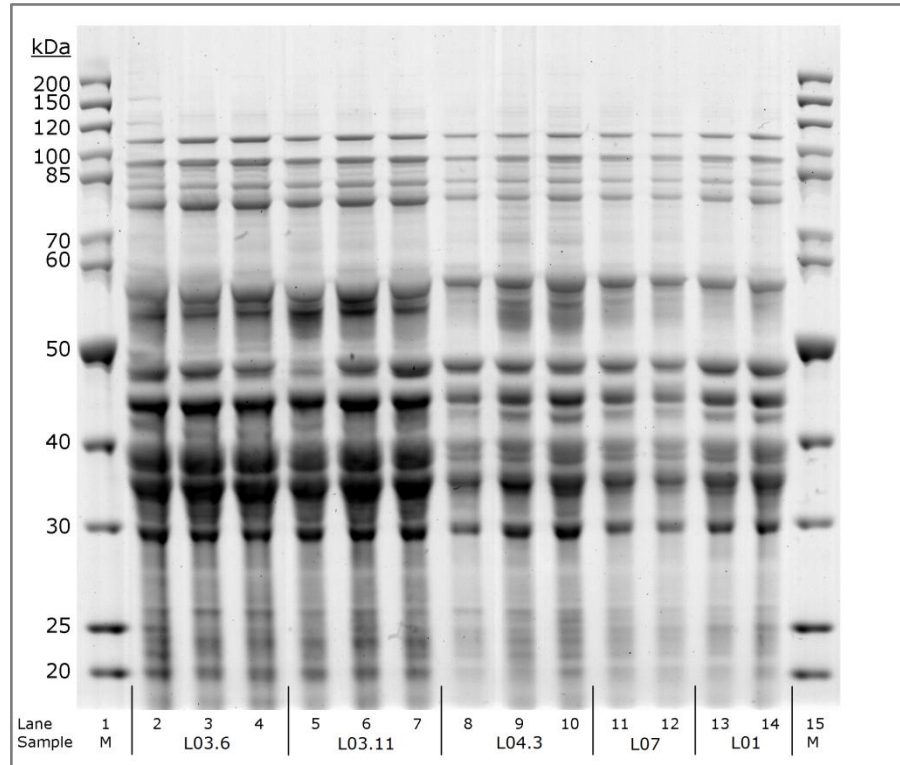
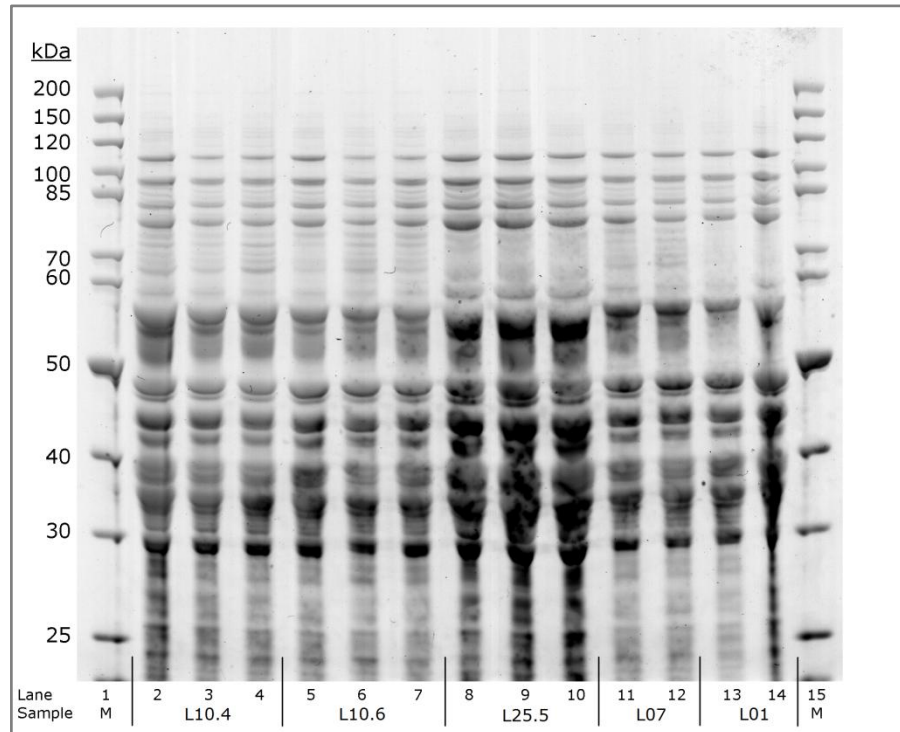


**Fig. 8.2 – SDS-PAGE of mature T2 seeds.**  
 Sizes of marker proteins are indicated on the left in kDa. Lane numbers and line names are displayed below the gels. L07 = T1 bar-only control line, L01 = T1 gold-only control line. M indicates a lane containing protein marker.

**A**

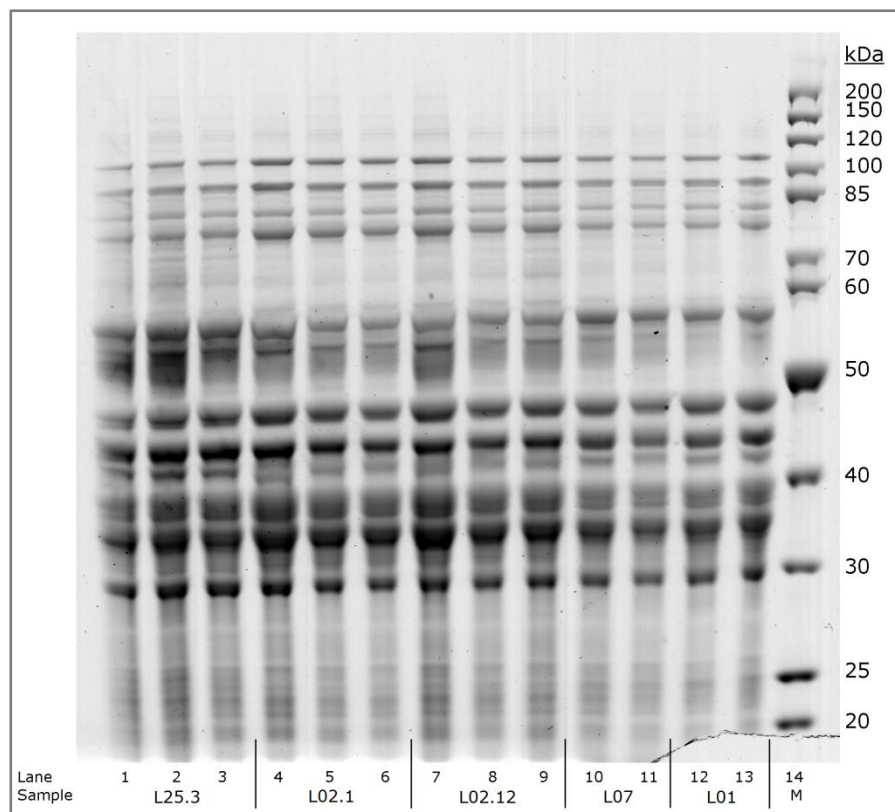


**B**



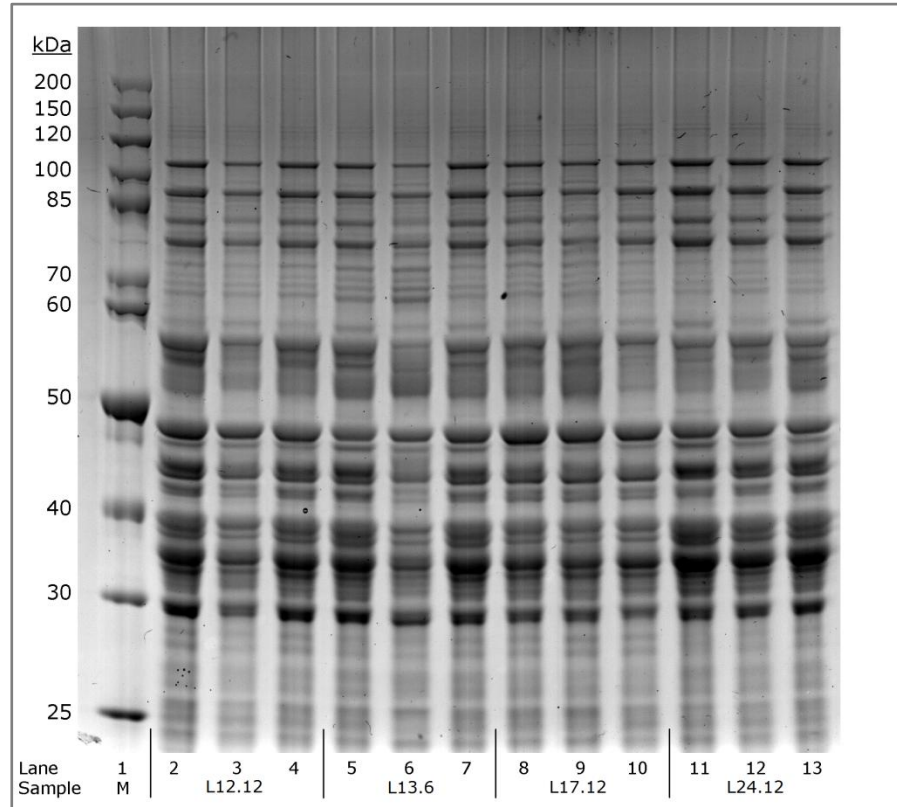
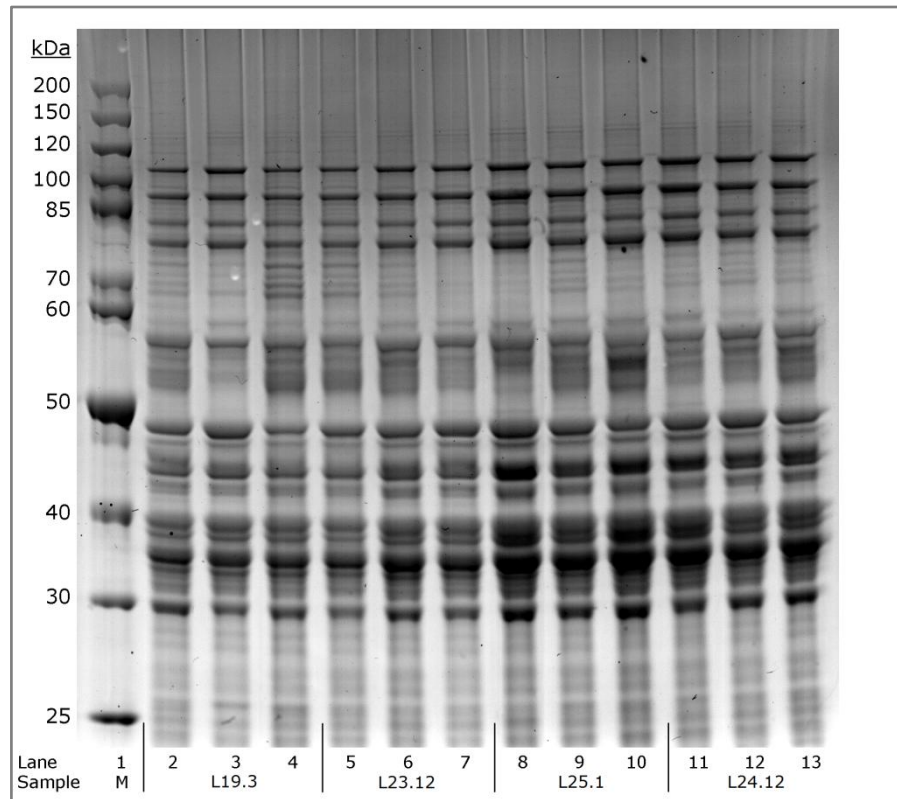
**Fig. 8.3 – SDS-PAGE of mature T2 seeds.**

Sizes of marker proteins are indicated on the left in kDa. Lane numbers and line names are displayed below the gels. L07 = T1 bar-only control line, L01 = T1 gold-only control line. M indicates a lane containing protein marker.



**Fig. 8.4 – SDS-PAGE of mature T2 seeds.**

Sizes of marker proteins are indicated on the right in kDa. Lane numbers and line names are displayed below the gels. L07 = T1 bar-only control line, L01 = T1 gold-only control line. M indicates a lane containing protein marker.

**A****B**

**Fig. 8.5 – SDS-PAGE of mature T2 seeds.**

Sizes of marker proteins are indicated on the left in kDa. Lane numbers and line names are displayed below the gels. L24.12 = T2 bar-only control line. M indicates a lane containing protein marker.

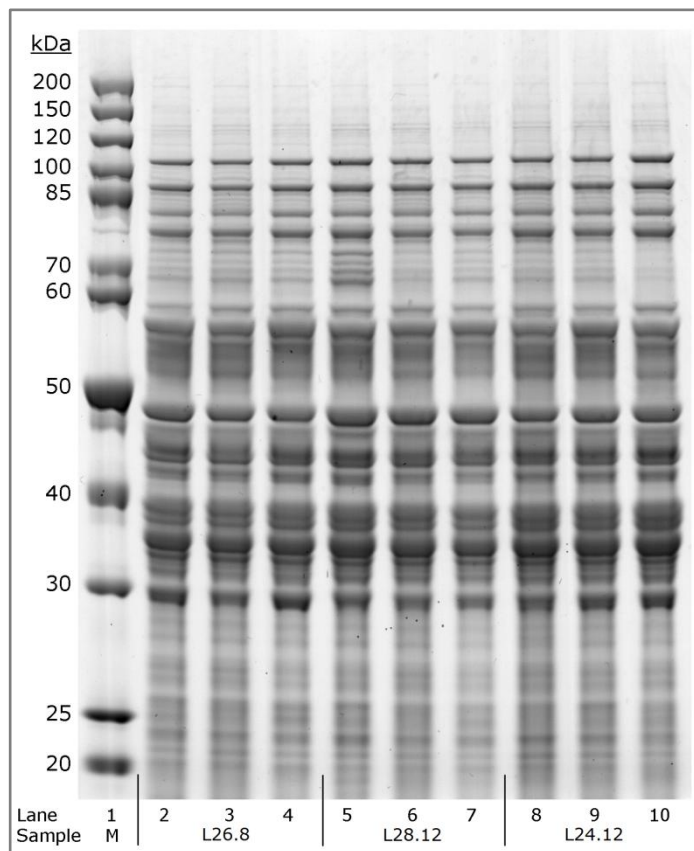


**Fig. 8.6 – SDS-PAGE of mature T2 seeds.**

Sizes of marker proteins are indicated on the left in kDa. Lane numbers and line names are displayed below the gels. L24.12 = T2 bar-only control line. M indicates a lane containing protein marker.